

AN ANALYSIS OF HOSPITALIZED MOTORCYCLISTS IN THE STATE OF MARYLAND BASED ON HELMET USE AND OUTCOME

Timothy Kerns

University of Maryland
National Study Center for Trauma & EMS
United States of America

Catherine A. McCullough

National Highway Traffic Safety Administration
United States Department of Transportation
United States of America

Paper No: 09-0061

ABSTRACT

In recent years, there has been a significant increase in mortality among motorcyclists. Despite high rates of morbidity and mortality associated with crashes among older riders, there have been relatively few studies on injured motorcyclists admitted to hospitals. In an ongoing study, data is being collected from motorcyclists involved in crashes in Maryland who were either killed or transported to the R Adams Cowley Shock Trauma Center (STC) in Baltimore, Maryland. Data on injured motorcyclists is captured from the trauma registry, hospital discharge records, autopsy reports, and through a linkage with police crash reports. Injured parties are assessed six-months and one-year post crash with the Short Form 36 (SF-36) questionnaire. The SF-36 is an evaluation tool used to determine long term outcome. Autopsy reports are obtained from the Office of the Chief Medical Examiner of Maryland (OCME).

Previous studies looking at head injuries resulting from motorcycle crashes have not been able to discriminate between operators using helmets that are and are not compliant with standards set forth by the United States Department of Transportation (DOT). Helmets will be categorized as DOT-certified, full-face, half-shell or uncertified novelty helmets. Fatal versus non-fatal crashes with resulting injuries are compared and matched by operator demographics, helmet use and type, and crash characteristics. It is anticipated that persons involved in a crash while wearing an uncertified novelty helmet have a higher risk of head injury than those who crashed while wearing a DOT-certified helmet.

From January 2007 through May 2008 there were 517 motorcycle operators admitted to the STC. The mean age of this group was 37 years and 25percent sustained a head injury with an Abbreviated Injury Score (AIS) between 1 and 6. Twenty-one percent of these helmets

were identified as DOT non-certified. A comparison of head injury and helmet type revealed that 50 percent (13/26) of those wearing a uncertified novelty helmet received a head injury (AIS 1-6) as compared to 23 percent (22/96) of those wearing a DOT certified helmet.($p<.05$).

INTRODUCTION

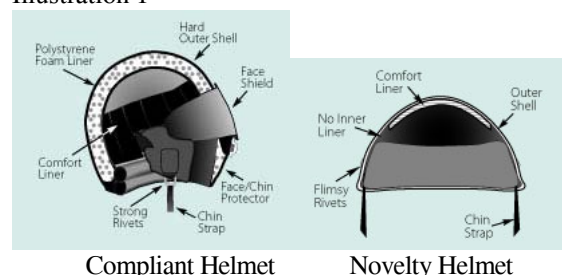
Motorcycles have become an increasingly popular mode of transportation; motorcycle registrations in the United States topped 8.1 million in 2007¹. Motorcyclists are particularly vulnerable to injury because their vehicles provide little or no protection in the event of a crash. Helmets have repeatedly been proven to reduce the severity of head injury in crashes. However, the number of motorcyclists injured (103,000) and killed (5,154) in 2007 continued a ten year upward trend.²

At the same time, there has been an increase in the average engine size of motorcycles, from a mean of 769 cc in 1990 to 999 cc in 2002.³ In addition, during the same period as the nationwide increase in fatalities, there has also been an increase in the number of states repealing or modifying motorcycle helmet use laws, as well as a decreasing rate among observed motorcyclists. While the use of a motorcycle helmet has been estimated to be 37 percent effective in preventing fatal injuries to motorcyclists who are involved in a highway crash, only 59 percent of motorcyclists who sustained fatal injuries were reported to be wearing a helmet at the time of their crash.⁴ Also, in a previous study of motorcyclist fatalities focusing on head injuries that was conducted at the National Study Center for Trauma & EMS (NSC) findings revealed that motorcyclists wearing helmets were significantly less likely to suffer a traumatic brain injury (TBI) than those who were unhelmeted.⁵

The US DOT created Federal Motor Vehicle Safety Standard FMVSS No. 218 in 1973. The purpose of this standard is to reduce deaths and injuries to motorcyclists and other motor vehicle users resulting from head impacts. To do so, the standard establishes a minimum performance requirement for helmets. These requirements include three performance tests: (1) An impact attenuation test; (2) a penetration test; and (3) a retention system test; as well as various labeling requirements.

Despite the passage of mandatory helmet laws in a number of states, the persistent use of ‘novelty’ helmets that do not meet the requirements of FMVSS No. 218 (Illustration 1) remains relatively unchanged.

Illustration 1



NHTSA has published an NPRM (73 FR 57297) on October 2, 2008, to amend FMVSS No. 218 to address the issue of novelty helmets. Some of the proposed amendments to FMVSS No. 218 would help realize the full potential of compliant helmets by aiding state and local law enforcement officials in enforcing state helmet use laws, thereby increasing the percentage of motorcycle riders wearing helmets compliant with FMVSS No. 218. The amendments would do this by adopting additional requirements and revising existing requirements to reduce misleading labeling of novelty helmets that creates the impression that uncertified, noncompliant helmets have been properly certified as compliant.

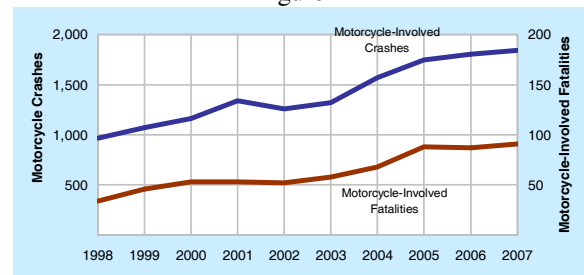
This study provides a general description of the characteristics of motorcycle crashes in Maryland and the injury patterns associated with those crashes. For this analysis, the prevalence of ‘novelty’ helmet use and subsequent head injury among motorcycle operators in Maryland who were transported to a trauma center as the result of a highway crash was examined.

METHODS

The Maryland Automated Accident Reporting System (MAARS) collects data on more than

100,000 crashes that occur annually. An analysis of this database was used to provide a general description of the number and type of motorcycle crashes that occur in the state. In addition, information on injuries and helmet type was collected from persons who were transported to the STC as a result of their crash during the period January 2007 through May 2008. During the course of their hospital stay, these crash-involved motorcycle operators were approached and asked to provide

Figure 1



consent for participation in the study. Upon consent, they were asked a series of questions about their riding habits and the type of crash in which they were involved and a series of questions about their general health and activity level prior to their crash. If available, the helmet they were wearing at the time of the crash was photographed. These photographs were used to identify any damage that may have resulted from the crash and to classify the helmet as being DOT-certified. Demographic characteristics and the nature and extent of the injuries sustained were captured from the STC trauma registry database. For this analysis, any documented brain or skull injury with a severity of 1 or higher, using the Abbreviated Injury Scale (AIS), was classified as a brain injury.

RESULTS

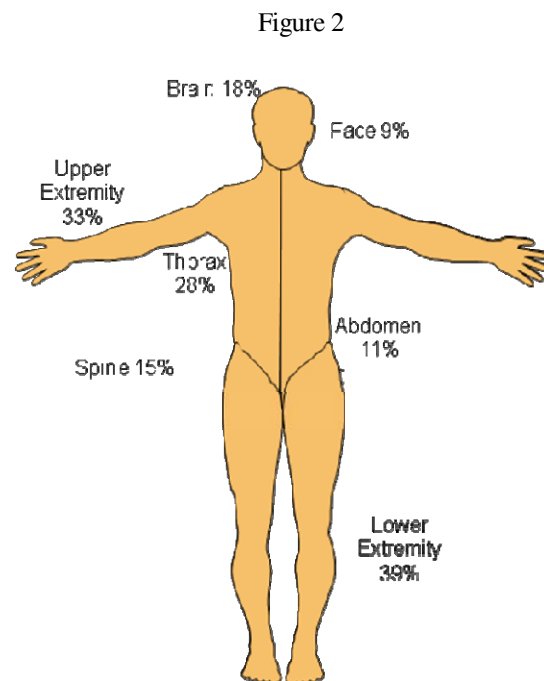
Crash Characteristics

During calendar year 2007 there were 1,841 motorcycle crashes and 96 fatalities that occurred on Maryland roads. Both numbers continue an upward trend in both crashes and fatalities that extends back to the late 1990's (Figure 1). The vast majority of the motorcycle operators involved in a crash was men (89 percent) and persons between the ages of 35 and 49 accounted for 34 percent of the riders involved in a crash. More than 40 percent of the crashes occurred on the weekend (Saturday - Sunday) and 60 percent occurred between the hours of noon and 8pm (Table 1).

Table 1 – Maryland Motorcycle Crash and Rider Characteristics					
Total Riders Involved in Crashes			Riders Killed in Crashes		
	N	%		N	%
Gender					
Male	1,680	89		87	99
Age					
<20	106	5.6		5	5.7
20-34	672	35.5		33	37.5
35-49	653	34.6		35	39.8
50-64	320	16.9		12	13.6
65+	32	1.7		3	3.3
Helmet Use					
Yes	1,403	74.0		77	87.5
Unknown	331	17.5		6	6.8
Total Motorcycle Crashes			Fatal Motorcycle Crashes		
Day of Week					
Weekday	1,046	56.8		49	53.8
Weekend	795	43.2		42	46.2
Hour of Day					
12am – 8am	231	12.5		12	13.2
8am – 12pm	199	10.8		6	6.6
12pm – 8pm	1,105	60.0		54	59.4
8pm – 12am	305	16.6		19	20.9

Injured Motorcycle Operators

From January 2007 through May 2008 there were 517 motorcycle operators admitted to the STC as the result of a roadway crash. The mean age of this group was 37 years and 25 percent sustained a brain injury. The distribution of injuries (AIS 2+) to other body regions for this group is illustrated in Figure 2. Injuries to the upper and lower extremities, as expected, were observed most frequently. The mean Injury Severity Score was 14.5 (range 1-75). Among this group of patients, 153 (30 percent) of those motorcycle operators who arrived at the trauma center provided consent to have photographs taken of the helmet they were wearing at the time of the crash. Based on these photographs, 21 percent of these helmets were identified as novelty (or DOT uncertified) helmets. Examples of helmets examined at the STC are presented in Figure 3. Case 1 illustrates a FMVSS No. 218 certified helmet with minor damage to the left side. Case 2 illustrates a novelty helmet affixed with a warning label on the inside warning that it will not protect against serious injury. Case 3 illustrates a novelty helmet that sustained significant damage as a result of the crash.



**Due to multiple body regions being injured as the result of a crash, percentages total more than 100%.*

Additionally 118 motorcycle operators provided answers to a general questionnaire that gathered information on their demographics, education level, and riding behavior. Selected characteristics of this group are provided in Table 2. Ninety-seven percent of the operators were men with a mean age of 39 years. Nearly 40 percent reported never having taken a motorcycle safety training course and the type of motorcycle ridden was distributed largely between cruisers (37 percent) and sport bikes (39 percent). Thirty-seven percent of the crashes involved a collision with another vehicle. Additionally, 65 percent reported to be wearing some type of protective clothing (excluding long pants/jeans) at the time of their crash.

A comparison of head injury and helmet type revealed that 50 percent (13/26) of those wearing a non-compliant helmet received a head injury (AIS 1-6) as compared to 23 percent (22/96) of those wearing a compliant helmet ($p<.05$). Those wearing 'novelty' helmets at the time of their crash were found to be significantly older (46.9 years vs 37.3 years, $p<.05$).

Table 2 – General Participant Characteristics		
		Percent
Gender		
	Male	97
Education Level		
	HS Diploma or less	45
Motorcycle Type		
	Cruiser	37
	Sport	39
Taken a MC training course		
	No	39
Type of Crash		
	Laid bike down	20
	Single vehicle, object impact	31
	Multiple vehicle	
	Intersection related	16
	Non-intersection related	21
Type of Road		
	Interstate	21
	City street/urban area	15
	Suburban area	26
	County road/rural area	29
Protective Clothing worn		65

DISCUSSION

Over the past ten years, there has been a steady and disconcerting increase in the U.S. in motorcycle crashes and fatalities. This national trend is also occurring in the state of Maryland. Maryland does have a universal helmet law, requiring all riders wear a DOT-certified helmet. This law initially helped lower the frequency of head injuries and fatalities from those injuries.⁵

However, several factors including the increase in the number of motorcycles on the highway has contributed to the overall upward trend of motorcycle crashes and their subsequent injuries and the use of uncertified helmets appears to increase the likelihood of a head injury as the result of those crashes. Anecdotally, some riders prefer the appearance and feel of these novelty helmets or may wear them to satisfy the minimum requirements of the law. Whatever their reason, uncertified novelty helmets do not provide the same level of protection as helmets certified to FMVSS No. 218 which have an energy attenuating liner and shell design to prevent excessive penetrations, and a

Figure 3

Case 1 – FMVSS No. 218 DOT Certified w/ damage



Case 2 – Novelty with warning label



Case 3 Novelty with damage



retention system that can withstand loads during a crash and therefore, will not protect the motorcyclist from a brain or skull injury in the event of a crash.⁶ This hypothesis has been supported by the research presented here. Of all injured riders, those wearing a non-compliant helmet were more likely to have sustained a head injury. It is important to note that the riders wearing uncertified novelty helmets were significantly older. Future analysis will incorporate injuries and helmet type for fatally injured motorcycle.

CONCLUSIONS

It has been shown that there are several distinct groups within the motorcycle riding community. Some studies have separated riders based on age, motorcycle type or riding experience. This study has provided a summary of the characteristics of motorcycle crashes and have focused on a sub-group of motorcycle operators who were injured in a highway crash and compared the occurrence of brain injuries with the helmet type, DOT-certified vs. uncertified. By analyzing riders who were injured, this project has shown that the likelihood of sustaining a brain injury increases when wearing a non-compliant helmet.

This study has provided further evidence regarding the effectiveness of use of DOT-certified helmets to reduce and prevent the severity of head injuries. Skeletal injuries have a higher likelihood of survival to positive outcomes, whereas brain injuries often lead to long-term disability or psychosocial issues. By preventing TBI, there is an increased likelihood of a positive outcome following a crash. Finally, this study exemplifies the use of the recommendation made in the Review of State Motorcycle Safety Program Technical Assessments⁷ by combining multiple datasets to evaluate multiple aspects of motorcycle crashes and their subsequent injuries.

REFERENCES

¹ Federal Highway Administration, Highway Statistics 2007, State Motor Vehicle Registrations 2007
<http://www.fhwa.dot.gov/policyinformation/statistics/2007/mv1.cfm>

² 2007 Traffic Safety Annual Assessments – Highlights, DOT-HS-811-017, August 2008

³Shankar, B.S., Ramzy, A.I., Soderstrom, C.A., Dischinger, P.C. and Clark, C.C. (1992). Helmet use, patterns of injury, medical outcome, and costs among motorcycle drivers in Maryland. *Accident Analysis and Prevention* 24 , 385-396

⁴Traffic Safety Facts – Research Note, DOT HS 809 861, August 2005.

⁵Auman KM, Kufera JA, Ballesteros MF, Smialek JE, Dischinger PC. Autopsy study of motorcyclist fatalities: the effect of the 1992 Maryland motorcycle helmet use law. *American Journal of Public Health*. 2002 Aug; 92(8):1352-5.

⁶ Traffic Safety Facts – Research Note, DOT HS 810 752, April 2007

⁷Review of State Motorcycle Safety Program Technical Assessments. DOT HS 811 082, January 2009

COMMERCIAL VEHICLE SAFETY TECHNOLOGIES: APPLICATIONS FOR TIRE PRESSURE MONITORING AND MANAGEMENT

Deborah Freund

Federal Motor Carrier Safety Administration
United States of America

Stephen Brady

Booz Allen Hamilton Inc.
United States of America
Paper Number 09-0134

ABSTRACT

Tire deficiencies often cause commercial motor vehicles (CMVs) to be cited for regulatory violations and to be taken out-of-service during roadside inspections. As part of a major safety technology project to assess the state of the practice and potential contributions of advanced sensor systems, the Federal Motor Carrier Safety Administration (FMCSA) sponsored three studies between 2003 and 2008 on tire pressure management systems (TPMS). The first study focused on obtaining baseline information. Fleet records and limited field collections were used to develop a database of inflation readings for 35,000 CMV tires, providing the first large-scale source of information on CMV tire inflation in the United States. The second study assessed the performance of TPMS in a controlled test-track environment. Multiple systems were installed on a truck tractor, a trailer, and a motorcoach. These were run under nominal operating conditions and with tire and system faults deliberately introduced. Although all the systems functioned at the levels specified by their manufacturers, some had limited ability to compensate for changes in ambient temperature, to reset pressure “alert” thresholds, and to withstand repeated tire installation and removal cycles. The third study, performed in an operational setting in an urban transit fleet, assessed the performance and maintainability of tire pressure monitoring devices. Three types of TPMS were installed on 12 buses that accumulated more than 1.28 million km, in aggregate, during the 12-month test period. The results of this study pointed to sensor durability and data integration challenges that need to be overcome for these systems to be used successfully in a severe service environment. These studies provided new information directly comparing the performance of TPMS in controlled and operational settings. Results are limited to the particular systems and applications tested. Study data are available from the FMCSA.

INTRODUCTION

The load carrying capability of a tire is critically linked to the inflation pressure. Fleet operators will generally select a particular “target pressure” for their trucks based on the unique load, operating, and environmental conditions in which they operate. If not properly inflated, the useful tire life, as well as vehicle handling and safety, are compromised.

CMV tires lose air pressure for a variety of reasons. Air can escape between the bead and wheel, as well as through improperly tightened valves, torn rubber grommets, or valve cores that have been blocked open by dirt and ice. Additionally, air molecules are small enough to diffuse through rubber (albeit very slowly), and an air pressure drop of up to two psi per month is not uncommon. Most tire companies recommend that tire pressure be checked weekly, using properly calibrated tire gauges. However, tire pressure maintenance is labor and time intensive. It takes 20 to 30 minutes to check all the tires on an 18-wheeled tractor-trailer combination vehicle and to add air to 2 or 3 tires that may be low. Due to this fact and the lack of time available, tires are often improperly inflated.

Improper tire inflation increases operating costs by reducing tire life and lowering fuel economy (an underinflated tire “flexes” and has higher rolling resistance). For the average fleet operator in the United States, improper tire inflation increases the annual procurement costs for both new and retreaded tires by about 10 to 13 percent. Due to improper tire inflation, fuel economy decreases about 0.6 percent for typical truckload (TL) and less-than-truckload (LTL) operations. According to road-breakdown management service providers, weakened and worn tires due to improper tire inflation are estimated to be responsible for one road call per year per tractor-trailer combination vehicle.

Although most industry stakeholders intuitively recognize the importance of proper tire inflation maintenance and its impact on operating cost and

safety, there was very little empirical data on CMV tire pressure maintenance practices. The extent of the under inflation problem had never been documented, and the costs of improper tire pressure maintenance had not been systematically analyzed. Although new tire pressure maintenance and management technologies have been introduced for the CMV market, such as automatic tire inflation systems and various types of tire monitoring systems, there was little information that fleet maintenance managers could use to determine whether those systems would provide a reasonable return on investment.

FIRST STUDY: TIRE PRESSURE SURVEY

The primary objectives of this project were to develop and document the impacts of tire inflation maintenance practices on CMV operating costs and safety and to provide a quantitative estimate of potential benefits of tire pressure monitoring sensors and automatic inflation systems. In order to address the dearth of comprehensive data on tire inflation practices, the study engaged in a cooperative effort with the Technology & Maintenance Council (TMC) of the American Trucking Associations to synthesize existing tire pressure survey data from a wide variety of truck and bus fleets and to collect new tire inflation field data for the owner-operator segment of the trucking industry. The study also gathered information from suppliers of tire pressure monitoring and automatic inflation systems and developed six hypothetical fleet operating scenarios to estimate potential costs and benefits from use of these systems.

Tire manufacturers perform fleet surveys for their CMV fleet customers to assist them with their tire maintenance programs and to determine the performance of their tires under various operating conditions. Experienced field service engineers use calibrated gauges to collect cold-inflation pressure data (the flexing of the sidewalls of tires in motion increases their temperature and leads to inaccurate air pressure readings). These fleet survey data provided the most accurate way to assess the relationship between a motor carrier fleet's target tire pressure and the actual cold inflation pressure of tires in service. The data are considered representative of motor carriers that participate in this type of maintenance program.

Conversely, no archival data from tire suppliers was available for tires on independent owner-operators' vehicles because owner-operators are generally responsible for their own operating costs. The only way to obtain cold tire pressure data was to collect it

at locations in which owner-operator drivers would be stopped for at least 3 hours, in order for their tires to cool down to ambient temperature. Trucker appreciation events held the most promise for this data collection. TMC assisted in recruiting a group of senior field service engineers who collected owner-operators' tire pressure data at the Walcott (Iowa) Truckers Jamboree and the Reno Truckerfest, both held during the summer of 2001.

A total of 6,086 units (3,261 tractors, 1,300 trailers, and 1,525 motorcoaches) and 35,047 tires (18,039 on tractors, 7,501 on trailers, and 9,507 on motor coaches) were checked, and the pressures recorded. The survey data also noted the type of motor carrier operation (for-hire LTL, for-hire TL, private, and public and private motorcoach).

Tire pressure survey results

The results focused upon four important metrics:

- *Proportion of tires 20 percent or more underinflated.* In general, fleets accept small deviations from the targeted pressure. However, if a tire is 20 percent or more underinflated, it indicates the problem is more serious and is likely the result of inadequate maintenance or quality control procedures. The survey found approximately 7 percent of all tires underinflated by 20 psi or more.
- *Proportion of tires within 5 percent of the targeted pressure.* Higher percentages indicate a well-executed tire maintenance program. It is generally accepted by the trucking industry that a good fleet operator will have 70 percent or more of his or her tires within ± 5 percent of the targeted pressure. The survey found only 44 percent of all tires sampled was within ± 5 psi of their target pressure.
- *Proportion of tires 50 percent or more underinflated.* This degree of under inflation would indicate a major tire failure and would generally be considered a flat tire. The percentage of such tires within a fleet could be an indication of either a tire product or tire-mounting problem or a poor tire inflation maintenance program, as indicated above.
- *Proportion of tires 10 percent or more overinflated.* A high percentage of such tires might indicate that the fleet is systematically over inflating the tires to compensate for lack of a good quality control program. Since overinflated tires also have negative impacts on tread wear, this is not considered a viable strategy.

Other key observations indicated differences among fleet operational categories, as well as among fleet size. For-hire carriers (LTL, TL, and owner-operators) generally reflected better tire inflation maintenance practices than private carriers did. As a group, sampled for-hire carriers had 7 percent of all tractor tires underinflated by 20 psi or more. In contrast, the sampled private carriers had 13.2 percent of all tractor tires underinflated by 20 psi or more.

Fleets with 50 or fewer power units had 19.1 percent of their tires underinflated by 20 psi or more. In contrast, fleets with more than 3,000 power units had only 2.1 percent of their tires underinflated by 20 psi or more. Similarly, motorcoach fleets with fewer than 50 power units had 11.8 percent of their tires underinflated by 20 psi or more, while fleets with over 500 power units had only 2.1 percent of their tires underinflated by 20 psi or more.

Study sample data showed that transit bus operators had better tire pressure maintenance than chartered motorcoach operators did. Only 3.1 percent of transit bus tires were underinflated by 20 psi or more, while 9.4 percent of chartered motorcoach tires were underinflated by 20 psi or more. Additionally, 49.9 percent of transit bus tires were within ± 5 psi of target, compared with only 34.2 percent of chartered motorcoach tires.

Tractors and trailers had a significant challenge with mismatched dual tires. Approximately 20 percent of all tractor dual tire assemblies had tires that differed in pressure by more than 5 psi. One out of four trailer dual assemblies (25 percent) had tires that differed in pressure by more than 5 psi.

SECOND STUDY: COMPARATIVE CONTROLLED TESTING OF TPMS

TPMS can offer safety and productivity benefits to CMV drivers and maintenance technicians. They can warn the driver and maintenance personnel if tire pressure drops to an unsafe level and can provide data to aid in problem diagnosis and resolution. They can alert the driver to a catastrophic tire failure (the loss of a trailer tire may not be noted through noise or vibration). Tires run at proper inflation pressures wear longer and have longer service lives. Systems that automatically maintain tire inflation pressure might offer additional benefits of increased fuel economy, provided they had a high level of reliability, were easy to maintain, and were considered affordable.

The overall objective of this second study was to document the performance, accuracy, and operational characteristics of several leading-edge technological approaches to commercial vehicle TPMS. The study focused on the ability of sensors to provide accurate tire pressure readings, detect both slow and rapid changes in tire pressure, and maintain tire pressure under adverse conditions, including partial failure of the device. The study examined three types of TPMS: dual tire equalizers to balance pressures between tires in a dual installation; tire pressure monitors; and tire pressure maintenance systems to maintain tire pressure at desired levels. The systems were installed on a conventional tractor-trailer combination vehicle and on a motorcoach. All testing was performed under controlled conditions on a high-speed test track at the Transportation Research Center in Columbus, Ohio.

The TPMS selected represented a sample of typical commercially available systems: two tire pressure-equalizing systems, five tire pressure-monitoring systems, and two central tire inflation systems. The systems and the vehicles on which they were installed are listed in Table 1.

Table 1.
TPMS Systems Used in Comparative Evaluation

Technology	Tractor	Trailer	Motor Coach	Recommended System for Testing
Dual Tire Equalizers				
Equalizing Systems #1	X	X		Cat's Eye (Link Manufacturing, Ltd.)
Equalizing Systems #2	X	X		Tire-Knight-S (V-Tech International, Inc.)
Tire Pressure Monitoring Systems				
Direct Monitoring System #1 (valve stem-mounted)	X	X		PressurePro (Advantage PressurePro, LLC)
Direct Monitoring System #2 (valve stem-mounted)			X	Integrated Vehicle Tire Pressure Monitoring (WABCO)
Direct Monitoring System #3 (wheel-mounted)	X	X		Tire-SafeGuard (HCI Corporation)
Direct Monitoring System #4 (wheel-mounted)			X	SmarTire (SmarTire Systems, Inc.)
Direct Monitoring System #5 (tire-mounted)	X	X		eTire (Michelin North America)
Tire Pressure Maintenance Systems				
Central Inflation System #1		X		PSI Tire Inflation System (Arvin Meritor)
Central Inflation System #2			X	Vigia (Gio-Set Corporation)

Dual Tire Equalizers

Tire pressure equalizer systems balance dual tire pressures by providing a pathway for air to transfer between two tires in a dual installation, and they also provide an indication of tire pressure. A pressure-actuated valve connected by hoses to the valve stems of the tires maintains an open position to allow air to flow between the tires when the combined pressure of the two tires is above a preset level (typically 90 psi). The pressure actuated valve closes and isolates the tires during slow leaks or instantaneous air losses (after the combined pressure of the two tires drops approximately 10 psi) to prevent both tires from going flat. A central fill valve incorporated in these devices allows both tires in the assembly to be aired simultaneously. The use of equalizers should improve irregular tire wear (i.e., cupping) caused by pressure differentials between dual tires. Visual indicators are also incorporated in the equalizers to provide the operator with a quick indication of the tire pressure levels during the pre-trip inspection without requiring the operator to perform a manual tire pressure check.

Tire Pressure Monitoring Systems

Tire pressure monitoring systems consist of a valve stem, wheel- or tire-mounted sensor, antennae, receiver, and display unit. The battery-powered sensors mounted on each valve stem, wheel, or tire on the vehicle transmit a radio frequency (RF) signal, which includes the tire pressure data, to an antennae mounted on the vehicle. A receiver, with an integrated electronic control unit (ECU), processes the signal transmitted to the antennae and displays the tire pressure information on a driver's cab-mounted display. The system also includes audible alarms and visible warning lights.

The study team tested five different tire pressure monitoring systems for this project. These included one tire-mounted, two valve-stem-mounted, and two wheel-mounted tire pressure monitoring systems. Figure 1 and Figure 2 display the Tire-SafeGuard and WABCO IVTM TPMS hardware respectively.



Figure 1. Tire-SafeGuard Wheel-Mounted System.



Figure 2. WABCO IVTM Wheel-Mounted/Tire Valve-Stem-Connected.

Automatic Tire Inflation Systems

Automatic tire inflation systems (ATIS) for tires use the air from the vehicle's air compressor that is stored in the air brake reservoirs (tanks) to maintain tire pressure at a desired level. The ATIS are plumbed to the vehicle's secondary reservoir that supplies air to the front brakes. The ATIS do not take air from the primary reservoir that supplies air for the rear brakes (which are responsible for the majority of the braking power of the CMV). These systems are plumbed either through the axle or externally, using a rotary union at the wheel hub. They automatically sense the tire pressures and inflate the tires when air is lost. The benefits of these systems are the elimination of manual tire pressure checks and the ability to continue operating the vehicle with minor air leaks in the tires. ATIS are available for all types of CMVs. In this test, one system was tested on the motorcoach and one was tested on the trailer of a tractor-trailer. Figure 3 shows the detail of the PSI trailer-mounted ATIS, and Figure 4 shows the Vigia ATIS mounted on a motorcoach.



Figure 3. PSI Trailer-Mounted ATIS.



Figure 4. Vigia ATIS Mounted on a Motorcoach.

Test Vehicles and Data Acquisition System

The test vehicles were a 2001 Freightliner FLD tractor, coupled to a 2001 Utility Trailer Manufacturing Co. 2000S tandem axle flatbed semi-trailer, and a 2003 MCI motorcoach. To acquire highly accurate pressure and temperature measurements (i.e., to establish "ground truth" against which readings from the various test articles could be compared), laboratory grade sensors were installed at each test wheel position. This required removing the wheels, machining replacement wheels for mounting thermocouples and pressure taps, and routing wire bundles to the data acquisition system (DAS) mounted in the cab of the truck and motorcoach. Figure 5 shows the installation location of each of the instrumentation packages on the tractor-trailer and motorcoach.

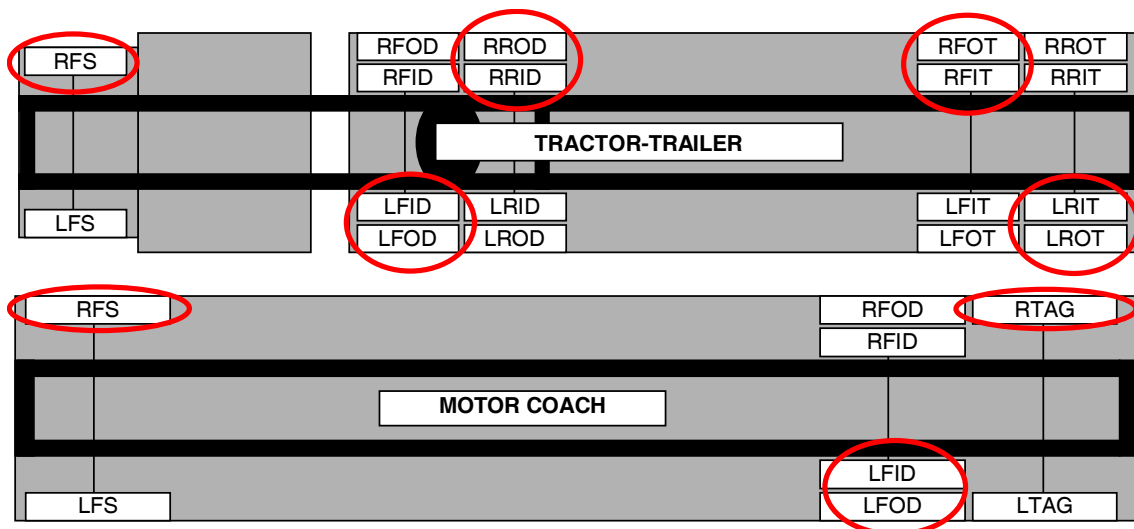


Figure 5. Tractor-Trailer and Motorcoach Instrumentation Package Location.

Additional test equipment consisted of: internal tire temperature thermocouples (nine, analog); tire pressure transducers (two, analog); custom-fabricated dual-flow combination rotary union and slip ring assemblies (five); a custom-fabricated pressure control manifold; primary and secondary brake reservoir and treadle valve pressure transducer (three, analog); a digital marker switch for the test driver's use to indicate when a warning was observed; and a digital non-contact fifth wheel. Figure 6 displays the details of the wheel end rotary union instrumentation package.

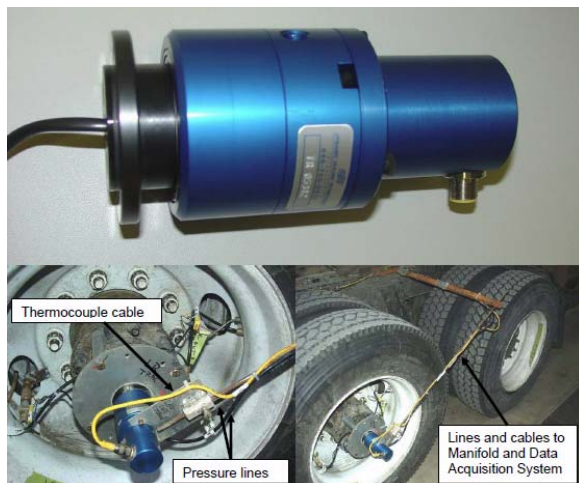


Figure 6. Rotary Union and Wheel Installation Detail.

The failure modes test required that the air brake systems be monitored to determine whether the central tire inflation systems degraded the vehicle's potential braking ability. Therefore, it was necessary to monitor the air brake system pressure at three

points: primary air reservoir, secondary air reservoir, and application pressure. Three pressure transducers, similar to those used for tire pressure monitoring, were spliced in a T into the brake lines at a T serving the primary air reservoir, the secondary air reservoir, and the application pressure gauge line upstream of the gauge.

The DAS was manufactured by Link Engineering Company, Detroit, Michigan. A PC-based laptop computer operated the system, stored data as it was acquired, and performed real-time analyses. The system software supported a variety of interface options, ranging from direct user interaction with the system during measurement to completely autonomous operation based on various pre-programmed trigger events that caused the system to begin data collection. The system was also capable of issuing prompts to a test driver or an instrumentation technician. The Link DAS system received information from 16 individual channels at a frequency of 10 Hz. The average TPMS test lasted about 10 to 30 minutes and generated approximately 5,000 to 10,000 data points. In total, the testing program generated approximately 450 Mb of data.

The test engineer was responsible for manually recording the test identification number and other information, including environmental conditions and tire(s) under test; as well as any specific warnings or indications by the TPMS. This was necessary because TPMS were self-contained and were not connected directly to the Link DAS, as they did not have signal outputs that could be tapped for direct recording.

Test Program

The test program included seven tests:

- *Functionality Test (Static and Dynamic).* This was an overview or shakedown test series, performed to characterize the operational, maintenance, and installation processes for each system.
- *Threshold Warning Level Test.* This test determined the thresholds at which low tire pressure warnings were given. In the case of the ATIS, the test determined the leak rate (psi/min) at which the inflation system could no longer keep pace and a low tire-pressure warning was given.
- *Loaded Test at High Speed.* This test examined the effects of tire heating, due to sustained high-speed driving, on the warning indicator/light of the systems.
- *Failure Modes Test.* This test had two components. For central tire inflation systems, this test determined whether a large or catastrophic air leak depleted the air supply for the pneumatic brakes or forced the system to run continuously, without giving the driver a warning that a tire had lost air. For systems where tires were interconnected (dual-tire equalizing and ATIS technologies), the purpose was to ensure that loss of inflation pressure in a single tire did not affect the interconnected tires.
- *Disablement Test.* This test determined the system's ability to provide a warning or advisory when it was disabled, either by an intentional act or because of a failure of a system or component.
- *Operator Interface Evaluation.* This test was a qualitative evaluation of the effectiveness of the driver interface.
- *Gate Reader Evaluation.* This test evaluated the performance and reliability of the drive-thru gate readers, used with tire-mounted monitoring systems. The objective was to determine the speed and consistency of the gate readers in capturing pressures of all 18 tires on the tractor-trailer.

Results of Comparative Tests

In general, all of the tested valve-, wheel-, or tire-mounted systems exhibited base-level functionality as specified by the manufacturer of the individual systems. The tire pressure values were generally accurate to within two to three psi of the values measured by calibrated pressure transducers.

Low-pressure warning thresholds were factory set on some systems but user-configurable on others. For those systems with factory settings, different warning levels, ranging from 12 to 25 percent below target pressure, were observed. All tested systems were generally within a 2- to 3-psi range of the expected warning threshold.

Many of the tested TPMS used RF communications to transmit data between the sensors and the display unit or ECU. The relatively long length of typical CMVs meant that additional on-board antennae were required for some of the systems to receive the sensor signals from trailer or tag axle tires. Disconnected or damaged antennae could lead to signal loss from the sensors.

The dual tire equalizer systems functioned as designed under both static and dynamic conditions, and they were found to be effective in balancing the pressures between the two connected tires. Figure 7 and Figure 8 show the equalization system balancing tire pressures under static and dynamic conditions respectively. The two systems tested prevented a total loss of pressure in one or both tires in every failure mode implemented, effectively isolating an intact tire from the adjacent tire with an artificially induced major air loss. Similarly, in a disablement test where a hose was cut to simulate damage from road debris, one tire of a dual installation sustained a total loss of air while the other tire was protected by a check valve. Figure 9 and Figure 10 demonstrate the effectiveness of the equalizer in isolating a slow and fast leaking tire from an intact tire.

Both tested equalizer systems included a visual indicator that provided a gross indication of whether tire pressure was within its target range. However, if the pressure fell below this range, they only showed a "low" pressure condition and did not indicate the extent of underinflation. Finally, although the indicators provided a good visual indication of tire pressure, they could be difficult to read as they were mounted on the wheel and could become obscured by dirt.

Despite their relative ease of installation, valve-stem-mounted TPMS had several limitations. When tire temperatures increased during high-speed driving, not all of these systems compensated for the related

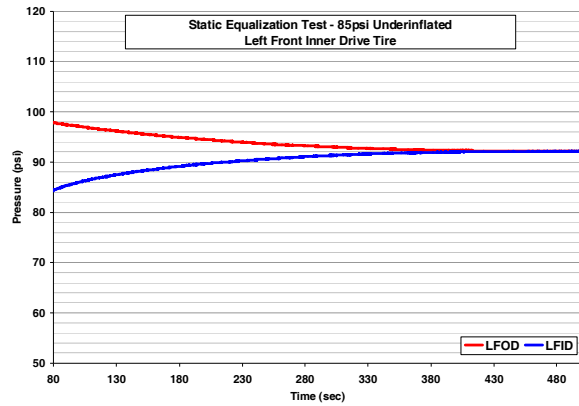


Figure 7. Static Equalization Test.

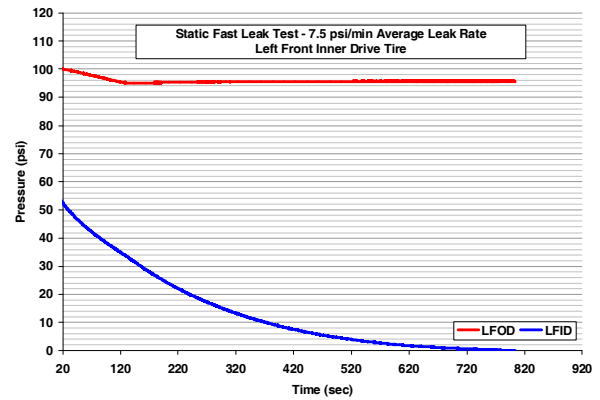


Figure 10. Equalizer Static Fast Leak Test.

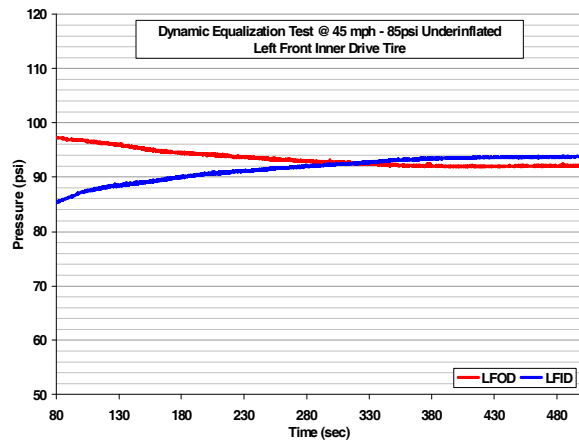


Figure 8. Dynamic Equalization Test.

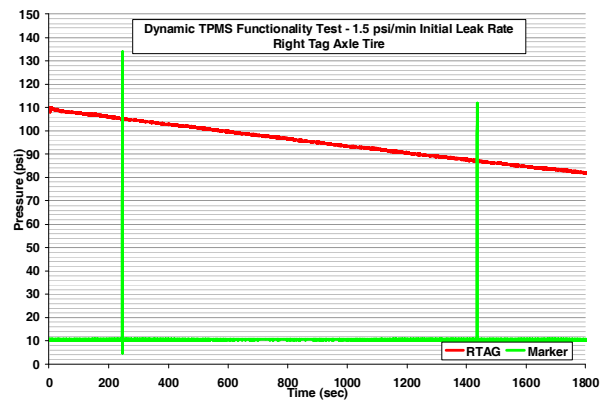


Figure 11. Initial Low Pressure Alarm and Second Critical Pressure Alarm Points.

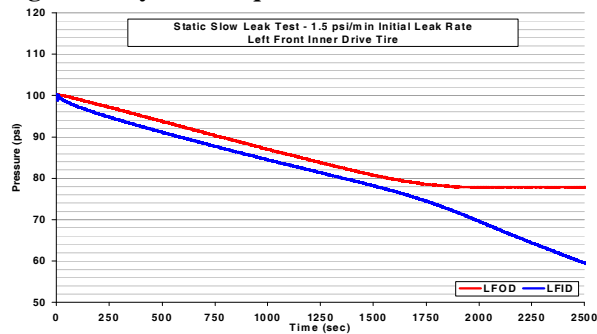


Figure 9. Equalizer Static Slow Leak Test.

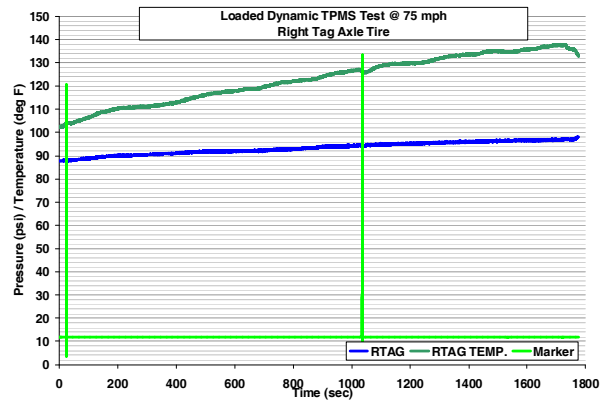


Figure 12. Initial Low Pressure Alarm and Point of Low Pressure Alarm Reset.

increases in tire pressure. One of the two tested systems in this study provided temperature compensation. One of the tested systems initiated a warning when the pressure fell below a preset value (~20 percent below target). Figure 11 shows the two alarm points on a wheel-mounted TPMS as the pressure in the tire bleeds down. However, the warning remained active until the tire was inflated to a higher value (~15 percent below target). This pressure band between the alarm pressure and alarm deactivation pressure prevented intermittent warnings to the driver. Lastly, valve-stem-mounted systems were susceptible to loss because they had to be removed during wheel mounting and dismounting for vehicle maintenance and inspection. Their relative ease of removal could also make them susceptible to theft.

With respect to wheel-mounted TPMS, product literature asserted that wheel-mounted technology included temperature compensation and typically provided the best performance in correcting for tire temperature. However, during the high-speed test sequences, both evaluated wheel-mounted systems had their active warnings disabled when tire pressure increased because of increased tire temperature. This occurred intermittently in various test runs and on different axles. Figure 12 shows the point where a low pressure alarm was cancelled due to increasing tire temperature causing a corresponding increase in tire pressure. However, the test data suggested that the systems were generally able to compensate for large increases in tire temperature (greater than 20 degrees Fahrenheit), but were less able to compensate when the temperature increases were lower. Increasing tire temperatures could prevent a low-pressure warning from being generated. In addition, the team found that the wheel-mounted technologies could be vulnerable to damage during tire mounting and dismounting.

The evaluated tire-mounted TPMS included temperature compensation. A handheld reader displayed both the temperature-corrected pressure and the uncorrected pressure at ambient tire temperature. This system was the only one that required the use of a handheld or gate reader to inspect tires. No in-cab display was available. Figure 13 shows the hand reader in the charger and download docking station.

The gate reader clearances were very tight and required very slow vehicle speeds, less than five mph. However, this particular system was unique among those tested in that it was linked to an Internet-based tire maintenance and tracking database

application hosted by the system manufacturer. Figure 14 and Figure 15 show the eTire tag and installation tools respectively.



Figure 13. eTire Handheld Reader.

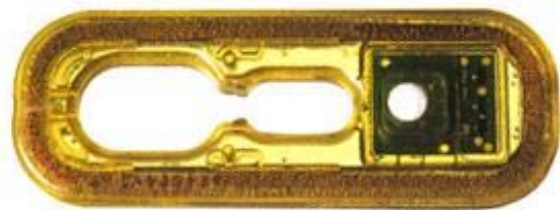


Figure 14. eTire Tire Tag.



Figure 15. eTire Mounting Patch and Installation Tools.

In general, the ATIS performed as designed and specified by the manufacturers and performed well in both static and dynamic conditions. Figure 16 displays the rate of inflation of the trailer-mounted ATIS from various initial inflation pressures. In the leak rate tests, the motorcoach ATIS was able to keep

up with leak rates up to 5 to 8 psi/min. Ultimately, this system's performance was limited by the vehicle's air compressor duty cycle and the compressed air supply and storage system design. The ATIS tested on the trailer could maintain adequate tire pressure with slow leakage rates (less than 1.0 psi/min) but did not maintain adequate tire pressure for higher leakage rates. This system appeared to be limited by its rate of airflow to the tires more than by a limitation of the onboard compressor and air system. Figure 17 shows the ability of the trailer-mounted ATIS to maintain pressure at various leakage rates.

During testing with heavy braking and simultaneous tire leaks, the vehicles' primary and secondary air reservoir pressures remained above the level required for safe brake operation. The compressor had no difficulty recharging the reservoirs without having to run continuously. Figure 18 shows the trailer-mounted ATIS maintaining pressure in the primary and secondary reservoirs during brake snub maneuvers with a leaking tire. Both tested ATIS protected the intact tires from deflating when a catastrophic air leak was simulated in one of the other tires in the system. In this regard, the systems functioned in a manner similar to the dual tire equalizers isolation circuits. Figure 19 shows the motorcoach-mounted ATIS maintaining pressure in a tire with a significant leak while operating at highway speeds.

Vehicle air systems are not optimized to support an ATIS with very high leakage rates; therefore, the functionality of the ATIS was often limited by the vehicle's air system. Additionally, there may be some long-term impact to the CMV's air system when subjected to a high leakage rate from the secondary reservoir, which the ATIS utilizes for its supply air. These leak rates would cause an increase in the duty cycle of the compressor and would increase maintenance requirements and decrease compressor service life.

Installation time for systems varied. In general, valve-stem-mounted TPMS and dual tire equalizers were less time consuming to install (generally, several hours), followed by wheel-mounted TPMS, tire-mounted TPMS, and ATIS that required up to a full day for installation.

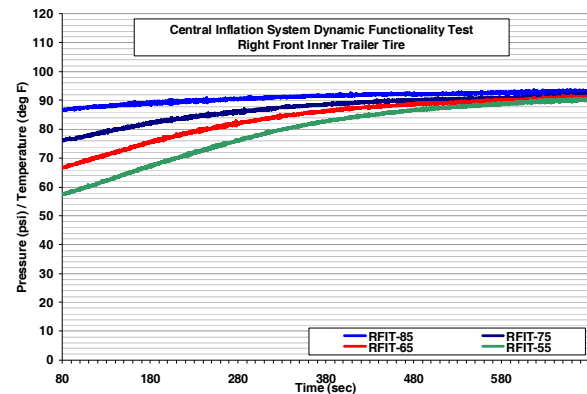


Figure 16. Trailer-mounted ATIS Static Inflation From Various Initial Pressures.

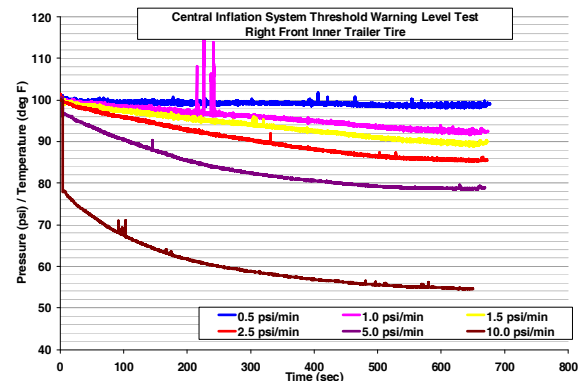


Figure 17. Trailer-Mounted ATIS With Various Leak Rates.

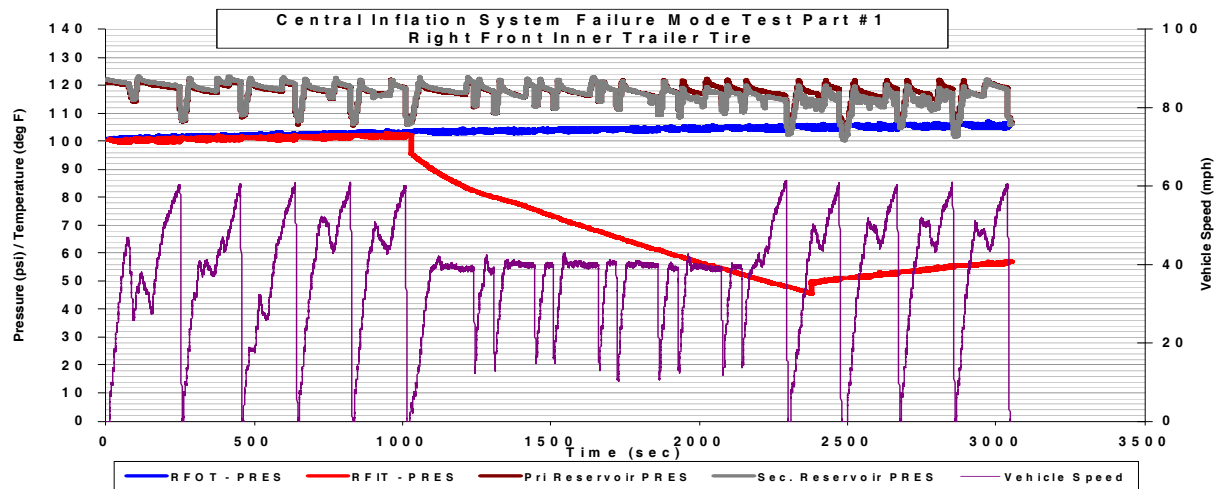


Figure 18. Trailer-Mounted ATIS Brake Snubs With Tire Leak.

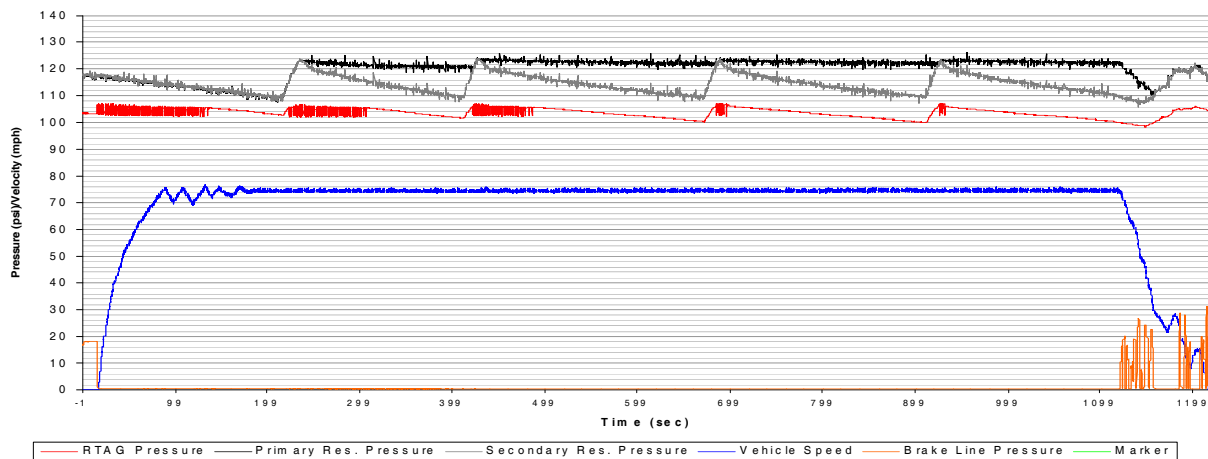


Figure 19. Motorcoach-Mounted ATIS Tire Leak at Highway Speed.

THIRD STUDY: TPMS MINI-FIELD OPERATIONAL TEST

The third study focused upon evaluating TPMS in a fleet setting. The study team sought to identify a commercial fleet operator (or host fleet) with characteristics that would allow for effective and fair evaluation of systems and technologies. These criteria included: an operating environment and duty cycle that could be considered severe for brake and tire wear; homogeneity of the fleet in terms of vehicle type, make, and model; consistency of operations within the fleet relative to driver assignments, routes, mileage accumulation, and maintenance operations; and a strong commitment by the host fleet in evaluating these systems in a controlled study for possible implementation in its own fleet.

The host fleet selected was the Washington Metropolitan Area Transit Authority (WMATA).

WMATA operates approximately 1,500 buses in the metropolitan Washington, D.C. area. Transit bus platforms were selected for this field test because their severe urban, stop/start duty cycle leads to accelerated brake and tire wear (thus challenging the sensor systems.) In addition, the fundamental brake and tire designs were very similar to a conventional tractor, thus allowing the results of this study to be extended to heavy-duty (class 8) trucks.

The test fleet consisted of 12 Orion VII series, 2005 model year, urban transit buses. The buses were a “low floor” design, 40 feet long and 102 inches wide, and operated on compressed natural gas. Each bus’s gross vehicle weight rating was 42,540 pounds. The passenger capacity was 41 seated and 36 standing passengers for a total of 77 passengers. The curb weight of the buses was 30,990 pounds.

The study team evaluated three TPMS (as well as three brake performance monitoring systems, as discussed in the companion paper) on 12 heavy-duty urban transit buses in revenue service for a period of 1 year. A control fleet of 12 identical buses was operated in a similar manner and used for comparison. A maintenance garage located in Arlington, Virginia was selected as the test site, based on the availability of buses of a consistent age and operating environment and because of the experience and low turnover of the maintenance staff. With the assistance of WMATA and TPMS system vendors, the study team retrofitted the candidate systems on the buses at the garage. The buses operated in an area covering approximately 300 square-miles south and west of Washington, D.C. The majority of miles were accumulated in an urban environment with minimal high-speed highway travel. The buses averaged 16 miles per hour in revenue service and were driven an average of 129 miles per day.

Over the course of the 12-month evaluation period, the systems were inspected weekly; and system data was downloaded as part of the test program. Additional data were collected in conjunction with WMATA's various maintenance inspections, which included a safety inspection every 3,000 miles and a comprehensive preventative maintenance inspection every 6,000 miles. WMATA staff recorded all maintenance and fueling activities and entered the data into a maintenance management database. This information was made available to the study team for evaluation. At the conclusion of the test, maintenance staff were interviewed about their experience operating and maintaining the systems. Other than the standard data-recording capabilities of the candidate systems, no additional (or special-purpose) data-logging devices were added to the vehicles. The system status displays were located out of the drivers' view per the request of WMATA fleet managers. The study team and WMATA technicians were responsible for monitoring the systems' display status. This was done to limit driver distraction, as well as to reduce the incidence of operators ceasing bus service because of information from the displays. Limiting vehicle-related information to the bus driver (system diagnostic information, dash-mounted warning lights, and fuel gauge readings) is common in the transit industry.

Three TPMS were installed in the test vehicles:

- *The WABCO Integrated Vehicle Tire Pressure Monitoring (IVTM) System* was developed in conjunction with Michelin and launched in the CMV industry in 2003. Each tire and wheel assembly is equipped with a sensor that attaches to the valve stem and is secured to the rim by two lug nuts. A pneumatic hose runs between the sensor and valve stem. Tire inflation pressure and temperature data are wirelessly transmitted to an ECU on-board the vehicle.
- *The HCI Tire-SafeGuard System* consists of pressure and temperature sensors, a transmitter, and a driver's display. The measurement sensor is strapped to the wheel inside the tire. Data are transmitted wirelessly, similar to the WABCO system.
- *The Michelin eTire System* for CMVs was introduced by Michelin North America in October 2002. The system includes an RF transmitter, pressure and temperature sensors, and an antenna, all of which are encased in impact- and heat-resistant plastic. The passive pressure and temperature sensors (which do not require batteries) receive power via RF transmissions from an external reader device. The eTire unit mounts to the inside sidewall of the tire via a molded rubber dock that chemically cures to the tire's sidewall. The system is designed to work with a tire pressure gate reader but can also be used with a handheld reader.

Results of Field Operational Test

To evaluate the performance (or accuracy) of the TPMS, manual tire pressure measurement readings were taken once a week on each bus and then compared with pressures as reported by the TPMS at the time of the manual measurement. Each bus was inspected approximately 56 times throughout the course of the test, resulting in a total of 3,714 tires inspected. Occasionally, certain buses were unavailable for a weekly inspection because a test bus was mistakenly put into service or a bus was removed from service and awaiting maintenance. Not all of the inspections yielded valid comparisons because of problems with the TPMS systems themselves or, in a few instances, because of problems associated with manually checking the tires.

Key observations related to the on-board monitoring systems include the following:

- The TPMS provided accurate tire inflation pressure data when compared to measured (tire-gauged) values. System sensors were found to be consistent and reliable in reporting tire inflation pressures. On average, the systems reported false positives (a false low-pressure reading) 6 percent of the time or false negatives (a missed low-pressure reading) 2 percent of the time. The more frequent issue, found in 17.6 percent of inspections, was “no reads,” resulting from missing sensors and sensors in the wrong wheel location.
- Keeping track of the individual wheel/tire sensor units themselves was a significant challenge during the field test. This logistical challenge arose because of the high frequency of tire changes. The sensor mounting locations were out of view of technicians and the lack of fleet-wide training on system awareness and operation accounted for lost or discarded sensors. Training was limited to the host depot, but occasionally tire and brake maintenance would occur at other depots. Training across the entire system would be required to prevent technicians from misplacing and inadvertently discarding sensors.
- The durability of two TPMS sensor designs was initially challenged by operating in transit service. Failures occurred with the wheel-mounted sensors just 2 months into testing. Excessive heat build-up caused the sensor housing to become brittle, crack, and fail. The sensor manufacturer provided a design change that consisted of an isolating pad on the bottom side of the sensor that contacted the wheel rim. This simple solution prevented further failures of this type from occurring. Failures also occurred with the sensors that adhere to the tire sidewall. Specifically, the plastic casings on these sensors were found to crack within the first few months of operation. The cracked sensor casings were determined to be caused by a manufacturing batch defect. Replacement sensors were found to be significantly more durable.
- An improvement in adherence to targeted tire pressures was not found on the test fleet compared to the control fleet. This may be because WMATA takes a pro-active role in maintaining target inflation pressures to comply with the tire vendor’s warranty. Average tire inflation pressure was 111 psi for both the test and control fleets (target pressure: 115 psi). Tire life and fuel economy were also similar in both fleets. This was likely the case because the real

time display of tire pressure readings was purposefully not made available to drivers but only to maintenance personnel and technicians. Therefore, drivers could not act immediately on such information to correct any tire pressure problems that may have been detected. In most commercial truck fleets, such real time information would have been provided to drivers; and drivers would have had the opportunity to act on the information as needed (for example, if low pressure was detected, adding air to tires at the next convenient time) thereby improving the average tire life and fuel economy of the fleet.

- Two tire blowouts could have been prevented during the course of the field test had the TPMS displays been visible to the bus operators. To maximize safety and operational benefits, system data need to be available to the driver in real time, as well as to maintenance staff.
- Technicians preferred the wheel-mounted tire pressure sensors for two reasons: (1) they were easier to install, and (2) tires could be changed without removing or disconnecting the system. Conversely, the technicians found valve-stem-mounted sensors difficult to connect to the inner tires on a set of duals. This issue may be unique to buses because the wheels and tires are surrounded by the structure of the vehicle. Tire-mounted sensors required more time to install (versus wheel- or valve-stem-mounted systems) because of the required tire surface preparations.

CONCLUSIONS

Tire pressure maintenance has been a significant and persistent problem for operators of CMVs. After brakes, tires are the most expensive maintenance item for fleets and the most common vehicle-related defect cited in crash reports. Tire deficiencies are the second-ranked reason for CMVs to be cited for defects during roadside inspections. A collection of tire pressure readings from over 35,000 tires provided the first large-scale source of tire inflation readings in the United States. A series of controlled test-track assessments of nine TPMS, representing the three types in the commercial marketplace, provided a comprehensive comparison of the characteristics and operation of these systems and suggested opportunities for improving their usability and performance. A 12-month field operational test of three monitoring-type TPMS provided information on tire pressure status that was useful for improving maintenance practices and detecting low tire pressures to perform timely repairs. This information had a significant impact on inspection practices and

enhanced the overall efficiency of operations at WMATA. While no firm procurement commitments were made, WMATA maintenance managers indicated that they would consider using one or more monitoring technologies on new vehicle procurements and the retrofit of existing buses. A study to test the TPMS technologies on commercial tractor-trailer fleets is currently underway.

REFERENCES

Kreeb, R. M., B.T. Nicosia, and P.J. Fisher, "Commercial Vehicle Tire Condition Sensors." Report FMCSA-PSV-04-002, November 2003.

Brady, S., B. Nicosia, R. Kreeb, and P. Fisher, "Tire Pressure Monitoring and Maintenance Systems Performance Report." Report FMCSA-PSV-07-001, January 2007.

Van Order, D., D. Skorupski, R. Stinebiser, and R. Kreeb, "Fleet Study of Brake Performance and Tire Pressure Sensors." Performed under Contract DTFH61-99-C-00025, Task Order 9, July 2005 – July 2008. Report forthcoming from FMCSA.

EFFECTIVENESS OF SEAT BELT USAGE ON THE ROLLOVER CRASHWORTHINESS OF AN INTERCITY COACH

Mehmet A. Güler

Department of Mechanical Engineering, TOBB University of Economics and Technology

Ali O. Atahan

Department of Civil Engineering, Mustafa Kemal University

Bertan Bayram

Research and Development, TEMSA Global

Turkey

Paper Number 09-0205

ABSTRACT

Safety of vehicle occupants jeopardized during rollover accidents when necessary safety measures are not taken. Structural adequacy and protection of occupants are the two significant measures that can be implemented to minimize occupant injury risk during vehicular rollover events. The aim of this paper is to evaluate the structural resistance and passenger injury risks and compare the effectiveness of safety belt usage in occupant during a simulated rollover event of a 13 meter long TEMSA bus. A total of eight occupants were placed at the structurally weakest locations of the bus. Three different occupant protection cases were considered: i. no safety belt, ii. two-point safety belt and iii. three-point safety belt. A standard rollover procedure was simulated using non-linear finite element code LS-DYNA. Head injury criteria and neck forces were calculated and compared to evaluate the effectiveness of seat belt usage on occupant protection. Simulation results clearly illustrated that when occupants had no seat belt protection they suffered serious risk of injuries. Moreover, two and three point safety belts provided somewhat similar protection levels for most of the occupants. Based on the findings, use of two point safety belt in all of the seats of the TEMSA busses was recommended.

INTRODUCTION

The most typical collision configurations involving busses and coaches are side, rear, frontal and rollover. Although rollover crashes did not happen very often, when they did, the number of seriously injured occupants was high compared to other crash types [1]. According to Enhanced Coach and Bus Occupant Safety (ECBOS) project final report [1], granted by the European Union, in the EC, every year 20,000

buses are involved in accidents which results in approximately 300,000 injuries per year. Unfortunately, some 150 of these persons suffer fatal injuries.

In EC, there is a strong movement towards establishing new safety requirements for buses or coaches operated in Europe in order to reduce fatalities. These safety requirements are continuously visited to improve passenger safety in these busses or coaches.

Albertson et al. [2] conducted one of the most comprehensive studies on rollover crash injuries. They analyzed 128 injured in Sweden with regard to the injury outcome, mechanisms and possible injury reduction for occupants when using a safety belt. Other studies found out that when the bus or coach rolls 90° or more, occupants would have high risks of sustaining injuries [3,4]. In fact, Matolcsy [5] collected a rollover accident statistics over 300 accidents which showed that the average casualty rate was 25 casualties/accident.

In case of a rollover, passengers run the risk for being exposed to ejection, partial ejection, projection, or intrusion and thus exposed to a high fatality risk [5,6]. However the most dangerous one is the intrusion, when due to the large scale structural deformation structural parts intrude into the passenger, or compress them (lack of the strength of superstructure) [5].

The difference for a bus or coach passenger, with respect to biomechanics and space, as compared to those of lighter vehicle passenger becomes obvious in a rollover crash. During a bus or coach rollover, the occupant will have a larger distance from the center of rotation as compared to that of a car occupant. For this reason, European regulation "ECE R66" titled "Resistance of the Superstructure of Oversized Vehicles for Passenger Transportation" is

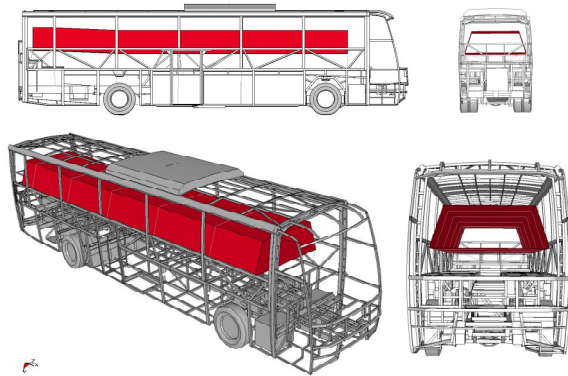


Figure 1. Placement of residual space in a bus.

in force to prevent catastrophic consequences of such rollover accidents thereby ensuring the safety of bus and coach passengers [7]. This regulation prescribes a test to be chosen between one of the following kinds

- A complete bus rollover test
- A bay section rollover test
- A pendulum test
- A numerical simulation of rollover.

The use of prototype to verify the design changes and doing real rollover, bay section or pendulum tests are often unsuitable because of the high costs and time. Therefore, among the alternatives, utilization of the numerical simulation is becoming more appealing to researchers. Friedman et al. [14] investigated using fiber-epoxy composite roof pillars under rollover (FEM). (FEM). In all of the above cases for the Regulation ECE R66 the effect of added mass of the passengers are not considered. The effect of passenger weight on the rollover crashworthiness is investigated by Guler et al. [15]. Results of that study shows that busses built with the current regulation does not comply if the passenger weight is considered. In another study by Belingardi et al. [16] FEM approach has been used to study the structural behavior of a M3 bus in a rollover accident and evaluate the structure resistance and passenger injury risks. In that study, only a bay section has been modeled with rotation axis parallel to the longitudinal bus axis. They also showed that the numerical analysis has given prominence to the inadequacy of the actual European regulation (ECE66), concerning passive safety.

METHODOLOGY

In this paper, results of a numerical rollover investigation study involving TEMSA bus with occupants are presented. FEM was used to construct a 12.8 m long bus with stainless steel material and special reinforced roll bar structure in the front and in the most rear. The FEM of the bus is developed by the specialized pre-processing software ANSA 11.3.5. and calculations are made using a non-linear, explicit, three dimensional, dynamic finite element computer code LS-DYNA. To verify the accuracy of the bus FEM, a series of laboratory tests were performed on a breast knot of side-body and on a roof edge knot of the vehicle and compared with those obtained from subsequent numerical simulations. A high degree of theoretical and experimental correlation was obtained, which partially confirmed the validity of bus FEM. Once the component validation process completed, a complete vehicle rollover test simulation was carried out. The finite element model in this study consisted of a validated vehicle [15] and occupant models. LS-DYNA Hybrid III dummy models were used as occupant models and are seated in 4 double seats located in critical places by considering structurally weakest sections of the bus.

The rollover simulations performed are intended to determine the damage mechanics and potential injury risks of the dummies. Three different occupant protection cases were considered: i. no safety belt, ii. 2-point safety belt and iii. 3-point safety belt. In each case head and neck injury criteria were used to evaluate the effectiveness of seat belt usage on occupant protection.

The ECE R66 Regulation

The purpose of the ECE R66 analysis is to ensure that the superstructure of the vehicle has the sufficient strength that the residual space during and after the rollover test on complete vehicle is unharmed. That means no part of the vehicle which is outside the residual space at the start of the test (e.g. pillars, safety rings, luggage racks) are intruding into the residual space. As shown in Figure 1, the envelope of the vehicle's residual space is defined by creating a vertical transverse plane within the vehicle which has the periphery and moving this plane through the length of the vehicle.

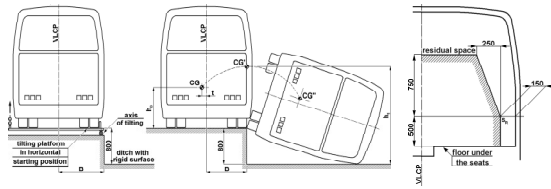


Figure 2. Details of rollover test according to ECE R66 [7]

The rollover test is carried out on that side of the vehicle which is more dangerous with respect to the residual space (see Figure 2). The decision is made by the competent Technical Service on the basis of the manufacturer's proposal, considering at least the following: i. the lateral eccentricity of the center of gravity and its effect on the potential energy in the unstable, starting position of the vehicle, ii. the asymmetry of the residual space, iii. the different, asymmetrical constructional features of the two sides of the vehicle, and iv. which side is stronger, better supported by partitions or inner boxes (e.g. wardrobe, toilet, and kitchenette).

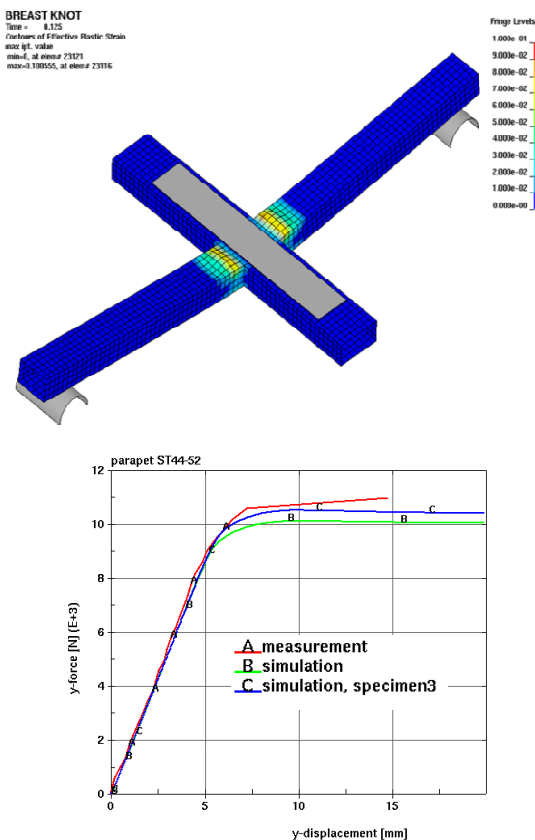


Figure 3. LS-DYNA simulation results for breast knot subassemblies



Figure 4. Test arrangements for breast knot and special roof profile subassemblies

Verification of Calculation

Before starting the ECE R66 simulation and certification process, a verification of calculation procedure set forth by the regulation ECE R66 was performed. Two separate specimens (breast knot and roof edge knot extracted from the vehicle) were prepared and sent to TÜV Automotive for experimental investigations. These parts were subjected to certain boundary conditions and quasi-static loads at TÜV's testing facility [17]. The same subassemblies were also modeled and simulated using LS-DYNA. Force-deflection curves obtained from both the experiments and simulations were compared and a good correlation between experiment and simulation results was obtained (see Figure 3 and Figure 4).

Description of the Computational Model

FEA model of the full vehicle (with seats) was comprised of 770,404 number of nodes, 785,940 first order explicit shell elements, 153 beam and 51,460

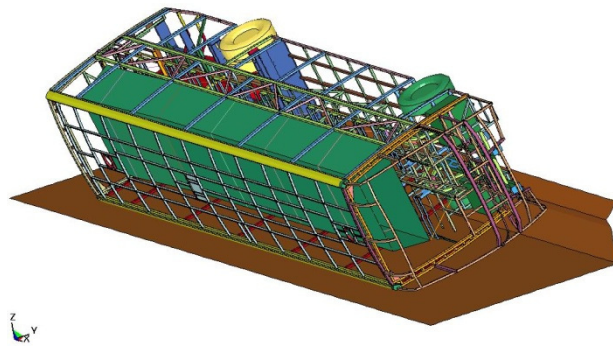


Figure 5. Finite Element Model of the whole bus rotated about the ground contact position

mass elements (see Figure 5). Element length is assigned to be 10 mm in the critical regions (A verified assumption coming from the verification of calculation) and for the regions under the floor (lower structure-chassis) element length up to 40 mm was used. The number of elements per profile width is at least 3 for the upper structure whereas the number of elements per width is 4 for side wall pillars which are significant for rollover deformation.

All deformable parts were modeled with the 4-node Belytschko-Tsay shell elements with three integration points through the shell thickness [18]. The shell element formulation is based on Belytschko-Lin-Tsay formulation with reduced integration available in LS-DYNA [19]. This element is generally considered as computationally efficient and accurate. The shell element that has been, and still remains to be, the basis of all crashworthiness simulations is the 4-noded Belytschko and Tsay shell. Upon completion of mesh generation of bare structure, masses were imposed according to a certain methodology. First, a list of masses of the vehicle was prepared. The engine, gearbox, air conditioner and fuel tank were roughly 3D modeled as rigid parts, the inertias were calculated analytically and mass and the inertia was imposed on a representative node (on the approximate center of gravity points for the relevant part) of these parts. The axles were modeled with rigid truss elements and the mass and the inertias were imposed using the same method. The masses particularly located were imposed by using mass elements. The distributed masses were imposed by changing the density of the related region. Further details on bus FEM can be obtained from the study by Guler et al. [15].

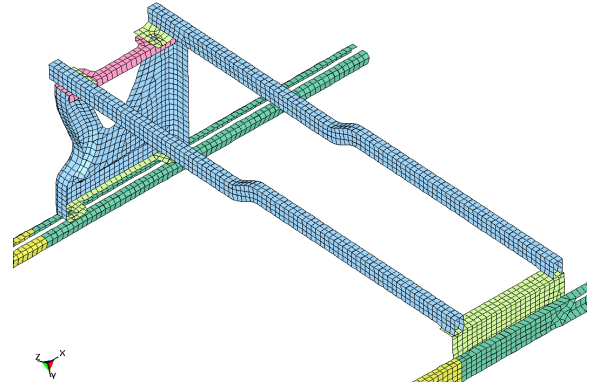


Figure 6. FEA Model of the seat structure

To model the seat structure, the geometry of the seat base was constructed using shell elements. The seat structure was connected to the floor elements located below using spotweld option in LS-DYNA. This option represented the closest approximation to an actual bolted connection due to its properties, such as bolt failure. A detailed representation of the spotwelds and finite element mesh of the seat structure is shown in Figure 6.

The Center of Gravity (C.G.) of the vehicle was measured using a test platform in TEMSA. The measured values were in a good agreement with the ones coming from the finite element model of the bus. To exactly match the measured and calculated C.G.'s, the C.G.'s of engine, gearbox and the axles were fine tuned in the model.

For obtaining the material data, tension tests were applied on several specimens at TÜV Automotive facilities. The true stress-strain curves were obtained and imposed in LS-DYNA accordingly. The material model for the deformable structure in LS-DYNA is the so called "MAT Type 24, Piecewise Linear Isotropic Plasticity model" [20]. This is an elastic plastic material model which uses the Young's Modulus if stresses are below the yield stress and the measured stress-strain-curve if the stresses are above the yield stress. Rigid parts (engine, gear box, fuel tank, axles, etc.) are modeled with the so called Rigid Material, MAT Type 20. For the definition of the survival space (residual space) "MAT Type 9, Null Material" is used.

Hybrid III 50th percentile dummy was used to represent passengers riding in the bus during a rollover accident. Dummy is a completely deformable finite element model (see Figure 7) and detailed information about the dummy can be found

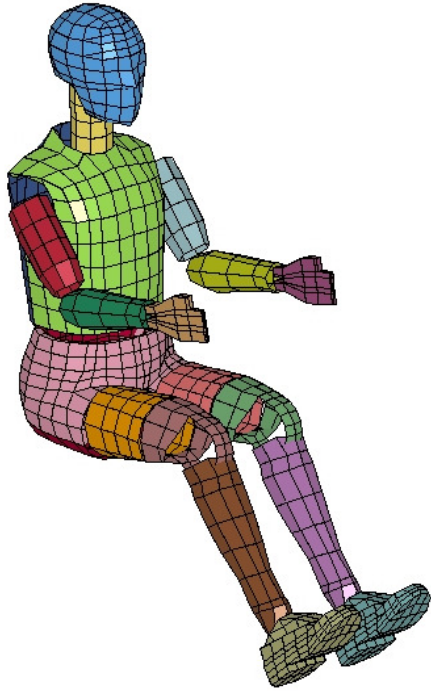


Figure 7. Hybrid III Dummy

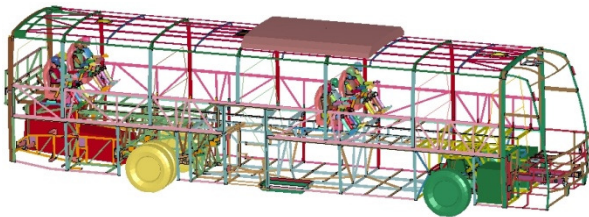
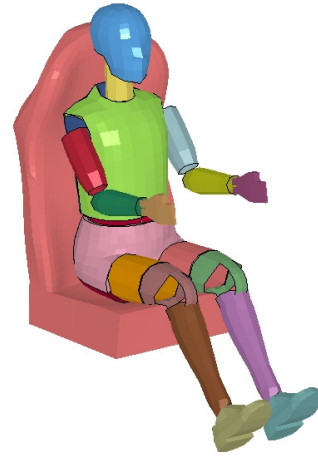


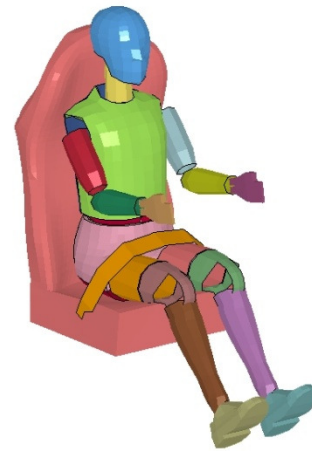
Figure 8. Positioning of Dummies in the bus structure

in [21]. A total of eight dummies were used in the rollover analysis. The dummies were placed in the weakest sections of the bus as shown in Figure 8. These locations were determined from the past experiences of the rollover study. The dummy positioning into the seats was done automatically using LS-DYNA.

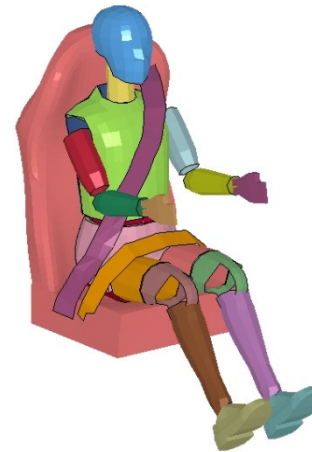
Two types of seat belts evaluated in this study are: two point or lap belt and three point or shoulder belt (see Figure 9). The top end of the seat belt near the shoulders of the dummy was positioned so that it fits the contours of the chest and the upper body of the dummy whereas the lap belts positioned to fit the contours of the thigh.



(a)



(b)



(c)

Figure 9. Finite Element Model of the dummy, seat and seat belt; (a) No seat belt; (b) two-point or lap seat belt; (c) three-point seat belt

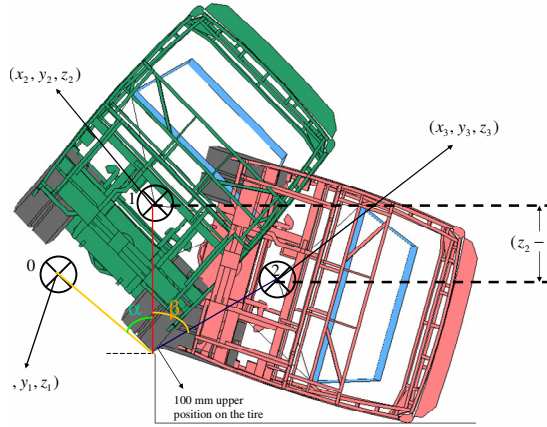


Figure 10. Rotation of the bus to the ground contact position

LS-DYNA Solution procedure

The solution procedure in general is described as follows: The total energy according to the formula indicated in the ECE R66 regulation:

$$E = 0.75Mgh \quad (1)$$

where, E is the total energy, M is the unloaded curb mass of the bus structure, g is the gravitational acceleration and $h = \Delta z = z_2 - z_3$ as shown in Figure 10. This energy is applied to the structure by applying a rotational velocity to all of the deformable and rigid parts of the vehicle. h is the vertical distance between the C.G. of the vehicle at free fall position (z_2) and the C.G. of the vehicle which is kinematically rotated up to the ground contact position (z_3).

First, the model is rotated around x axis until the mass center of the whole vehicle reaches its highest position. At this point the coordinate of the C.G. in the z direction is recorded. Then, the bus is rotated around the 100 mm obstacle until the vehicle contacts the ground (an offset is left considering the shell thickness of the ground and the corresponding vehicle structural part). The z coordinate of the C.G. at this position is recorded as well. Then, as shown in Figure 10, the vertical distance between these two points is determined and recorded as h .

Initial velocity generation is done with *INITIAL_VELOCITY_GENERATION card in LS-DYNA.

*CONTACT_AUTOMATIC_NODES_TO_SURFACE was used to establish contact between the vehicle super-structure (body-in-white) and the ground. On the other hand, *CONTACT_AUTOMATIC_SURFACE_TO_SURFACE was used between the seat structure and the seat rails on the side-wall and on the sill (see Figure 6). The static friction coefficient between all parts was set to 0.1 and the dynamic friction coefficient was set to default which assumes that it is dependent on the relative velocity of the surfaces in contact. Shell thickness change option in *CONTROL_SHELL is enabled assuming that membrane straining causes thickness change during the deformation. Mass scaling was applied to the smallest 100 elements which resulted in negligible change in overall mass. This provided a significant computational time savings.

The solutions are performed with SMP version of LS-DYNA. The analyses run approximately 12 hours for belted dummies and 20 hours for unbelted dummies on an AIX IBM P5+ series work-station with four P5 processors. Simulations lasted until dummies become stationary. Simulation time was 500 ms for unbelted dummies and 300 ms for belted dummies with results output required after every 5000 time steps..

Head Injury Criteria

The Head Injury Criteria (HIC) is used to assess the risk of injury to the head of bus occupants. This criteria is first introduced by Versace [22] and later modified by modified by The National Highway Traffic Safety Administration's NHTSA. HIC is a commonly used injury criterion for the assessment of the level of head injury risk in frontal collisions. A HIC of 1000 is conventionally accepted as the threshold where linear skull fractures will begin to appear, but NHTSA changed this value to 700 in March 2000 [23]. HIC is calculated as:

$$HIC_{t_2-t_1} = \left[\frac{1}{t_2 - t_1} \int_{t_1}^{t_2} a(t) dt \right]^{2.5} (t_2 - t_1) \quad (2)$$

where $a(t)$ is the resultant linear acceleration at the center of gravity of the head and t_1, t_2 are arbitrary instants of time when head experiences acceleration of deceleration. The HIC was analyzed using 36 ms time interval in this study.

It should be noted that in this study, neck injury criteria was not used. Instead, neck forces obtained from simulation was compared with limit values to assess the severity of neck injury during rollover event.

DISCUSSION OF RESULTS

In order to check the accuracy of the simulation results, the first thing to check is whether the total energy remains constant during the simulation time period. The graph showing various energy distributions obtained from the rollover simulation of the bus structure is given in Figure 11. As shown in this figure, the total energy remains constant which is one of the indications for correct analysis results. It can be observed that the kinetic energy drops and transforms into internal energy (strain energy + sliding energy) over the time and the hourglass energy remains negligible.

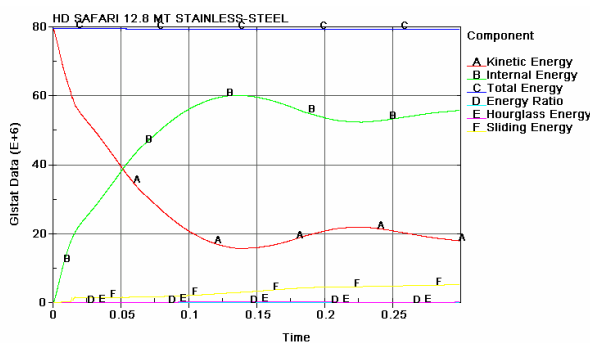


Figure 11. Energy distribution versus time

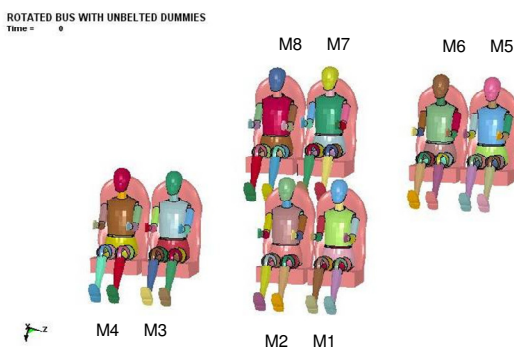


Figure 12. The arrangement of dummies

To clarify the dummy referencing, labels shown in Figure 12 were used. So, the dummies seated in the bus model were labeled from M1 to M8. According to the arrangements, dummies M1 to M4 and M5 to M8 are sitting near the front and back of the bus, respectively.

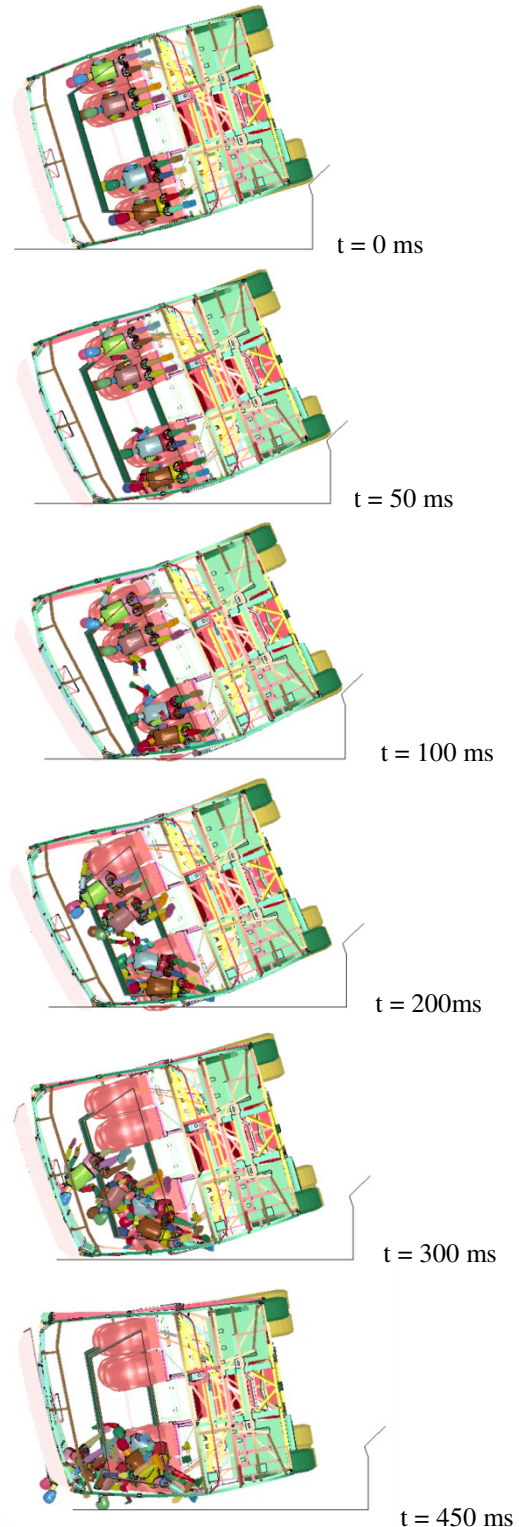


Figure 13 Sequential pictures showing behavior of unbelted dummies during ECE R66 test simulation.

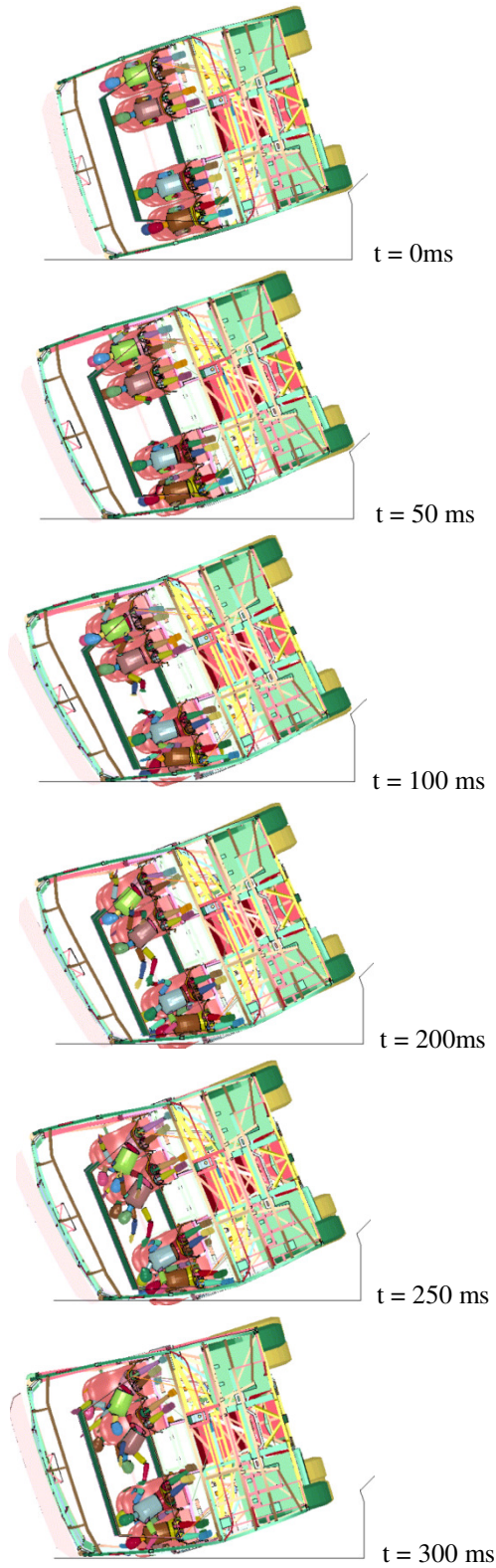


Figure 14 Sequential pictures showing behavior of lap-belted dummies during ECE R66 test simulation.

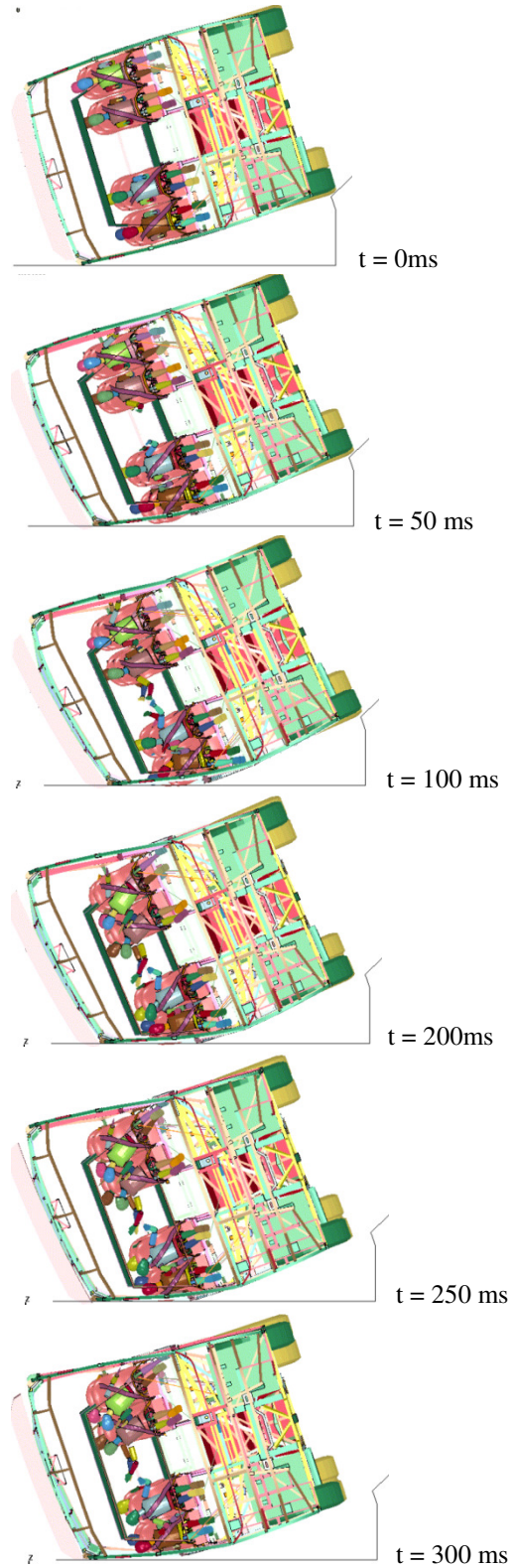


Figure 15 Sequential pictures showing behavior of three-point-belted dummies during ECE R66 test simulation.

Time histories for selected time steps are illustrated are presented in Figure 13 for the unbelted dummies. The rollover behavior is typical such that bus first comes into contact with the ground and then starts absorbing energy by elasto-plastic deformation through bending at the plastic hinge zones. After sufficient deformation occurs the bus starts sliding. Since the dummies are not belted, it is obvious that the dummies M1, M2, M5 and M6 would fly in the space and quite possibly hit either the dummies sitting on the rollover side (Dummies M3, M4, M7 and M8) or hit the luggage compartment or sealing of the bus structure. In reality, a full ejection or partial ejection of passengers occurs which is very common in the rollover traffic accidents. As it can be seen from Figure 14, Dummy M3 first collides with M4 at 150 milliseconds and after that M2 falls down to M3 at 295 milliseconds. The situation is similar for the dummies sitting at the back of the bus. In this case dummy M8 is hit by M7 at 145 milliseconds and M6 falls down to M7 at 290 milliseconds.

Sequential pictures for the two-point or lap belted dummies rollover simulation are given in Figure 14. During the rollover event, the passengers seating near the window from the rollover side (in our case dummy M4 and dummy M8) typically hit their head to the window or side pillars of the bus. As shown in Figure 14, seat belt usage clearly showed positive effect on protecting the passengers. In fact, simulation results showed that passengers seating across the rollover side were prevented from partial or full ejection due to the employment of two-point seat belt.

Finally, time histories of the rollover simulation for three-point belted dummies are presented in Figure 15. In this case neither partial nor full ejection of dummies are observed.

For the standpoint of injury criteria, HIC and neck forces observed during the rollover simulation for the unbelted dummies case are given in Table 1. All of the dummies HIC values are greater than 1000 and neck forces are greater than 4000 N except dummy M3 and dummy M7 indicating series injury of all of the passengers. Dummy M3 is coming into contact with dummy M4 in 150 ms and with dummy M2 in 295 ms. Also Dummy M7 is coming into contact with dummy M8 in 145 ms and with dummy M6 in 290 ms.

For the two-point or lap belted dummies the HIC and neck forces are given in Table 2. Observe that only dummy M8 has a HIC value higher than 1000 due to the fact that it comes into contact with

the ground in 105 ms and dummy M7 is colliding with dummy M8 in 185 ms. Neck forces are in allowable range for the belted dummies.

For three-point belted dummies, HIC and neck forces are given in Table 3. As shown in this table, all of the HIC values and neck forces are within the acceptable limits. The highest HIC value is observed in the dummy M4 due to the fact that it collides with side pillars at 125 ms.

Analysis results showed that the three-point belt usage provided the best occupant protection since it results in the lowest values in terms of HIC. However, as it can be seen from the Tables 2 and 3, wearing the three-point belt generally increases the neck forces during a rollover accident. Since the values of HIC values are in acceptable range for two-point seat belts, wearing two-point seat belts seems to be a good alternative to more complex three-point seat belts.

SUMMARY AND CONCLUSIONS

A state-of-the-art computational nonlinear explicit dynamic analysis was employed to assess the behavior of bus occupants during a rollover event. Vehicle model was partially validated using subassembly experimental data which proved the accuracy of the bus model used in the rollover simulation study according to ECE R66 regulation.

As predicted by the rollover analysis presented in this paper, unbelted bus passengers are in a great risk of partial or full ejection resulting in serious injuries. Simulation results showed that passengers wearing two-point or lap belts are very likely to remain seated during rollover which prevents passengers flying in vehicle and consequently hitting the windows or pillars of the bus structure or other passengers.

Three-point belt usage resulted in the lowest values in terms of HIC. However, three-point belt usage increased the neck forces during a rollover. Since the HIC values obtained from two-point belt simulations are in acceptable range, it is recommended to use two-point seat belts rather than three-point seat belts to achieve improved passenger protection. It should be added also that incorporation of two point belt system into busses are easier and more cost-effective for bus manufacturers. This aspect should also be considered during the manufacturing phase.

Table 1 HIC values and Neck Forces for unbelted dummies

Dummy	HIC36	Neck Forces (N)	Description
M1	2390 @ 0.450 s	6400 @ 0.450 s	Collision with ground @ 450 ms
M2	2170 @ 0.435 s	4800 @ 0.435 s	Collision with ground @ 435 ms
M3	695 @ 0.295 s	2390 @ 0.150 s	Contact with Dummy M4 @ 150 ms and with Dummy M2 @ 295 ms
M4	1280 @ 0.075 s	1070 @ 0.335 s	Contact with side pillar @ 75 ms
M5	2530 @ 0.490 s	5700 @ 0.490 s	Collision with ground @ 490 ms
M6	3200 @ 0.375 s	5200 @ 0.450 s	Contact with side pillar @ 375 ms
M7	460 @ 0.290 s	3200 @ 0.145 s	Contact with Dummy M8 @ 145 ms and with Dummy M6 @ 290 ms
M8	1350 @ 0.095 s	2370 @ 0.235 s	Collision with ground @ 95 ms

Table 2 HIC values and Neck Forces for two-point or lap belted dummies

Dummy	HIC36	Neck Forces (N)	Description
M1	308 @ 0.230 s	1400 @ 0.280 s	No contact
M2	160 @ 0.210 s	1600 @ 0.270 s	No contact
M3	175 @ 0.120 s	1950 @ 0.215 s	No contact
M4	255 @ 0.110 s	2840 @ 0.100 s	Collision of hand with side pillar @ 110 ms
M5	295 @ 0.230 s	1450 @ 0.280 s	No contact
M6	155 @ 0.210 s	1570 @ 0.270 s	No contact
M7	640 @ 0.185 s	2700 @ 0.245 s	Contact with Dummy M8 @ 185 ms
M8	1130 @ 0.105 s	1210 @ 0.135 s	Contact with ground @ 105 ms

Table 3 HIC values and Neck Forces for three-point belted dummies

Dummy	HIC36	Neck Forces (N)	Description
M1	290 @ 0.220 s	1400 @ 0.270 s	No contact
M2	160 @ 0.210 s	1600 @ 0.280 s	No contact
M3	175 @ 0.120 s	2300 @ 0.210 s	No contact
M4	750 @ 0.125 s	3400 @ 0.100 s	Contact with side pillar @ 125 ms
M5	205 @ 0.225 s	1050 @ 0.192 s	No contact
M6	155 @ 0.216 s	970 @ 0.200 s	No contact
M7	225 @ 0.200 s	1750 @ 0.185 s	No contact
M8	345 @ 0.112 s	2450 @ 0.112 s	Belt contacts with the neck of the dummy @ 112 ms

It should be noted that the FEM used in this study did not include the trim parts of the interior of the bus structure. Since the presence of trim parts would have an effect on the HIC values its inclusion in a future study is strongly recommended. Also increasing the number of dummies in the vehicle and using more sophisticated dummies would result more accurate

analysis results. Finally, improvements on seatbelts FEM is recommended for further studies.

The influence of the belted occupants must be considered by adding a percentage of the whole passenger mass to the vehicle mass. That percentage depends on the type of belt system and is 70% for passengers wearing 2-point belts and 90% for

passengers wearing 3-point belts [24]. In authors' earlier study [15], it was shown that adding passenger weight to the bus structure significantly changes the rollover crash scenario increasing the initial kinetic energy of the whole system and causing much more damage than expected to the structure of the bus. Hence for further studies it is recommended that a full passenger's weight must be added to the bus structure or dummies equal to the passenger number must added to the finite element model and authors believe that this should be adapted in the ECE R66 regulation.

ACKNOWLEDGEMENTS

Authors wish to acknowledge Ibrahim Eserce director of R&D division and Kadir Elitok research engineer at TEMSA Bus Company and Ulrich Stelzmann of CADFEM for their contributions to this study. Financial support for this project was provided by TUBITAK TEYDEB project number 3060183.

REFERENCES

- [1] Kirk, R. Grant, (2001),ECBOS Workpackage 1 Task 1.1 "Statistical collection" Final Report, European Union.
- [2] Albertsson, P., Falkmer, T., Kirk, A., Mayrhofer, E. and Bjornstig, U. (2006) 'Case study: 128 injured in rollover coach crashes in Sweden–Injury outcome, mechanisms and possible effects of seat belts', *Safety Science*, Vol. 44, pp.87–109.
- [3] Albertsson, P., Björnstig, U., Falkmer, T., (2003). The Haddon matrix, a tool for investigating severe bus and coach crashes. *International Journal of Disaster Medicine* 1 (2), 109–119.
- [4] Albertsson, P., Falkmer, T., (2005). Is There a Pattern in European Bus and Coach Incidents? A Literature Analysis with Special Focus on Injury Causation and Injury Mechanisms. *Accident Analysis and Prevention* 37 (2), 225–233.
- [5] Matolcsy, M., (2007), "The severity of bus rollover accidents", *ESV Paper 989*, 20th ESV Conference, Lyon, France.
- [6] Rona Kinetics and Associates Ltd. (2002). Evaluation of occupant protection in busses. Transport Canada, Report RK02-06, British Columbia, Canada.
- [7] United Nations. Strength of the superstructure of large passenger vehicles. Regulation 66. Revision 1. Available at: <http://www.unece.org/trans/main/wp29/wp29regs/r066r1e.pdf> [accessed March 09, 2009].
- [8] Kumagai K., Kabeshita Y., Enomoto H., and Shimojima S., (1994). An analysis method for rollover strength of bus structures. 14th International Technical Conference on Enhanced Safety of Vehicles, Munich, Germany, 351-357
- [9] Ni N. and Nakagawa K., (1996). Rollover analysis method of a large-sized bus. 15th International Technical Conference on the Enhanced Safety of Vehicles, Melbourne, Australia, 985-992.
- [10] Castejon L., Miravete A. and Larrodé E., (2001). Intercity bus rollover simulation. *International Journal of Vehicle Design*, 26(2/3), 172-184.
- [11] Elitok K., Guler M. A., Avci F.H. and Stelzmann U., (2005a). Bus rollover simulation, validation of a new safety concept. 23rd CADFEM Users' Meeting, International Congress on FEM Technology, Bonn, Germany.
- [12] Elitok K., Guler M. A., Avci F.H. and Stelzmann U., (2005b). Regulatory bus rollover crash analysis using LS-DYNA. Conference for Computer-Aided Engineering and System Modeling, İstanbul, Turkey.
- [13] Kwasniewski, L., Bojanowski, C., Siervogel, J., Wekezer, J.W., Cichocki, K., "Crash and safety assessment program for paratransit buses", *International Journal of Impact Engineering*, in-press
- [14] Friedman, K., Hutchinson, J., Weerth, E. and Mihora D., (2006), "Implementation of composite roof structures in transit buses to increase rollover roof strength and reduce the likelihood of rollover", *International Journal of crashworthiness*, Vol. 11, No. 6, pp. 593 – 596.
- [15] Guler, M.A., Elitok, K., Bayram, B., Stelzmann, U., (2007), "The influence of seat structure and passenger weight on the rollover crashworthiness of an intercity coach" *International Journal of Crashworthiness*, 12 (6), pp. 567 - 580.
- [16] Belingardi, G., Gastaldin, D., Martella, P., Peroni, L., (2003), "Multibody analysis of M3 bus rollover: structural behaviour and passenger injury risk", 18th International Technical Conference on the Enhanced Safety of Vehicles, ESV, Nagoya, Japan.
- [17] TÜV Süddeutschland, (2004). Experimental limit loads of columns, Technischer Überwachungsverein, Unpublished Research Report, Filderstadt, Germany.

- [18] T B Belytschko, J I Lin and C S Tsay, 'Explicit algorithm for the nonlinear dynamics of shells', Comput Methods Appl Mech Eng, 1984 43, 251–276.
- [19] LS-DYNA theoretical manual (2006).
Livermore, California: Livermore
SoftwareTechnology Corporation.
- [20] LS-DYNA Keyword user's manual. (2006)
Livermore, California: Livermore Software
Technology Corporation.
- [21] LSTC (2006) LS-PREPOST, Livermore
Software Technology Corporation, Livermore, CA,
Online Documentation, <http://www.lstc.com/lsp>
- [22] Versace J. (1971) A Review of the Severity
Index. Proceedings of the Fifteenth Stapp Car Crash
Conference SAE Paper No. 710881
- [23] Eppinger, R., Sun, E., Bandak, F., Haffner, M.,
Khaewpong, N., Maltese, M., Kuppa, S., Nguyen, T.,
Takhounts, E., Tannous, R., Zhang, A., Saul, R.,
(1999). Development of improved injury criteria for
the assessment of advanced automotive restraint
systems. II. National Highway and Traffic Safety
Administration.
- [24] Mayrhofer E., Steffan H. and Hoschopf H.,
(2005). Enhanced coach and bus occupant safety.
Paper Number 05-0351, Graz University of
Technology, Vehicle Safety Institute, Austria.

INFLUENCE OF ALCOHOL CONCENTRATION AND BRAKING PROCEDURE ON MOTORCYCLIST BRAKE REACTION TIME USING A MOTORCYCLE RIDING SIMULATOR

Chun-Chia Hsu

Chih-Yung Lin

Lunghwa University of Science and Technology

Chin-Ping Fung

Oriental Institute of Technology

Ming-Chang Jeng

National Central University

Taiwan

Paper Number 09-0213

ABSTRACT

The statistical data published by National Police Agency, Taiwan, indicated that the motorcycle induced the highest accident rate, and drunk driving ranked first among the traffic fatality causes in 2007. The high traffic accident rate was attributed to the alcohol decaying driver reaction and the increase of frequency of using motorcycle in daily life as the car parking space and driving cost were considered. A motorcycle riding simulator, integrating a stationary real motorcycle and virtual reality system, was developed to measure motorcyclist brake reaction time under different drunken levels and braking procedures. The motorcyclist encountered an emergence that a pedestrian went across the road abruptly in a simulated driving scene. The time between an emergence and the activation of brake lever was recorded as the brake reaction time. Ten young participants, ranging from 20 to 25 years of age, were recruited in this study. Drunken levels for motorcyclist were designed to breath alcohol concentrations (BrAC) of none, 0.15 mg/l and 0.25 mg/l. In addition, two different braking procedures, subject positioned his fingers on brake level or had his fingers wrapped around the handlebar, were tested. The experimental results showed that a longer brake reaction time was induced by the motorcyclist under higher BrAC. Additionally, the brake reaction time is also significantly influenced by braking procedure. The results in this study gave really useful information for driving education and skill in the field of motorcyclist driving safety. As the motorcycle riding simulator in this study did not involve a motion platform, participants cannot experience emergency motions induced from abrupt acceleration and braking. However, by using state-of-the-art computer graphic technologies the

simulator gave a reallike scene of emergency traffic event.

INTRODUCTION

The statistics of the Department of Health, Taiwan, indicated that the unintentional injury was the fifth of top ten death factors in Taiwan in 2007 [1], and the traffic accident was the main cause of the injury. Driving is part of daily life in modern society and, of course, induces risk to some extent. However, as the car driving cost has been gradually risen, the increase of frequency of using motorcycle becomes an inevitable result. The statistical data published by National Police Agency [2], Taiwan, showing that the car type inducing the highest accident rate was the motorcycle, reflected the unsafety of motorcycle driving. Furthermore, the statistical data [2] showed that drunk driving ranked first among the traffic fatality causes in 2007. The proposing a toast in Taiwanese culture can be attributed to the drunk driving. People usually toast each other in different dinner parties, and drink excessive alcohol unwittingly. However, most people underestimate the order of severity of drunk driving in safety. The drunk driving becomes a very serious problem nowadays in Taiwan.

The speed of driver response to the changing in traffic situation has a direct influence on driving safety. When driver receives stimulus from surrounding traffic, through the sense of sight and hearing, the information is processed in brain and then decision is made. Simultaneously, command is sent to motor organ such as hands and feet to response. The time of the process from receiving stimulus to making response is the reaction time. In generally, when safety is considered the driving ability is indicated by the reaction time. Driver

concentration on driving, body condition, driving experience, drinking alcohol or using drug would all influence reaction time to different extents. It is commonly known that alcohol influences reaction. This view was supported by scientific research. Kruisselbrink et al. [3] examined how consuming low to moderate quantities of beer over an evening affected adult females. The study found that reaction time did not significantly change the next morning as a function of alcohol dose, and suggested that consuming moderate quantities of beer affects decision making but not physical and physiological performance in adult females the next morning. Fillmore and Blackburn [4] examined how an expectancy-induced adaptive response could reduce the impairing effects of alcohol on response activation, while at the same time increase its impairing effect on response inhibition. Their experimental results showed that subjects led to expect slowed reaction time displayed faster reaction time but fewer inhibitions under alcohol, compared with those who received no such expectancy. The findings demonstrated that an alcohol expectancy reduce impairment of one aspect of performance under the drug while increasing its impairing effect on another. Alcohol can further affect driving ability. Lenné et al. [5] point out that driving performance would drop if the driver is intoxicated. In their study, a driver's ability of keeping the vehicle running inside the lane is lessened, leading to an increase in lane shifts and direction deviation angle. Meanwhile, the driver's ability of maintaining his speed is weakened, which contributes to more volatile changes in speed. His response time would likewise become longer. Leung et al. [6] discover in their study that intoxicated drivers' perception of danger on curved roads would be impaired; as a result, their response would become slow. Most of the research studies exploring the effect of alcohol on driving ability focus on car drivers. In comparison, no objective data or complete research have been obtained or conducted so far on the effect of alcohol concentration on motorcyclists' response capacity. Through a drunk driving experiment participated in by motorcyclists, the real response of the motorcyclists can be determined. However, the traffic environments that the motorcyclists will face are complicated. If the drunk driving experiment with real motorcycles is carried out, then it is bound to threaten the safety of the participants and other passers-by. During the past few years, virtual reality technology has grown rapidly, and the integration of virtual reality technology into a motorcycle simulator can not only protect the participants and reduce costs, but realize the design of experimental items, guarantee the experimental significance, and simulate varied dangerous contexts as well. Therefore, considering driver safety and experiment cost, this study conducted drunk driving experiments using motorcycle riding simulator to investigate the effects

of alcohol concentration on motorcyclist brake reaction time.

EXPERIMENTAL METHODS

The study employed a motorcycle riding simulator to access the influence of alcohol concentration and braking procedure on motorcyclist brake reaction time. The participants, simulator equipment, experimental design, and data analysis are described as follows.

Participants

This research employs 20 participants, composed of 13 males and 7 females, between 20-25 years old and holding a motorcycle license. All the participants are healthy, and have no habit of excessive drinking.

Motorcycle riding simulator

The motorcycle riding simulator integrated a real motorcycle, a virtual reality-based visual and audio system, and a host computer system to create a virtual environment of motorcycle riding. The motorcycle is a real scooter, the most common motorcycle type in Taiwan. The motorcycle front wheel is mounted on a rotationable disk. The disk allows motorcyclist to change driving direction by turning steering handlebar, and the orientation and turning angle of the front wheel are detected by a rotary-type resistance equipped on the disk. Linear variable differential transformer is attached to the brake lever to detect the position of the lever as motorcyclist applies braking. The three-dimensional models of pedestrians, vehicles and buildings in the virtual environment are created using 3DS MAX 5.1 to create. The virtual environment is presented, and the interactions between the virtual models and human being are designed, using EON studio 5.2. The virtual scene is displayed on a 100-inch rear-projection rigid screen providing 85.5° horizontal × 69.4° vertical field of view. The audio system provides simulated noises from the engine and traffic environment. The control of all the input and output of software and hardware is integrated into a main program developed using Visual Basic 2005.

Experimental design

The experiment employed a 3×2 factorial within-subject design that compared motorcyclist reaction time based on different alcohol concentrations (none, 0.15 mg/l, 0.25 mg/l) and braking procedures (cover mode, uncover mode). The braking procedure of cover mode was that subject positioned his fingers on brake level. The uncover mode was that subject had his fingers wrapped around the handlebar. The different

conditions were presented in random order to participants.

Driving Scenario

A simulated driving scene was created using the VR system for motorcyclist undergoing the driving experiment in safety. When the motorcyclists are riding on the simulator, they will meet any number of pedestrians standing on the sidewalks five times during the driving process. Only in three cases will the pedestrians abruptly cross the road from the sidewalk at a quick trot, as shown as Figure 1. The pedestrians will be standing at their places 3 meters away from the middle of the lane. The pedestrians' speed when crossing the road is set at 7.2km/hr. The event of the pedestrian crossing the road will be triggered when the distance between the motorcycle and the place where the pedestrian is standing reaches 20 meters. The speed of the motorcycle is fixed at 50km/hr. If the motorcyclist does not take any action to brake after the event is triggered, the pedestrian will run into the motorcycle after 1.5 seconds. To obviate the expectations held by the participants to the events, which will then cause the collected data to lose objectivity, the times the three events of the pedestrian crossing the road are arranged randomly.



Figure 1. Pedestrian goes across the road abruptly.

Experimental procedure

The experimental procedure starts from the registration of the participants. First of all, the participants register and then fill out an experimental questionnaire. After that, the experimental process is explained by an assistant and how to use the motorcycle simulator is taught, allowing each participant to practice with the motorcycle simulator so as to ensure they are familiar with the experimental process. After the participants learn how to operate the motorcycle simulator well, the simulating experiment of conscious driving is set out

to do.

During the drunk driving experiment, participants must drink the prepared alcoholic drinks within 10 minutes and then rest for 20 minutes. The drink volume is calculated according to the information provided by the participants. Next, an alcohol detector is used to check whether the breath alcohol concentration of the participants has reached 0.15mg/l (± 0.03 mg/l). If the desired concentration is reached, the experiment is set out to conduct. After the experiment is finished, the alcohol concentration of the participants is tested and recorded again. Then, the second round of experiments will be made. The participants will be asked to drink the second cup of alcoholic drink and then rest for 20 minutes. An alcohol detector is then used to check whether the breath alcohol concentration of the participant has reached 0.25mg/l (± 0.03 mg/l). If the desired concentration is reached, the experiment is set out to conduct. After the experiment is finished, the alcohol concentration of the participants is tested and recorded once more. After all the experiments are finished, hot tea and other drinks will be provided to the participants to relieve the effects of the alcohol. The participants can take a rest for one to two hours after the experiment before leaving.

On the day before the commencement of the experiment, the participants should not eat any food containing any alcoholic ingredient to prevent alcohol from remaining within the body or the problems of alcoholic metabolism from appearing. Moreover, the participants should not stay up late, making sure to have plenty of sleep. Finally, they should keep away from food containing high oil, sugar, or caffeine content within two hours before the experiment so as not to affect the absorption of alcohol.

Data analysis

The braking response time is counted beginning from the moment the pedestrian begins to move and ends when the activation of brake lever. All experimental data are sorted out and statistically analyzed using the SPSS15.0 Statistic Application Software.

RESULTS AND DISCUSSION

Braking response times using uncover mode and cover mode for brake preparation action under different alcohol concentrations are listed in Table 1. Mean braking response time using uncover mode for brake preparation action without alcohol is 0.665 second, longer than the 0.49 second braking response time using uncover mode. This discrepancy has reached a statistically significant difference ($P < 0.001$). When the breath alcohol concentration is 0.15mg/l, the mean braking response time using uncover mode (0.680 second) for the brake preparation action is longer than mean braking

response time when using uncover mode (0.490 second). Again, this discrepancy has reached a statistically significant difference ($P < 0.001$). When the breath alcohol concentration is 0.25mg/l, the mean braking response time using uncover mode for the brake preparation action without alcohol is 0.692 second, longer than of the mean braking response time of 0.578 second when using uncover mode. This discrepancy has likewise reached a statistically significant difference ($P < 0.001$). The experimental result shows that despite the intake of alcohol, or under varied alcohol concentrations, the mean braking response time using uncover mode for the brake preparation action is longer than the mean braking response time when using cover mode, and that the discrepancy between them has reached a statistically significant difference. The results of this study indicated that the brake reaction time is significantly influenced by braking procedure. The results gave really useful information for driving education and skill in the field of motorcyclist driving safety.

Table 1.
The reaction time in different braking procedures and alcohol concentrations

alcohol concentrations	braking procedures	Average	S. D.	P value
0 mg/l	Uncover mode	0.665	0.138	0.000
	Cover mode	0.479	0.126	
0.15 mg/l	Uncover mode	0.680	0.106	0.000
	Cover mode	0.490	0.105	
0.25 mg/l	Uncover mode	0.692	0.158	0.000
	Cover mode	0.578	0.152	

The participants' braking response time under different breath alcohol concentrations when pedestrians cross the road at a quick trot is shown in Table 2. When the participants have not drank any alcohol, the braking response time is 0.572 second; when the breath alcohol concentration is 0.15mg/l, the braking response time 0.585 second; when the breath alcohol concentration is 0.25mg/l, the braking response time is 0.610 second. The statistical analysis result indicates that the effect of different breath alcohol concentrations on the braking response time reaches a statistically significant difference ($p < 0.032$). Tukey post-hoc tests showed the difference between 0 mg/l and 25 mg/l was significant. On the other hand, there was no

difference between 0 mg/l and 15 mg/l, and between 15 mg/l and 25 mg/l. The results of this study indicated that the brake reaction time is significantly influenced by alcohol after driver drank at some level of alcohol concentration.

Table 2.
The reaction time at different alcohol concentrations

alcohol concentrations	Average	S. D.	P value
0 mg/l	0.572	0.161	0.032
0.15 mg/l	0.585	0.142	
0.25 mg/l	0.610	0.176	

CONCLUSIONS

The study investigated motorcyclist reaction time based on different alcohol concentrations (none, 0.15 mg/l, 0.25 mg/l) and braking procedures (cover mode, uncover mode). It was found from the experimental that the brake reaction time is significantly influenced by braking procedure. The brake reaction time for subject had his fingers wrapped around the handlebar was much longer than the time for subject positioned his fingers on brake level. The results gave really useful information for driving education and skill in the field of motorcyclist driving safety. The experimental results showed that a longer brake reaction time was induced by the motorcyclist under higher BrAC. The brake reaction time is significantly influenced by alcohol after driver drank at some level of alcohol concentration.

ACKNOWLEDGEMENTS

The authors would like to acknowledge the assistance of Uen-Jau Tian for his help with the experiment in this study.

REFERENCES

- [1] Main death factors. Available from: <http://www.doh.gov.tw/CHT2006/DisplayStatisticFile.aspx?d=61564>. Accessed September 14, 2008.
- [2] Traffic accident analysis. Avail from: <http://www.npa.gov.tw/NPAGip/wSite/ct?xItem=39220&ctNode=11398&mp=1>. Accessed September 14, 2008.
- [3] Kruisselbrink, L.D., K.L. Martin, M. Megeney, J.R. Fowles, and R.J.L. Murphy. 2006. "Physical and psychomotor functioning of females the morning after consuming low to moderate quantities of beer." *Journal of Studies on Alcohol*, Vol. 67: 416-421.

[4] Fillmore, M.T. and J. Blackburn. 2002.
“Compensating for alcohol-induced impairment:
alcohol expectancies and behavioral disinhibition.”
Journal of Studies on Alcohol, Vol. 63: 237-246.

[5] Lenné, M.G., T.J. Triggs and J.R. Redman. 1999.
“Alcohol, time of day, and driving experience: effects
on simulated driving performance and subjective
mood.” Transportation Human Factors, Vol. 1:
331-346.

[6] Leung S. and G. Starmer. 2005. “Gap acceptance
and risk-taking by young and mature drivers, both
sober and alcohol-intoxicated, in a simulated driving
task.” Accident Analysis and Prevention, Vol. 37:
1056-1065.

Evaluation of needs and possibilities to change the requirements in the regulations regarding the possibility of observing the surroundings in the N_1 vehicles

Krzysztof Olejnik

Motor Transport Institute

Poland

Paper No. 09-0399

ABSTRACT

The lack of information from the surrounding of the vehicle is one of the reasons of collisions and accidents. There is a radical limitation of unobstructed observation of the whole area surrounding trucks of N_1 category in comparison to the car of M_1 category. Vehicles which have the same body and which are designed to transport people – M_1 category or load – N_1 category, they have different equipment, such as side glazing and back walls. Those who are driving these vehicles don't have comparable and identical visibility. Technical progress and development in the area of visual transfer devices helps to use them in the vehicles in order to improve the possibility of observing the surrounding of the vehicle. There is an important need to change the regulation as far as construction and vehicles equipment is concerned. The regulation should compel the vehicles manufacturers to ensure such construction of the vehicle that the driver will have a possibility of observing the surrounding of vehicle in the range of scope and placement visible area would be comparable to the car. Setting this kind of requirement will force the producers to ensure visibility from the trucks comparable to that of cars. This will help avoid collisions and accidents which are caused by the substantial limitation of the possibility to observe the surrounding of the vehicle. These facts speak for the necessity and need of changes to the regulations. This paper offers the change of the philosophy of the regulations requirements in the area of visibility. The novelty is the definition of the needs and possibilities of changes in the regulations concerning visual transfer for trucks. There is no reason to tolerate the worse visual transfer in the vehicles N_1 category. It is possible and is imperative to introduce regulations which will obligate the vehicles manufacturers to equip trucks in such a way that the possibility of observing the surrounding will be the same as in the passenger car version.

Key words: demands, visibility, construction of the car

INTRODUCTION

Ensuring the visibility of the road and around it, conforming to the regulations does not always guarantee the good visible transfer for drivers (inside the vehicle) – sufficiently good visibility.

Often the regulations on the road formation do not cater for the limitations of visibility resulting from the constructional features of the vehicle.

The open load-carrying body in the truck creates the screen obscuring of the big part of the vehicle's surrounding which precludes the direct observation of the considerable area.

The devices of the indirect visibility enable to observe only the part of the area which is directly invisible.

THE SUBJECT OF THE TESTS

The subject of the tests is the car construction aimed at ensuring possibility to observe the car surroundings while driving

The figure 1 presents the areas around the vehicle which the driver should have the possibility to observe while driving it (making various manoeuvres) during a day and at night – with the street lighting and without it.

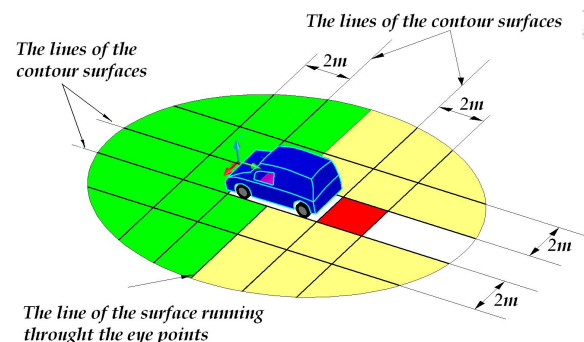


Figure 1. The areas around the vehicle which must be visible

The practical realization of the need to have a visibility of surroundings (according to the current regulations in force) is considerably different from the ideal. In spite of the installation of indirect visibility devices in the cars, the big part of directly invisible area is still invisible.

The figure no. 2 shows the area surrounding the vehicle of N_1 category, observed directly by the driver through the windows forward and on each side and also indirectly through the mirrors. Areas A and B – observed areas. Areas D – minimal areas

demanded by regulations. Areas C – areas the observation of which is impossible till now.

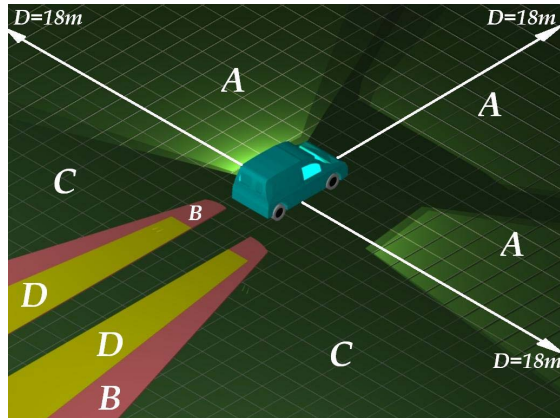


Figure 2. The areas around the vehicle category N_1 which are visible

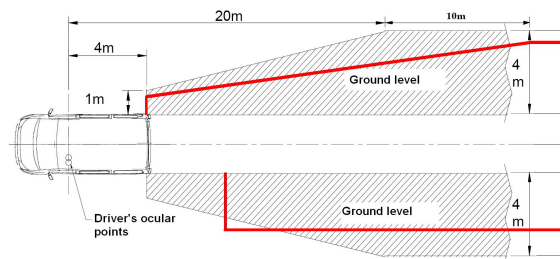


Figure 3. Placement and vastness of the visibility field for the main rear view mirrors of class III – by thickened line denotes requirements hitherto in force - $d_{mc} \geq 2000$ kg

In order to estimate the degree of divergence between the ideal and the real situation the visibility of surroundings of the M_1 category car and the N_1 category truck were tested. The estimation was conducted on the example of the Renault Kangoo vehicle in the passenger car version and in the truck version. The similarity exists between the vehicles of categories M_1 and N_1 of the same brands and models in the range of the external resemblance of the body but big differences in the visibility outward. The cars with the identical bodies dedicated for the transport of people – category M_1 and goods – category N_1 , have the various sets of equipment, among other thing, as far as glazing of side walls and rear wall are concerned. The test was made using the method presented in the directive 2003/97 EC, 77/649/EC. The results of visibility tests of car surroundings were presented at the figure no. 5. From the comparison of figures no. 1, 2 and 3 it transpires that the driver does not have any possibility to observe this part of the area around the car which should be observed during manoeuvring of the car to avoid the collision and accident.



Figure 4. Vehicle Renault Kangoo – truck and car – body versions

Moreover the drivers of the above do not have identical possibilities to observe the surroundings. In the truck of category N_1 the area which can be observed by the driver is radically reduced. Is it needed, is it necessary, and is it possible to eliminate the difference in the “surroundings visibility” of trucks in comparison with the passenger cars, especially these which are based on the identical body. The lack and also insufficient information from the cars surroundings during driving are one of the causes of the rise of collisions and accidents. Unobscured observation of all the area surrounding the vehicle is radically limited, in the small trucks of category N_1 in comparison with passenger cars of M_1 category. It is particularly easy noticeable and perceptible in the vehicles of categories M_1 and N_1 of the same brand whose bodies are similar. In the vehicle of the passenger car version the side walls and the rear wall have the glazed windows, through which the driver can observe surroundings. Additionally it is equipped with the indirect visibility devices which are identical as in the version of the truck except the interior mirror. In general the interior mirror is not mounted in the truck. In the truck, in the area behind the driver, in general the windows in the side walls and in the rear wall are not fitted or used. As a result the driver can observe considerably smaller area of his surroundings.

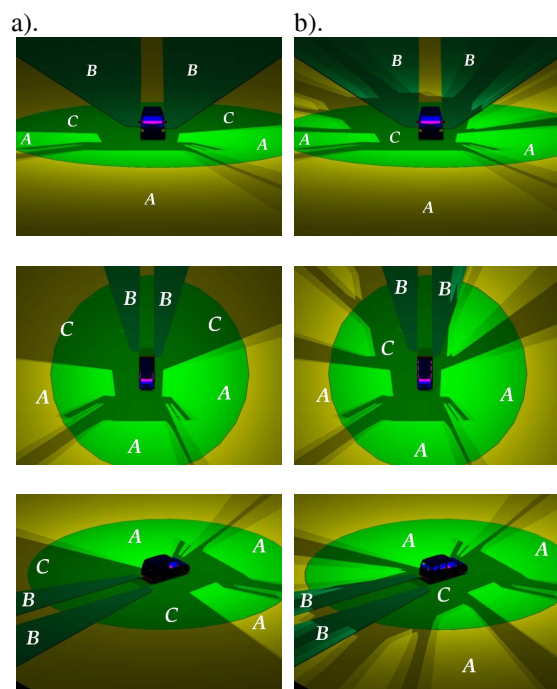


Figure 5. The direct and indirect visibility field for Renault Kangoo: a). truck category N_1 and b). car category M_1

The perceptible technical progress and the development of the visibility devices allow to equip the vehicle in such a way that the driver of the truck could observe the areas surroundings comparable with passenger cars.

RECAPITULATION AND CONCLUSIONS

The vehicle the driver does not have any chance to receive the visible transfer from the significant part of the area surrounding and thus to have the possibilities to act adequately to the situation during the car driving.

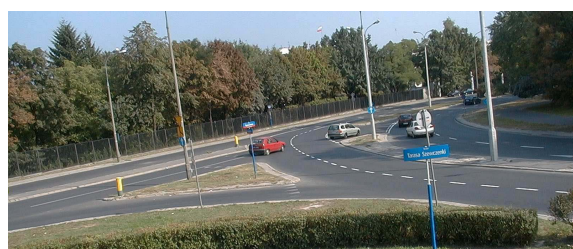


Figure 6. Situation on the angular intersection with reduced visibility on the right side of the vehicle

This problem is particularly important on oblique road crossings when the angle of the cutting of their axes is considerably different from the right angle – difference exceeds the value of 15° . With

reference to vehicles in use, insufficient (for the most part of cases) visible transfer from the surroundings is the essential cause of rise of collisions and accidents taking place in the road traffic. The increase of possibilities to observe areas of the vehicle surroundings (in the newly designed constructions), which till now couldn't be supervised, is the step in the proper direction. It is possible to change the regulations and to change the vehicles equipment by the manufacturers. It is expected to radically extend the visibility and to diminish the danger of accidents in the vehicles of N_1 category which were caused by the previous visibility limitations

REFERENCES

- [1] OLEJNIK K.: Operating problems of buses and trucks – safe reversing. Journal of 17th European Maintenance Congress, 11th – 13th of May 2004 Barcelona – Spain, 343–348.
- [2] OLEJNIK K.: Critical analysis of the current traffic regulations concerning visibility from the position of a vehicle driver. Quarterly Motor Transport 2/2003 distributed by Motor Transport Institute, Warsaw, Poland, 69–80.
- [3] Regulation no. 46 ECE UN. Uniform provisions concerning the approval of devices for indirect vision and of motor vehicles with regard to the installation of these devices.

INITIAL SITE INSPECTION OF MOTORCYCLE COLLISIONS WITH ROADSIDE OBJECTS IN NEW JERSEY

Allison Daniello
Ben Powell
Nicholas Schaeffer
Aaliyah McClinton
Yusuf Mehta
Rowan University
United States

Kimberly Swanseen
Hampton C. Gabler
Virginia Tech
United States

Paper Number 09-0450

ABSTRACT

This paper details the methods used to investigate motorcycle collisions with roadside objects and the initial findings of the study. One factor associated with the frequency and severity of motorcycle collisions with roadside objects may be the design and maintenance of the road. Two methods of analysis were used to investigate the influence of the road geometry and design of roadside environment on motorcycle collisions. Satellite imagery was used to develop an overview of different collision sites. Individual site visits for 34 motorcycle-roadside object crashes were conducted to record details about each site, including types of guardrails and distance of the object struck from the road.

INTRODUCTION

Motorcyclists are overrepresented in guardrail collisions. Motorcycles comprise only 2% of vehicles on the roads, but account for 42% of all guardrail collisions (Gabler, 2007). Motorcyclists are more vulnerable on the road than other vehicle passengers due to the instability of their vehicle as well as greater exposure to the outside environment. There are various causes of motorcycle crashes, including the design and maintenance of the road. Roadside environments were further investigated to determine characteristics that may lead to a higher risk for motorcyclists running off the road. Potential design factors include road curvature, superelevation, barrier type, and barrier offset distance from the travel lane. Road surface factors of interest include the presence

of rumble strips, potholes, cracking, painted areas, and gaps between the road surface and bridge decks.

OBJECTIVE

The objective of this paper is to describe the methods used to develop a database with detailed information about roadside object motorcycle collision sites and to report the findings of the initial analysis of the cases investigated to date.

METHODS

The cases used in this study were extracted from the New Jersey Crash Records Database (NJCRASH) for calendar years 2005-2008. NJCRASH is a complete collection of police accident reports which are available in electronic form. Of particular value to this project, most crashes have been geocoded with the latitude / longitude coordinates of the crash site. The geocoded locations of motorcycle-roadside object collisions were investigated using two methods: a satellite image analysis and an individual site inspection. For this pilot study, a subset of these cases was investigated to determine the feasibility of our approach. Motorcycle collisions with guardrails, concrete barriers, poles, and trees were investigated.

Satellite Imagery Analysis

The imagery analysis gave a first look at the different guardrail collision sites. Using the latitude and longitude data recorded in the NJCRASH database, sites were located on satellite images using Google Earth Pro. A screenshot was taken of each collision

site and incorporated with data tables that displayed information about the accident based on the coded NJCRASH Data. The tables incorporated data about the time and date of the crash, location, information on the rider and motorcycle, and sequence of events to give an overall description of each accident.

The radius of curvature was also investigated through the satellite imagery analysis. Collisions that occur on any size curve are listed simply as 'curve' in the NJCRASH database. NJCRASH does not describe the radius of the curve. However, it is important to know the radius of a curve: curves with smaller radii may be more dangerous for riders (FEMA, 2000). Thus, comparing the radii of curves on which collisions occurred may help in determining the geographic locations where accidents are occurring.

Google Earth Pro was used to measure the radii of curves where collisions occurred. The circle tool used to draw a circle on the image. The tool measures the radius of the circle, which can be adjusted by dragging the endpoint of the radius on the map. The center of the circle can also be adjusted by dragging the center to a new location. Using these two operations, the circle was fit as best as possible to the curve (Figure 1). The median of the road was used as guidance in determining the curvature of the circle, and, when possible, the circle was fit to the median. On roads where there was no median, the lines on the road were used as reference if they were visible in the satellite imagery.



Figure 1. Example radius of curvature measurement from Google Earth Pro. This collision occurred in Mercer County on Route 640. The radius of curvature is 200 feet.

Once the circle was fit to the curve, the radius of the circle was recorded to the nearest foot. The Google Earth Pro tool records the radius to the nearest hundredth of a foot; however, the rounding was made in order to compensate for human error in fitting the circle to the curve.

Site Survey Data Collection

Though satellite imagery provided an introduction to the area where a crash occurred, the imagery is not of a high enough resolution to determine smaller characteristics of the road, such as variations in the surface and the type of guardrail surrounding the road. Motorcycles are more vulnerable to these variations as they are significantly less stable than other motor vehicles. Data currently available through NJCRASH does not include detailed information about the roadside objects, such as the distance of a struck object from the road or the condition of the object.

Site visits were conducted to methodically document the characteristics of the roadway, roadside, and barrier at each crash site. A data collection form was used to ensure the same information was gathered at every site. It allowed for investigators to select specific characteristics from a list of options, with the option of adding characteristics that were not included. This format allows for simpler analysis of data as opposed to a sheet without any options because there are a finite amount of responses to each question. Photographs were taken in order to compare the road conditions and surrounding environments around each crash site. The data collection sheet contains a check list of photographs to be taken to ensure that common features can be compared. The data elements collected in each site inspection are presented in Table 1.

Table 1.
Information gathered at sites by data element type

Data Element	Characteristics
Barrier Characteristics	Concrete Barrier
	Type
	Height
	Damage
	Guardrail
	Rail type
	Post type
	Blockout type
	Terminal type (if applicable)
	Distance between posts
	Damage to rail/posts
	Additional features

Table 1 (continued).

Data Element	Characteristics
Roadside Characteristics	Shoulder presence
	Rumble Strip
	Surface
	Division
	Potholes
	Patches
	Notable Cracks
	Contaminants
Dimensions	Object to pavement edge
	Distance
	Slope
	Pavement edge to lane end
	Distance
	Slope
	Ground to bottom of rail (if applicable)

The main focus of the collection process was on motorcycle-guardrail collisions. Several different characteristics about the guardrail were observed through site visits. First, the type of rail was recorded since this is the main component of the guardrail. Moreover, the height of the rail from the ground was measured. In the event of a collision a motorcyclist can fall from his/her motorcycle and slide under the guardrail, potentially colliding with the post. Second, the type of post was recorded. Posts prove to be one of the greatest hazards to motorcyclists as they have narrow faces and edges which concentrate the force. Lastly, it was noted if any additional safety measures, such as an additional W-beam or metal guard, were used on the guardrail at the collision site. Characteristics of other roadside objects were incorporated such as type of concrete barrier, pole type, and any distinguishing features.

Characteristics about the roadway were also observed to see if there were common aspects of the road that could potentially be a cause of an accident. It was noted if there were any potholes, patches, or cracks in the road, as a motorcycle can lose stability from riding over one of these defects. Any abrupt changes in the elevation were noted as these are also hazardous to motorcyclists. However, these characteristics may have changed from the time of the crash. Several design aspects of the road were also examined. First, it was noted if there was a rumble strip in the shoulder as the high surface variation may cause a rider to lose control. It was also noted if there was paint on the road, as this has a different coefficient of friction from the road surface

and this change, though not significant to other motor vehicles, may cause a rider to lose control.

Measurements of the shoulder width, slope, and distance between the object and end of the pavement were also taken at each site. A diagram was included in the survey sheet to clarify the required measurements (Figure 2). The distance of the object from the road may have an effect on the severity of a collision; if the object is further away from the flow of traffic, the motorcyclist will have more time to slow down before colliding with it.

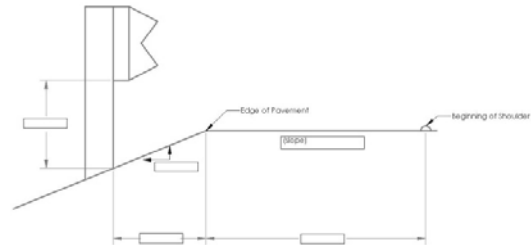


Figure 2. Guardrail and Road Environment Measurements. This figure was included in the site survey sheets to gather data about the distance of the object from the road and the slope of the road.

Police reports for each site visited were obtained from the New Jersey Department of Transportation before most site visits. The police reports contained more information about the occurrences of the accident, sometimes including a diagram. This additional information facilitated finding the site and exact location of the collision, as many sites had multiple poles, trees, or lengths of guardrails.

RESULTS

To date, a database of 34 collisions which have occurred at 31 crash sites has been developed. Four crashes occurred at the same location. Table 2 presents the composition of the resulting dataset. This includes 17 guardrail collision sites, 11 pole collision sites, 4 tree collision sites, and 1 concrete barrier collision site. The majority of the collisions (29) occurred in either 2007 or 2008.

Table 2.
Composition of Data Set of Motorcycle-Roadside
Object Collisions (NJCRASH 2005-2008)

Variable	Number of Cases
All	34
Year of Crash	
2005	1
2006	4
2007	25
2008	4
Object Struck	
Guardrail	17
Concrete Barrier	1
Poles	12
Trees	4
Injury Severity (KABCO)	
Fatality	5
Incapacitating Injury	7
Moderate Injury	15
Complaint of Pain	7
Property Damage Only	0

Example Case

On Route 579 in Bethlehem Township in Hunterdon County, a crash location was investigated where there were 4 motorcycle-guardrail collisions in 2007. The posted speed limit on the road is 35 mph, with a reduction to 10 mph around the curve. The road took a sharp turn left, and disappeared from vision due to the downgrade of the road (Figure 3). There were two driveways ending at the curve.



Figure 3. Route 579, Bethlehem Township, Hunterdon County. Four motorcycle-guardrail collisions took place at this site in 2007.

There were at least 5 areas of damage along the W-beam guardrail, suggesting other vehicle crashes had occurred on the same curve (Figure 4). Some of the steel strong posts were also bent and damaged.



Figure 4. Damage to guardrail. There is notable damage to the rail and the posts in multiple areas.

The distance of the guardrail from the edge of the lane gradually narrows as the road curves left. The guardrail-road offset distance was measured in three places to be 7.4, 5.0, and 4.0 feet from the edge of the lane. Along the curve, the guardrail was located only 0.75 feet from the edge of the pavement. The guardrail is in place to protect vehicles from the wooded slope behind it. The road slopes 11° in the direction of the road. The road angled 23° toward the center of the curve.

During the site visit, a street cleaner was seen at the site, implying that the site is well kept. There was little debris noticed on the side of the road as well. There were no potholes, patches, or large cracks in the asphalt surface of the road. However, the road was rough and uneven (Figure 5), which may be more hazardous for motorcycles than other vehicles.



Figure 5. Road Surface. The surface of the road was noted to be rough and uneven.

The geometry of the site was analyzed using Google Earth Pro. The radius of curvature of the site was measured to be 49 feet (Figure 6). This is a very narrow curve as none of the other sites investigated using the satellite imagery were found to have a radius under 100 feet.



Figure 6. Radius measurement of example site.
The radius of the curve was measure to be 49 feet.

Site Survey Data Collection

In our dataset, seventeen motorcycle-guardrail collision sites were investigated. The guardrails all had W-beam rails with steel strong posts (10), steel weak posts (2), or wood strong posts (5). The blockouts used in the strong post guardrail also varied between steel (9), wood (4), recycled material (1), and none (1). This composition is consistent with national guardrail inventories which are primarily strong post w-beam systems.

The distances of the objects from the edge of the lane varied greatly amongst the sites (Figure 7). There were sites where the guardrail was on the edge of the pavement on a street with no shoulder, and others where the guardrail was offset from the edge of the pavement on a road with a significant shoulder.

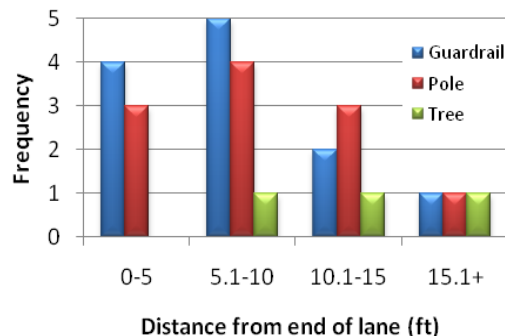


Figure 7. Distance of object from lane edge by object struck.

Of the 31 crash sites investigated, 17 occurred on curves. After visiting the sites it became evident that some of the curves created an obstruction of view. The road surface at the majority of the sites was free of debris and blemishes. There were no evident potholes at any sites, and only 5 sites had notable cracks in the surface.

Satellite Imagery Analysis

A separate analysis for 139 guardrail collision sites in New Jersey from 2005-2007 was conducted. The main component of each site investigated through the use of Google Earth was the radius of curvature at each site. Fifty-eight (41.7%) of the collisions investigated occurred on curves, 41 of which (33.6%) occurred on a curve with a radius of curvature of less than 1000 feet.

The distribution of the crashes across New Jersey was also found after each crash was analyzed (Figure 8). Most motorcycle-guardrail collisions were in northern New Jersey.

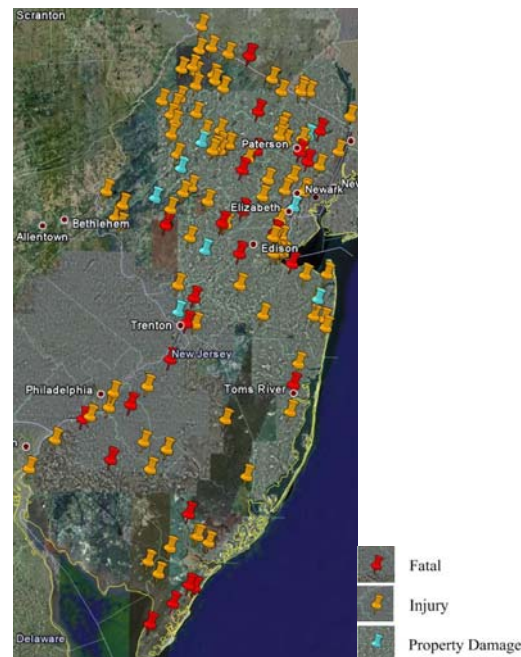


Figure 8. Distribution of motorcycle-guardrail collisions in New Jersey (2005-2007).

DISCUSSION

Two methods of evaluating motorcycle collisions with roadside objects were used to develop an enhanced database about the roads on which these crashes are occurring. Using satellite imagery from Google Earth, the radius of curvature at collision sites was obtained. It was seen that approximately 1/3 of crashes occurred on roads with a radius of curvature of less than 1000 feet. However, these data are limited by the precision of the user to fit a curve to the road.

Motorcycle collision sites were also analyzed through site surveys. Thirty-one sites have been visited to

date. One challenge was the occasional unavailability of latitude and longitude data from the NJCRASH database. Most of the recent crashes (2007-2008) were geocoded with these coordinates; however, there were some crashes that were neither geocoded nor included an exact location. In some cases, positioning coordinates appeared to be inaccurate. In several cases, the investigators' judgment was used to deduce the location of the crash.

A second challenge has been to obtain safe access to the sites for physical measurements. Many of the collisions occurred on main roads with higher speed limits. These roads sometimes have no place for investigators to safely stop for the inspection. For sites that were too dangerous to investigate thoroughly, a drive-by investigation was completed. This allowed for general information to be gathered about each site, though no measurements could be taken.

A third challenge was the need to promptly visit a crash site after the incident. We investigated several sites years after the incident with the hope that characteristics, e.g. barrier type or road curvature, would be unlikely to have changed. Some characteristics however, e.g. defects in the roadway surface or barrier damage, may have been repaired prior to our site inspections. To account for this possibility, our protocol required that the investigator note any indications of repair, e.g. new barriers or poles.

CONCLUSION

This paper has presented the design of a novel database containing detailed road design and maintenance information about motorcycle collision sites with roadside objects. This database extends the traditional databases of police-reported crash reports with engineering data such as guardrail type and distance of object struck from the road. Thus far, 31 sites have been investigated, supplemented with an analysis of satellite imagery. This database will provide researchers with more information to determine what environmental aspects are characteristic of motorcycle crashes. Identifying these characteristics and taking action to modify them, making them more motorcycle-friendly, will lead to a reduction in the severity of motorcycle crashes with roadside objects.

ACKNOWLEDGEMENTS

We gratefully acknowledge the New Jersey Department of Transportation and Motor Vehicle Commission who provided support for this project.

REFERENCES

1. Gabler, H.C., "The Risk of Fatality in Motorcycle Crashes with Roadside Barriers", Proceedings of the Twentieth International Conference on Enhanced Safety of Vehicles, Paper No. 07-0474, Lyons, France (June 2007).
2. The Federation of European Motorcyclists' Associations (FEMA). "Final Report of the Motorcyclists & Crash Barriers Project," <http://www.fema.ridersrights.org/crashbarrier/index.html>, 2000.

MODIFICATION OF A TRUCK FRONT FOR IMPROVED KINEMATICS IN RUN OVER ACCIDENTS

Michael Hamacher

fka - Forschungsgesellschaft Kraftfahrwesen mbH Aachen
Germany

Sven Fassbender

ika - Institut für Kraftfahrzeuge RWTH Aachen University
Germany

Florian Feist

Jürgen Gugler

Graz University of Technology
Austria

Paper Number 09-0458

ABSTRACT

A major problem of the predominantly flat fronts of trucks used in Europe with respect to accidents involving vulnerable road users are the kinematics of the vulnerable road user after the impact. Contrary to car versus vulnerable road user accidents the flat truck front pushes the vulnerable road user to the road rather than lifting him. This effect causes a high risk of a run over.

The main idea of the presented safety device is to change the flat front to a tapered shape deflecting the vulnerable road user sideways by using the impact impulse. The achieved deflection reduces the risk of a run over. The tapered truck front has been designed and analysed within the EC funded APROSYS integrated project.

For a principal investigation the tapered shape is realised by an add-on structure mountable to the front of a reference truck. Hence, a direct comparison of the flat and the tapered shape is possible. Regarding a practically relevant application of this safety concept with respect to technical and economical feasibility the tapered shape has to be implemented directly in the cabin design. During the development phase of the new front structure a large number of design versions are generated and assessed. The resulting final principal shape is compared to the basis truck in various numerical simulations with different accident scenarios, pedestrian models and parameter settings.

Due to these results it can be concluded that a convex truck front significantly reduces the risk of a run over. It is most effective in accidents with higher speed (> 20 km/h) and the additional deformation space allows to reduce the contact forces at the primary impact. In this regard it has to be discussed whether the implementation of passive

safety devices in trucks should implicate a revision of the vehicle length regulation.

INTRODUCTION

Statistics indicate that more than 1400 vulnerable road users in the current EU member states lose their lives every year due to accidents with heavy vehicles. This number is much larger in the Eastern Europe countries. A major problem of the predominantly flat fronts of trucks used in Europe with respect to accidents involving vulnerable road users are the kinematics of the vulnerable road user after the impact. The flat truck front pushes the vulnerable road user to the road, which causes a high risk of a run over. Car versus vulnerable road user accidents show a different characteristic. The primary contact is followed by a flight phase, in which the vulnerable road user is moved away from the car before the secondary impact and the sliding phase occur. A further contact to the car, the so called tertiary impact, is compared to accidents with trucks quite seldom.

Currently there are no existing pedestrian safety requirements for trucks. The main idea of the safety device described within this paper is to change the flat front to a tapered shape deflecting the vulnerable road user sideways by using the impact impulse. The achieved deflection reduces the risk of a run over and the additional deformation space allows to decrease the contact forces at primary impact. Due to the shape of the optimised truck front, there is not only a benefit in scenarios, where the truck is driving straightforward but also in cornering scenarios. The tapered truck front has been designed and analysed within the EC funded APROSYS integrated project [1].

To ensure a direct comparison of the flat and the tapered shape, it is realised by an add-on structure mountable to the front of a reference truck. The reference truck is a MAN LE. Regarding a practically relevant application of this safety

concept with respect to technical and economical feasibility the tapered shape has to be implemented directly in the cabin design. However, the results of the add-on device give sufficient implications on the benefits and difficulties to be expected for a tapered truck front in accidents between a truck and a vulnerable road user.

DEVELOPMENT OF A DEFLECTING FRONT SHAPE

The first step on the way to a final design is to determine the most appropriate general design.

Front geometry versions

In total the number of front geometry versions developed and assessed amounts to 90. The differences between the single versions are often only marginal. This approach is reasonable to examine the effect of a specific geometry or to improve positive effects. However some versions show exaggerated shapes. These versions are meant to provide information about the accident kinematics but are not practical for an actual application. An overview of the different development stages is given by the 12 examples shown in Figure 1.

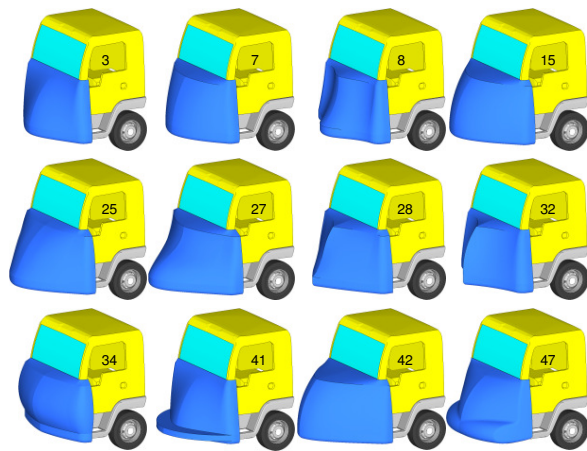


Figure 1. Examples of the 90 front geometry concepts.

Regarding the current regulations a practical front structure solution should be as flat and even as possible. Versions 3, 7 and 8 fulfil these requirements but do not provide a sufficient deflection of the pedestrian. Version 15 shows a highly improved deflection effect. The front structure of the versions 3, 7 and 15 is rather steep, which leads to a straight and direct impact of the pedestrian. An effect that throws the pedestrian slightly upwards can be achieved with the versions 25 and 27, which show a more shallow shape. Examples of front structures bending sharp to the centre of the front are the versions 28 and 32. The

aim of these versions is to deflect the pedestrian even from a centre position sufficiently to the side. Unfortunately, these solutions have not shown the expected effect. In addition they are critical because of the disadvantageous primary impact on the sharp and stiff edge formed by the centreline, which might cause severe injuries of the pedestrian. The idea of design concept 34 is a primary contact of the arms and torso of the pedestrian instead of the lower extremities. Due to its bad test results this design is not regarded in further concepts.

To achieve the effect of throwing the pedestrian up but having a short front version 41 has been designed with a forward reaching plateau at the lower end of the nose. In contrast to this, version 42 shows the maximum geometrical design space regarded within the study. As of a certain length further improvements can not be achieved by extending the nose. Version 47 is an optimisation of version 41 and forms the basis for the remaining 43 versions, where the design is further optimised. This concept can be seen as the summary of all experience gained in the previous designs. The dominant concept idea is the surrounding plateau at the bottom. In addition to the effect of throwing the pedestrian up the plateau improves the compatibility to cars.

Assessment of the front geometries

During the development of the different designs the versions have to be assessed regarding their impact kinematics. Due to the large number of different versions this can only be done by a reduced number of accident scenarios.

The assessment of the different versions comprises six tests, but for most of the versions less tests are conducted if they do not show appropriate results. The complete scope includes three crash-scenarios in a forward-driving and three crash-scenarios in a right-cornering situation. The simulations for the determination of the general shape are carried out with a 50 % male pedestrian model only. Later on for the assessment of the final design more scenarios and pedestrian models will be considered. The assessment only assesses the crash kinematics and the position of the pedestrian after the impact. In this context the two terms run over and roll over are used. Both cases are critical since the pedestrian gets underneath the truck, whereas roll over implies a contact of the pedestrian to the tyres.

Determination of the best front geometry -

Regarding the different front geometries the curvature of the plateau along the width of the truck front has an important influence. After all, a curved platform shows better results because of the stronger side deflection of the pedestrian. Additionally, a steeper design of the plateau has a positive

effect on the impact kinematics. A slight tapering of the outer edges of the plateau has advantages in the right-cornering scenarios when the impact occurs at the corner of the truck front. Front geometry 84 offers all these positive effects (Figure 2).

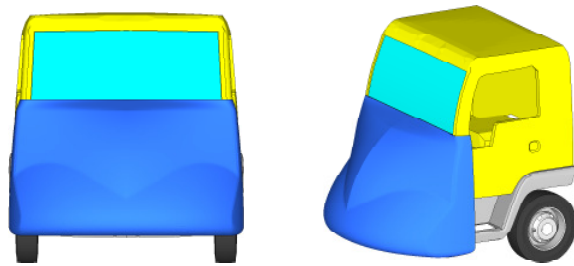


Figure 2. Front geometry 84.

The kinematics of the pedestrian model can be seen in Figure 3. Shortly after the primary impact the pedestrian model loses contact to the ground and turns away from the truck. When touching the ground the right leg is already beside the plateau. The rest of the body is deflected to the side. During the secondary contact the pedestrian model rolls to the side and rests at a sufficient clearance to the truck wheels.

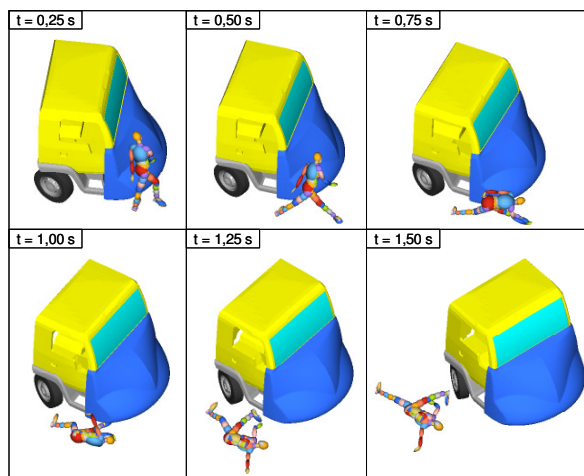


Figure 3. Deflection of the pedestrian in a right-cornering scenario (Version 84).

For the simulation of the run over tests the multi-body simulation software MADYMO (mathematical dynamic modelling) is used.

ASSESSMENT OF THE FINAL DESIGN

For the definition of a run over test procedure the knowledge of typical accident constellations is necessary. This includes the knowledge of the predominant scenarios as well as the knowledge of the most frequent locations of the primary contact in accidents between trucks and vulnerable road

users (VRU). Accident scenarios and assessment parameters can be deduced from those results to cover a broad spectrum of real world accidents.

Accident analysis

In countries of the European Union about 1400 pedestrians (year 2006) and cyclists lost their lives after an accident with a truck. Accident experts expect a possible decrease of about 30 % through new design concepts, test methods and development guidelines. The injury severity of a VRU is depending on different aspects. The collision speed plays an important role beside the geometry of the vehicle front and the position during the primary impact. But also age and height of the pedestrian are relevant. At last, the secondary impact has an influence on the severity of the injury.

The results of a previous APROSYS study [2] showed that accidents with pedestrians are more crucial than accidents with cyclists. Especially the danger of a fatal accident by being rolled over is higher. In the APROSYS study 26 truck-pedestrian accidents from the GIDAS (German In-Depth Data Analysis Study) data base and 30 cases of DEKRA have been regarded amongst further in-depth studies. In 94 % of the cases the truck was driving straight-forward. For inner city areas the scenario of a right cornering truck is relevant as well with a rate of 6 %. Accidents with left-cornering trucks do not occur in the studies. The in-depth data show three characteristic situations for accidents between trucks and pedestrians (Figure 4).

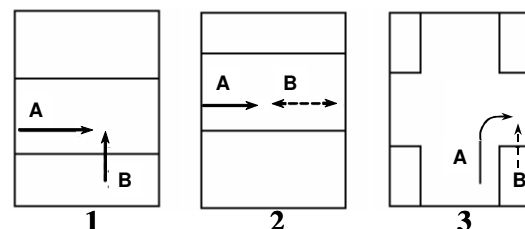


Figure 4. Characteristic situations of truck-pedestrian accidents. [2]

In the first situation a pedestrian tries to cross the road and approaches from the right side. In the second situation the pedestrian walks in or against the driving direction of the truck. Right cornering is the third characteristic situation for an accident. Situations 1 and 3 are typical inner city accident situations whereas situation 2 is more common on non-urban roads.

Regarding the straightforward driving direction of the truck (situation 1 and 2) it is obvious that most impacts occur at the front, whereas the right corner is involved most frequently. The area behind the front axle is not very relevant (only 10 %).

The front right corner of the drivers cabin is also the predominant impact area in situation 3. This scenario is crucial because the affected section is hardly visible or even not visible at all from the drivers seat. As a result the accident partners are rolled over in many of these cases. However the hit pedestrian gets not necessarily underneath the truck in place of the primary impact. Depending on the impact constellation the pedestrian is run over at a subsequent location. 81 % are run over before the right front wheel, 62 % of those are actually rolled over by the front or the rear wheels during the turning process. In contrast to the right side the left side is less relevant. Only 10 % of VRU's impact here and reach under the truck. The results of the accident analysis are used as a basis for the assessment of the optimised front design. [3]

Accident scenarios

Within the APROSYS project the straightforward driving truck turned out to be the predominant accident scenario. Beside this, also the right-cornering situation is relevant. Both situations are regarded for the assessment of the final design. The straightforward driving scenario is comparable to the first situation in Figure 4 with a pedestrian approaching from the right side of the street. The pedestrian model is placed sideways in a walking position in front of the truck. The right-cornering scenario is defined according to situation 3 in Figure 4 but differs in an important aspect. Here the pedestrian model is hit at the entrance of the curve and not at its end as it is shown in the picture. Correspondingly, the pedestrian model is placed in a walking position sideways directly in front of the truck. Because of the curve radius the truck moves also in lateral direction towards the pedestrian. Thereby the position of the pedestrian moves, relatively to the truck, to the front centre. As a result the cornering counteracts a deflection to the right side of the street. This effect has to be compensated additionally (worst case). Both driving scenarios are displayed in Figure 5.

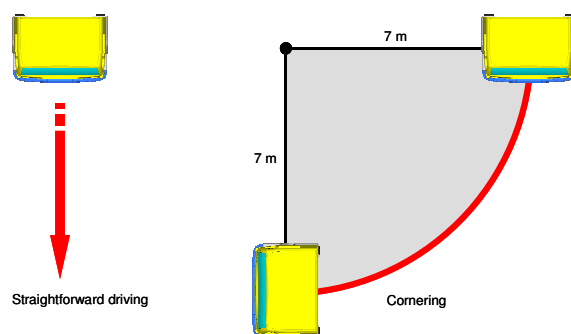


Figure 5. Movement of the truck model.

Another important aspect for the definition of the cornering scenario is the curve radius. The used

radius of 7 m is deduced from the turning circle of the MAN LE 2000, which is 14 m in diameter. DEKRA determined radii of 10 to 15 m, but there are also smaller radii of about 6 m, therefore the chosen 7 m radius represents a good estimation and represents the more critical constellation with respect to side deflection.

Pedestrian models - MADYMO offers a full body pedestrian model. The model is available in five different body heights reaching from a three year old child to the 95 % male model. The three year old child model is not regarded in the tests, due to the low protection potential in an accident with a truck. The included models are shown in Figure 6.

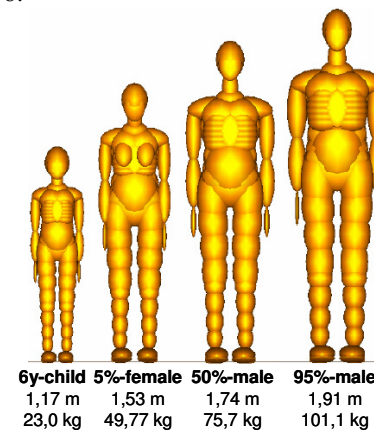


Figure 6. Regarded full body pedestrian models from MADYMO. [4]

The kinematics of the pedestrian models were precisely determined. The legs are able to break at the tibia and the femur. Thereby the impact kinematics can be described more exactly. For the analysis in the tests measuring points record the accelerations, forces and moments. Predictions concerning impact kinematics and the behaviour of throwing the pedestrian up are feasible. Head impact speeds are simulated with a good tendency. Head movements, impact angles and impact points can be simulated accurately. Precise predictions of injuries are not possible. Adequate predictions can be deduced from the measured accelerations.

In addition to the kinematics of the human models also the head impact speeds at the primary and secondary impact are regarded within the assessment of the final design. The head impact point of the primary contact is determined to identify the influence of the different body heights.

Collision speed - An essential factor during a crash is the collision speed of both opponents. This speed has to be chosen appropriate to deliver realistic results. Since both regarded accident scenarios occur in urban areas the speed range is

limited. For the straightforward driving scenario a truck speed of 40 km/h is chosen, which is about 20 % lower than the inner city speed limit and covers a wide field of possible accidents. This speed corresponds to the speed in several full-scale and component tests.

The truck speed in the right cornering scenario is inevitable lower. 87 % of the trucks collide in a right-cornering situation with a speed of only up to 20 km/h, whereas the speed range in most of the accidents analysed by DEKRA reaches from 11 to 15 km/h. Regarding the side deflection behaviour a higher speed would reduce the demands for the side deflection as it would contribute to the impulse given by the shape. Therefore a collision speed of 14,4 km/h (4 m/s) is chosen in the right cornering scenario. Together with the narrow turning circle this scenario sets high demands for the new front structure.

Analyses reveal that the pedestrian is in movement prior to the crash. But within the run over assessment the pedestrian model has no initial speed, which correlates with the common procedure. This approach is acceptable as the pedestrian model is set up directly in front of the truck and due to the low kinetic energy of a walking pedestrian.

Positioning of legs and arms - The positioning of the legs and arms has an important influence on the accident kinematics. Two different postures are simulated to consider this effect. In position 1 the left leg and the right arm are moved forward (walking position). Position 2 is set contrary. The two postures are shown in Figure 7.

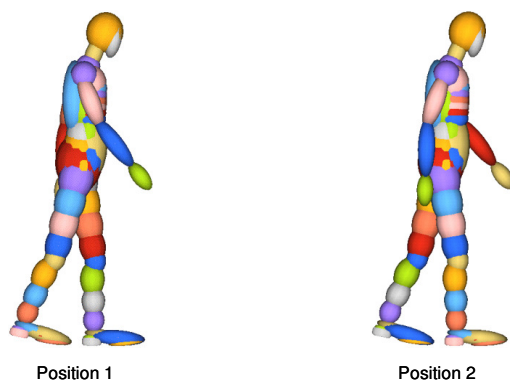


Figure 7. Positioning of the pedestrian model.

Collision angles - Besides the angles of arms and legs the orientation of the human model in relation to the truck defines the pedestrian positioning and the resulting collision angle. Extensive in-depth analyses of car-pedestrian accidents revealed that in more than 90 % of the accidents the pedestrian crossed the street and was hit laterally. In more than 80 % of these cases the pedestrian was

caught in a 3-o'clock or 9-o'clock position by the vehicle front. As the accident analysis records the hit angle with an accuracy of 15°, two different orientations are used for the assessment of the final design. In addition to the 90° orientation of the pedestrian model an angle of 75° is regarded. Both collision constellations are shown in Figure 8.

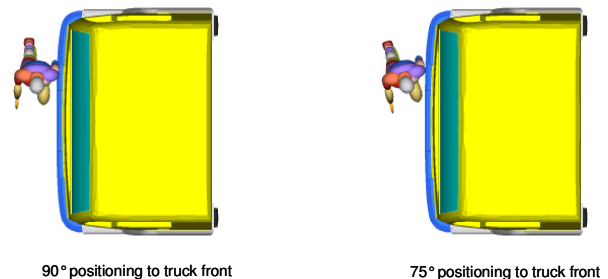


Figure 8. Impact constellations.

Lateral positioning of the pedestrian model -

Three different lateral positions of the pedestrian model in front of the truck are defined for each scenario. The classification in right and left front side is carried out in driving direction.

In the straightforward driving scenario the pedestrian is positioned 50 cm left and right of the trucks longitudinal axis. That matches with the respective middle of each front half of the truck. The third position addresses the centre of the truck with an offset of 15 cm to the right of the longitudinal axis. This offset is necessary, because with respect to a side deflection an exactly centred position represents an instable and undefined situation. By the offset the direction of the deflection is predetermined. Furthermore an exactly centred impact is very improbable. The simulation of a corner impact is not necessary for the straightforward driving scenario, because a sufficient deflection can be taken for granted when the pedestrian isn't run over in the first two positions. This has been proven by several simulations.

The focus in the cornering scenario lies on the right front edge of the truck, which represents the predominant impact area for this scenario. For this reason the pedestrian is positioned in a distance of 80 cm and 100 cm from the trucks longitudinal axis. Since the truck is turning right a wheel angle of 25° is defined. The left side is not as critical as the right side in this scenario, because here the truck moves away from the pedestrian. This effect supports the movement out of the critical area. Therefore a position closer to the centre of the truck front is chosen. Corresponding to the value of the straightforward driving scenario the pedestrian is positioned at a distance of 50 cm from the trucks longitudinal axis. All positions are displayed in Figure 9 by vertical lines.

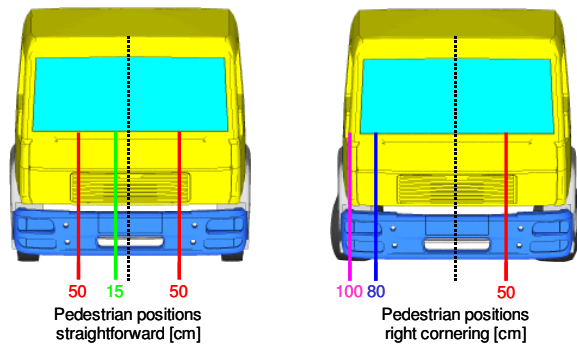


Figure 9. Positions of the pedestrian model relative to the longitudinal axis.

Simulation matrix – The shape of the optimised front has been mainly designed for the 50 % male. The entire assessment described above covers necessarily a much broader spectrum of tests. All tests are also carried out with the basis truck front as a reference. Altogether the parameters defined lead to 192 simulations. The associated simulation matrix is shown in Table 1.

Table 1.
Simulation matrix for the assessment of the final design

Parameters	Test scope	Factor
Crash scenarios	Straightforward driving and cornering	2
Pedestrian models	6 y. child, 5 % female, 50 % and 95 % male	4
Collision speed	One collision speed per crash scenario	1
Positioning of arms and legs	Two postures per pedestrian	2
Collision angle	Two constellations	2
Pedestrian positions	Three positions per crash scenario	3
Truck models	Basic and optimised version	2
Total amount of simulations		192

For the comparison of the improved truck front to the basic design the kinematics, the head speeds and the impact points of the pedestrian models are regarded. Variations of several simulation parameters complete the assessment.

Results of the basis model

The steep front shape of the basis model is representative for existing truck designs in Europe. Only the slight forward reaching front bumper of the MAN LE 2000 is a non-typical feature but is positive for the loads at the primary contact. Nevertheless the steep front shape causes disadvantageous kinematics with the pedestrian rotating to the street.

Accident kinematics - In all scenarios the pedestrian model is thrown straight in front of the truck after the impact and is rolled or run over. Severe injuries are expected in 80 of 96 cases (83,3 %). Only in the 16 cases of the right cornering scenario, where the pedestrian model is positioned on the left side, the results are not as crucial. Here the truck moves away from the pedestrian after the impact. In these cases the essential parts of the body remain in a sufficient distance to the front wheels but still the lower limbs are rolled over. Table 2 gives an overview of the crash characteristics of the basis model.

Table 2.
Overview of the crash characteristics of the basis model for 6 year old child (Ch), 5 % female, 50 % male and 95 % male

Scenario	Position	Ang	Ch	5%	50%	95%
Straight-forward driving	15 cm right	Pos 1	75°			
			90°			
		Pos 2	75°			
			90°			
	50 cm right	Pos 1	75°			
			90°			
		Pos 2	75°			
			90°			
	50 cm left	Pos 1	75°			
			90°			
		Pos 2	75°			
			90°			
Right cornering	100 cm right	Pos 1	75°			
			90°			
		Pos 2	75°			
			90°			
	80 cm right	Pos 1	75°			
			90°			
		Pos 2	75°			
			90°			
	50 cm left	Pos 1	75°			
			90°			
		Pos 2	75°			
			90°			
	Roll over of outer limbs without life threatening injuries					Run or roll over of essential body regions

Fields marked in orange highlight situations where essential body regions of the pedestrian model are run or rolled over. Both effects have to be avoided in respect of an improved pedestrian safety. Only a rolling over of arms and lower legs can be allowed without risking life-threatening injuries. These cases are marked in green.

Despite the missing contact to the wheels a run over implicates a great danger for the pedestrian and is almost as critical as a roll over. Therefore roll and run over of a pedestrian model are rated equally. Besides a roll over can only be determined for the front axle with the available model. Further axles are not regarded and the roll over of pedestrians by the rear axles can not be detected.

Figure 10 shows an example of a run over situation in the straightforward driving scenario. The sequence shows the 5 % female at a collision angle of 75° positioned 50 cm right from the front centre. Arms and legs are in position 1. As a result of the steep front it cannot be avoided that the pedestrian reaches under the truck. In the sequence the model is only run over but in 11 of the 16 cases within this scenario the pedestrian model is actually rolled over. Five of these cases are highly crucial as essential body regions are rolled over.

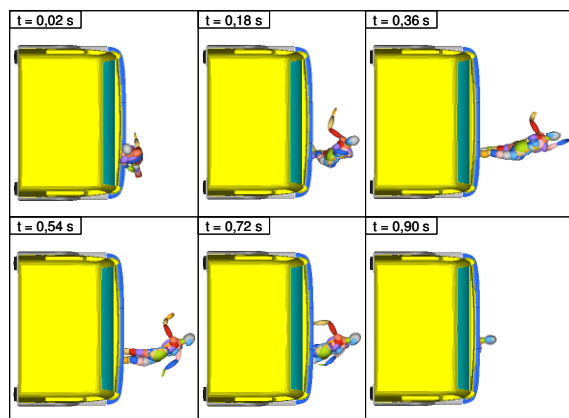


Figure 10. Kinematics of the 5 % female in the straightforward driving scenario.

In the right cornering scenario all cases with an impact at the right truck side result in a run or roll over situation. Figure 11 shows an according crash with a six year old child model.

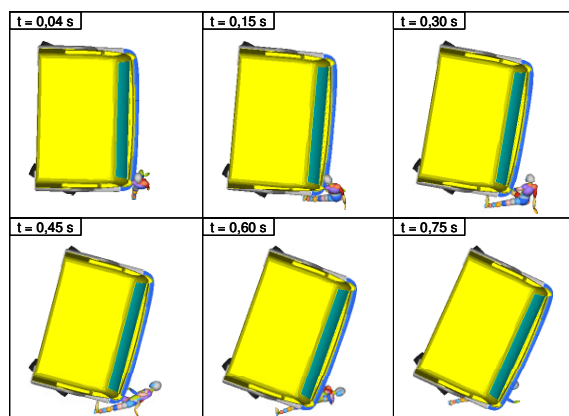


Figure 11. Kinematics of the six year old child in the cornering scenario.

Head impact areas - Body height and collision constellation affect the head impact area. Due to the fact, that the pedestrian models are positioned directly in front of the truck the head impact points are nearly identical to the initial head position. In four cases of the six year old child, a second impact of the head occurs. This happens in the cornering scenario when the model is hit by the edge of the truck. The head strikes the bumper while the model is falling down.

The head impact areas can be seen in Figure 12 divided into straightforward driving and cornering scenario. On the left side impact areas of the six year old child and the 5 % female are illustrated. The right side shows the impact areas of the male pedestrian models. Each mark represents one of the defined scenarios and comprises all impact points of the corresponding model within this scenario. A missing mark indicates, that a head impact has not been detected in all of the four belonging cases.

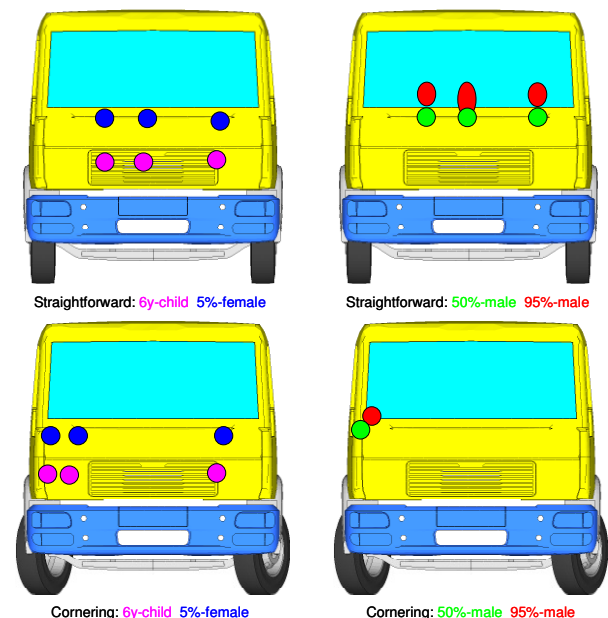


Figure 12. Head impact areas.

Summary - The pedestrian safety potential of the basis structure can be estimated as very poor. All crash situations lead to run or roll over events. The flat front design pushes the pedestrians straight in front of the truck. Regarding pedestrian protection, this is a big disadvantage of today's truck front designs. Measurements, like rounding the edges, that decrease the severity of injuries at the primary impact are not sufficient as long as there is such a high risk for the pedestrian of getting under the truck.

The head impact speeds of the primary impact can be regarded as relatively good, except for the six year old child. In many cases there is even no

contact of the head with the front due to the straight impact of the pedestrian model. The simulations reveal high head impact speeds during the secondary impact. The burden on the head is significantly higher compared to the primary impact. In this context it is interesting to what extent the deflection effect of the optimised front shape will influence the speed level of the secondary impact.

Results of the optimised model

The optimised front leads to completely different kinematics compared to the basis truck. Due to the effect of throwing the pedestrian model up with the resulting rotary motion towards the truck a head contact to the front is very probable. So it can be expected that compared to the basis model there will be less cases without a head contact. As before the roll over of non essential body parts like feet, lower legs and arms are regarded as non critical. Nevertheless, the predominant aim of the new front structure is the entire prevention of run and roll over situations.

Accident kinematics – Only 16 cases of the basis model fulfil the requirements for a non critical assessment. The optimised model reveals a highly improved behaviour with 84 cases rated uncritical (87,5 %). So in most cases fatal injuries resulting from a run or roll over of the pedestrian can be avoided. Regarding the 12 cases with fatal injuries the 95 % male model is affected six times, the six year old child is involved four times and the 5 % female two times. The right cornering scenario with a position of the pedestrian model 80 cm right from the longitudinal axis shows the highest number of critical cases. Table 3 gives an overview of the simulation results of the optimised front. The results for the 50 % male model are particularly good, because the front geometry has been designed for it.

Out of the three situations of the straightforward driving scenario the impact of the pedestrian model next to the front centre is the most challenging constellation for the new structure. In this situation a maximum deflection of the pedestrian is required. Four critical cases occur, where the deflection is not sufficient. A roll over of essential body parts is identified for the six year old child in both constellations with arms and legs in position 2. Due to the low impact point of the child model the plateau geometry is here mainly responsible for the kinematics. Near to the front centre the plateau shows only a slight curvature. Thus a strong deflection impulse cannot be generated for the child model, although its low weight has a positive influence. A negative effect of posture 2 can also be detected for the other pedestrian models.

Table 3.
Overview of the crash characteristics of the optimised model for 6 year old child (Ch), 5 % female, 50 % male and 95 % male

Scenario		Position		Ang	Ch	5%	50%	95%
Straight-forward driving	15 cm right	Pos 1	75°					
			90°					
		Pos 2	75°					
			90°					
	50 cm right	Pos 1	75°					
			90°					
		Pos 2	75°					
			90°					
	50 cm left	Pos 1	75°					
			90°					
		Pos 2	75°					
			90°					
Right cornering	100 cm right	Pos 1	75°					
			90°					
		Pos 2	75°					
			90°					
	80 cm right	Pos 1	75°					
			90°					
		Pos 2	75°					
			90°					
	50 cm left	Pos 1	75°					
			90°					
		Pos 2	75°					
			90°					
	No run or roll over / Roll over of outer limbs without life threatening injuries					Run or roll over of essential body regions		

Figure 13 shows an example of a prevented run over situation in the straightforward driving scenario. The sequence shows the 95 % male model in posture 1 with an impact angle of 90°.

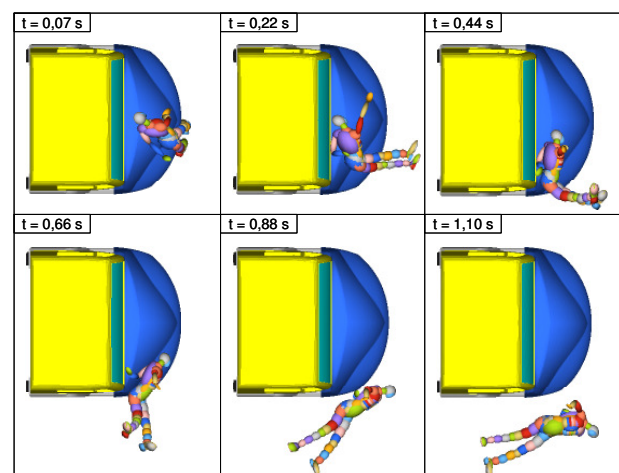


Figure 13. Kinematics of the 95 % male in the straightforward driving scenario.

Although the impact occurs next to the centre of the truck front and despite the height and weight of the 95 % male the model is deflected far enough to the side. This is a good example for the potential of the tapered front structure. With only four critical cases in 48 situations of the straightforward driving scenario its effectiveness can be regarded as good in comparison to the basis model showing a run or roll over of vital body parts in all constellations.

In Figure 14 an example of the right cornering scenario is displayed. It shows the kinematics of the six year old child model with arms and legs in position 2 and a collision angle of 90°. In the illustrated position at 100 cm right to the centre of the truck front only one case is critical. The torso of the 95 % male dummy is rolled over due to a disadvantageous drop behaviour caused by a broken shinbone. In all other cases the kinematics are good.

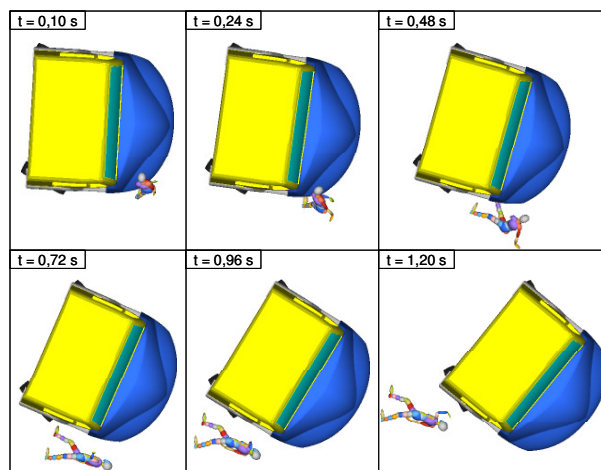


Figure 14. Kinematics of the 6 year old child in the cornering scenario.

In the second constellation (position 80 cm to the right) of the cornering scenario it becomes apparent that the design is optimised for the 50 % male model. The 50 % male dummy is sufficiently deflected to the side in all cases while the 95 % male dummy is rolled over after fractures of the shinbone. The 5 % female shows one critical situation. The kinematics of the six year old child depend on the collision angle. Both situations with a collision angle of 75° show good kinematics without a roll over of body parts. However under a collision angle of 90° the torso is rolled over. The kinematics of the 50 % male for a collision angle of 75° and with arms and legs in position 1 are shown in Figure 15.

No roll over is identified in the third crash constellation of the cornering scenario with the impact on the left front side. This scenario is not as critical as the other scenarios. The basis model has

no critical cases in this scenario as well. Nevertheless, the pedestrian safety is improved. In the basis model the lower extremities are rolled over. This can be avoided with the improved front structure

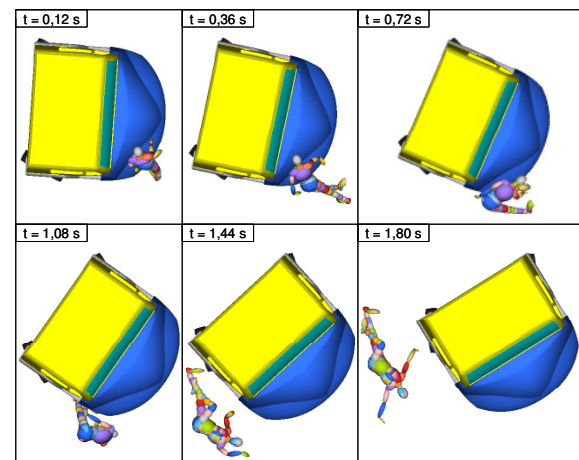


Figure 15. Kinematics of the 50 % male in the cornering scenario.

Eight critical cases are detected in the cornering scenario. That is two times as much as in the straightforward driving scenario but still relatively low compared to 48 cases tested.

Head impact areas – As expected the head impact occurs more frequently with the optimised front. One example is given in Figure 16, where the impact of the 50 % male model next to the front centre is shown for both models. Whereas there is no impact of the head at the truck front with the basis model, the kinematics caused by the optimised shape lead to a head contact.

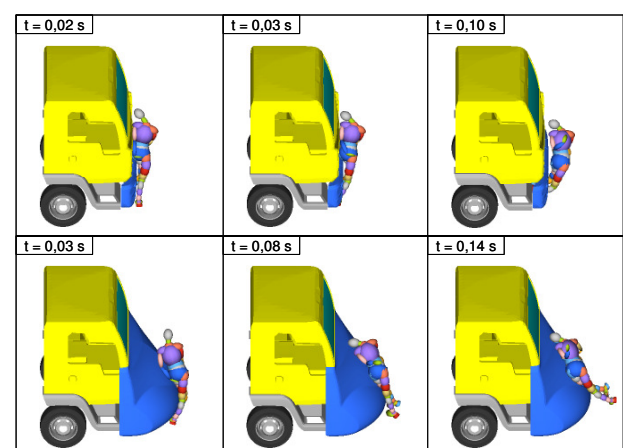


Figure 16. Comparison of primary contact with basis and optimised front (50 % male).

Despite the throwing up effect in three cases still no head impact can be detected for the 95 % male model.

The head impact areas are displayed in Figure 17 divided into straightforward driving and cornering scenario. On the left side impact areas of the six year old child and the 5 % female are illustrated. The right side shows the impact areas of the male pedestrian models. Each mark represents one of the defined scenarios and comprises all impact points of the corresponding model within this scenario.

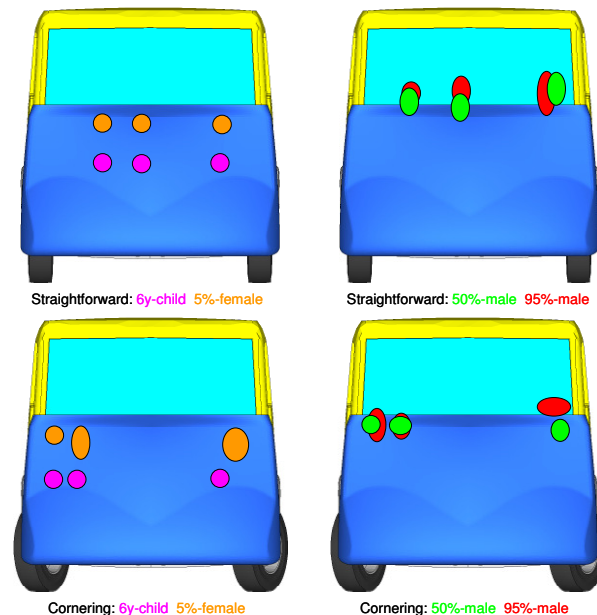


Figure 17. Head impact areas.

Head impact speeds - Overall the head impact speeds in the straightforward driving scenario vary only in single cases from the basis model. Positive and negative deviations are found. However the rotary motion of the pedestrian models caused by the optimised shape has a bad influence on the secondary impact. In the regarded constellations the head of the pedestrian hits the road first. As a result high head loads can be assumed. An evaluation within the parameter studies has to show if this effect depends on the truck speed or occurs in general.

In the cornering scenario the kinematics caused by the new front structure have a beneficial effect on the head speeds. Especially the more critical secondary impact shows lower values in most of the cases. However higher speeds are detected for the primary impact due to the effect of throwing the pedestrian up, which makes a contact of the head with the truck front more probable.

Parameter studies - The parameter variations for both accident scenarios are assessed with the 50 % male pedestrian model at a collision angle of 90° and arms and legs in position 1. This corresponds with the constellation during the design phase of the optimised front.

In the straightforward driving scenario a speed of 16 km/h leads to a sufficient side deflection when the model is positioned 50 cm next to the front centre. For positions closer to the side of the truck the speed is even less critical. The rotary motion of the pedestrian, which occurred in many simulations, shows a relevant effect at speeds higher than 30 km/h. At that speed the pedestrian model is rotated so far into a horizontal position, that it hits the road with the back of the head first.

Increasing the speed from 4 to 5 m/s in the cornering scenario leads to bad results for the male models. The shinbone breaks at that speed and loses its supporting function. The model falls right in front of the truck. However, a reduction of speed to 3 m/s is uncritical. Despite the low speed a sufficient deflection is still achieved and a roll over of the pedestrian model can be avoided.

Another varied parameter is the positioning of arms and legs. In the straightforward driving scenario also an upright (not walking) posture provides a sufficient side deflection. A positive effect with this constellation is the missing rotary motion of the pedestrian model. Thus the head is not the first body part which hits the road at the secondary impact. It can be concluded that the rotary motion results from the walking posture of arms and legs. Figure 18 shows the kinematics of the standing pedestrian model. The model is sufficiently deflected to the side and is not rolled over by the truck.

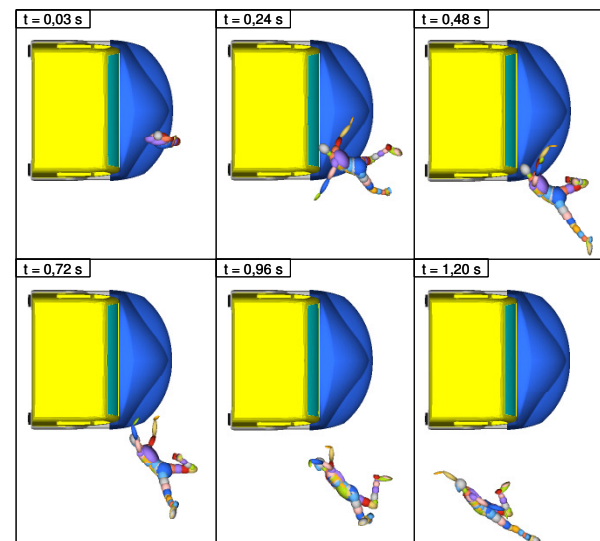


Figure 18. Kinematics of the standing 50 % male model.

In the cornering scenario a sufficient deflection for the upright posture can only be achieved for an edge impact. For the walking postures a position 70 cm right from the longitudinal axis is critical. The pedestrian model is no longer deflected far

enough out of this position. It remains within the unsafe area.

Beside the parameter studies also strength and HIC analyses have been conducted with a FE-model of a detailed designed add-on solution. It has been proven, that despite lightweight design such a structure is able to withstand a pedestrian impact. Also the HIC values at primary impact are improved by the optimised front.

Experimental test – A prototype of the optimised front out of EPP foam is tested in a straight-forward driving scenario at a speed of 30 km/h. For good control of the impact speed the truck is not driven by its own engine but pulled with a towing device. The driver inside the truck is only steering (Figure 19). [5]



Figure 19. Connection of prototype to the truck. [5]

Due to the risk of possible damage caused by a run over, the pedestrian model used for the test is a simplified 50 percentile dummy without instrumentation and a weight of 75 kg. It is positioned exactly between the centre of the truck and the right truck side in a walking position with the leg that is standing forward facing the truck front. Consequently, the dummy is impacted laterally.

Figure 20 shows a picture sequence of the experimental run over crash test. It can be observed that the pedestrian model is deflected to the side as intended instead of being run over. As a result of the simple pedestrian dummy mainly set up from rigid body parts connected by standard joints the biofidelity is limited. However, the experimental test shows good consistence compared to the simulation of the same accident scenario. The picture sequence of the respective simulation is presented in Figure 21. The good correlation between experiment and simulation shows the principal applicability of numerical simulation for the risk evaluation of a run over.



Figure 20. Experimental test. [5]

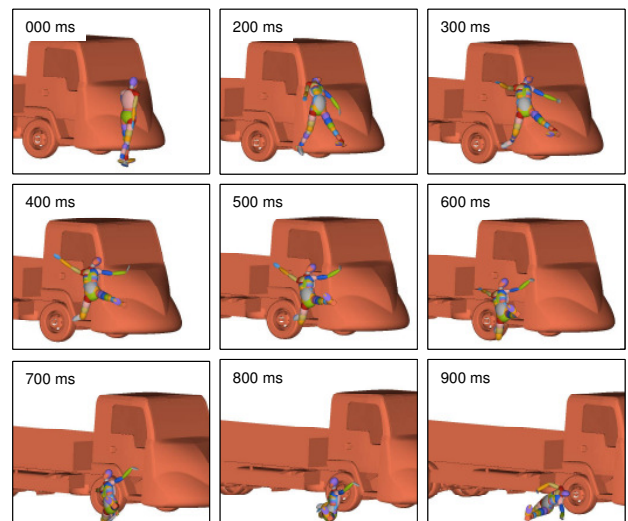


Figure 21. Simulation with parameters of experimental test.

Summary - The results of the performed tests prove the effectiveness of the optimised front. The simulations show that the optimisation of current truck front designs can lead to a significant improvement. The passive safety is enhanced because serious roll over accidents are avoided in 87,5 % of the simulated cases.

In the straightforward driving scenario, according to accident analysis the most important scenario, a sufficient deflection can be guaranteed in a wide range of constellations even for low speeds of the truck. Only an impact very close to the centre of the front is sometimes critical and requires a certain velocity for a sufficient deflection.

The right cornering scenario is more sensitive. Impacts closer than 80 cm to the longitudinal axis lead to run or roll over situations on the right side.

Within the effective area of the front especially the 95 % male pedestrian model shows critical results. On the one hand there are anthropometrical reasons for this but on the other hand a main problem is the fracture of the shinbone at the primary impact. Further tests have to indicate if this issue can be improved by the designated structural foam in the bumper, which has not been regarded within the simulations. In general better results are achieved with an impact angle of 75° . Referring to the real accident this is advantageous, because due to the cornering an impact angle of exactly 90° is rather unlikely.

INTEGRATED DESIGN APPROACH

An add on solution of the optimised front as used for the crash test is not an efficient solution with respect to costs, weight and appearance. In order to fully exploit the benefits of such a design the shape has already to be considered in the early design phase and must be an integral part of the cabin. Figure 22 indicates how such a cabin could look like.

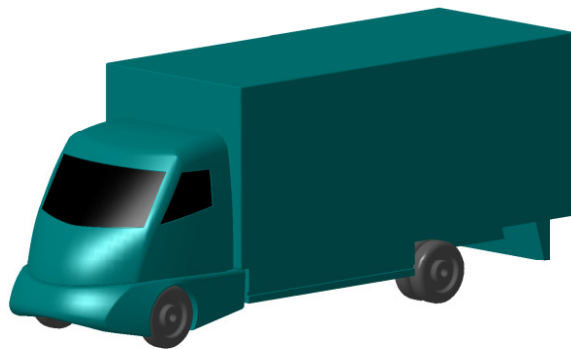


Figure 22. Integrated design approach.

The design study by DAF, shown in Figure 23, could also be considered as a first approach for a design with an improved pedestrian safety.

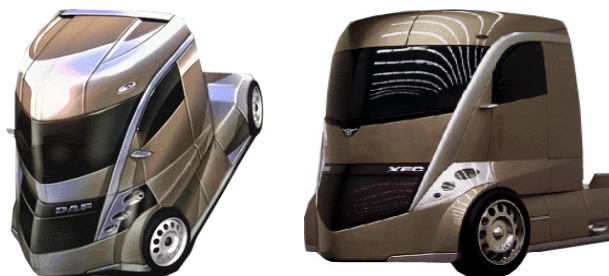


Figure 23. Design study by DAF.

Moreover, with respect to the current European legislation that limits the total length of trucks the market implementation of such a tapered shaped front design is unlikely, since the loading space would have to be reduced. Discussions during the

APROSYS final workshop have disclosed that the truck manufacturers are principally supporting the implementation of passive safety devices at the truck front in case legislation allows an increase of the total vehicle length for those measures.

Aerodynamics

Beside the improved passive safety the optimised design seems also to have potential in reducing fuel consumption due to its streamline design. A 1:10 model is used to study the wind resistance of this design versus a flat front design (Figure 24).

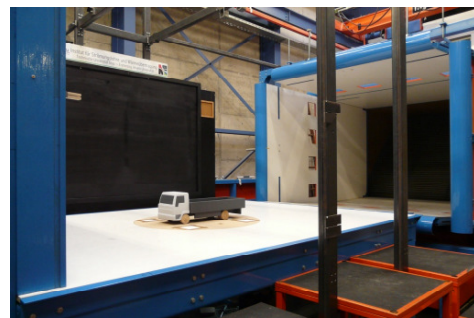


Figure 24. Overview of wind tunnel with truck model. [6]

The truck is modelled of wood and foam. The wind tunnel tests are performed with velocities up to 40 m/s. Measurements are forces and moments in all directions. The calculation of the drag coefficients is referenced to the truck width or the cross section area (characteristic dimensions). During the tests the airflow is made visible by artificial fog. This shows clearly the benefits of a homogenous airflow around the vehicle as it is illustrated by Figure 25 and Figure 26.

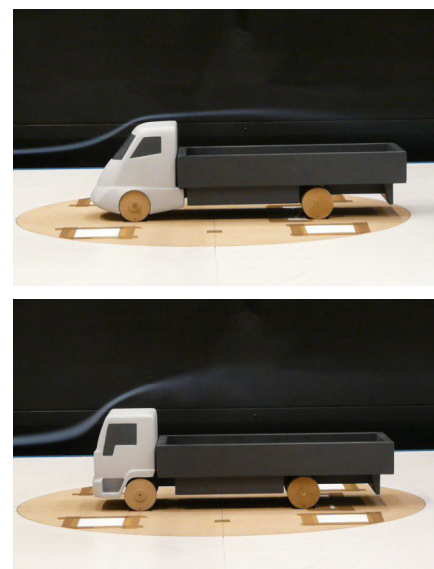


Figure 25. Visualisation of aerodynamics in the wind tunnel for a tipper type truck. [6]

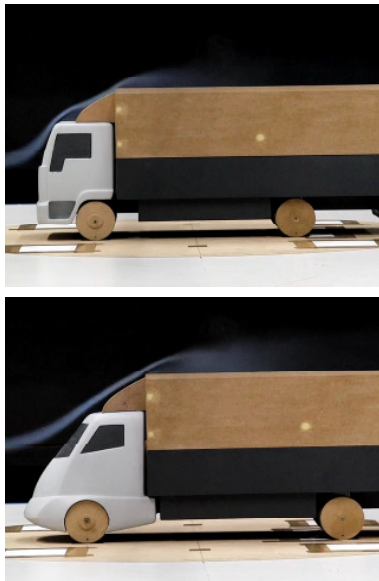


Figure 26. Visualisation of aerodynamics in the wind tunnel for a box truck with spoiler. [6]

The optimised design shows a clearly lower drag coefficient compared to the standard truck. The decrease of the drag coefficient lies between 0.10 and 0.33. This is equivalent (not taking into account the scale of the model) to a reduced fuel consumption of 1.2 to 3.6 litres per 100 km. [6]

CONCLUSIONS

The results of the performed tests prove the effectiveness of the optimised front. The simulations show that the optimisation of current truck front designs can lead to a significant improvement. The passive safety is enhanced because serious roll over accidents are avoided in 87,5 % of the simulated cases.

Numerical simulations and experimental testing have not only shown the relevance of the primary impact for serious injuries. The secondary impact on the ground is just as important as the primary impact. Further studies of enhanced front structures should also consider post-impact kinematics and the secondary impact of the VRU.

In general a tapered shaped truck front is a simple and cost efficient passive measure to reduce the risk of a run over of VRUs by heavy vehicles. Beside this main purpose there are also positive effects on:

- Contact forces at primary impact of the VRU (additional crush space)
- Vehicle to vehicle compatibility (improved frontal underrun)
- Occupant safety (additional crush space)
- Aerodynamics (streamline shape)

- Package (more space due to longer cabin)

The introduction of an optimised front design for trucks requires a reconsideration of the vehicle length regulations. With the current legislation the vehicles are designed to maximise loading space and payload. Because the main business is to carry freight with the heavy goods vehicles, optimisation is made with regard to maximum loading (volume and payload) under current length. All measures reducing payload or volume are not taken into account. Therefore the allowance for additional vehicle length for the implementation of safety features is a basic requirement with respect to an improved passive safety of current trucks. The presented design is also transferable to other transportation systems like trams or buses.

REFERENCES

- [1] Faßbender, S.; Feist, F.; Niewöhner, W. Demonstrator module for new design concepts APROSYS SP2.1 Deliverable D2.1.3, 2007
- [2] Mesina, C.T.; Margaritis, D.; de Vries, Y.W.R.; Niewöhner, W.; Ruijs, P.A.J. Characteristics of Heavy trucks versus Pedestrians and/or Cyclists APROSYS SP8.3 Deliverable D8.3.5, 2006
- [3] Niewöhner, W.; Berg, F. A. Gefährdung von Fußgängern und Radfahrern an Kreuzungen durch rechts abbiegende Lkw BAST report F 54 DEKRA Automobil GmbH, Stuttgart, 2005
- [4] N. N. MADYMO Human Models Manual Release 6.3.1 TNO, 2006
- [5] Faßbender, S.; Feist, F. System description of the experimental safety module APROSYS SP2.1 Deliverable D2.1.5, 2008
- [6] Faßbender, S.; Feist, F.; Gugler, J. Guidelines for integrated design and evaluation of advanced vulnerable road user protection systems APROSYS SP2.1 Deliverable D2.1.7, 2009

EVALUATING CRASH AVOIDANCE COUNTERMEASURES USING DATA FROM FMCSA/NHTSA'S LARGE TRUCK CRASH CAUSATION STUDY

Kristin J. Kingsley

National Highway Traffic Safety Administration
United States of America
Paper Number 09-0460

ABSTRACT

Real world crash data are used to estimate the size of crash populations addressable by crash avoidance countermeasures. Until the release of the data from the Large Truck Crash Causation Study (LTCCS) that was conducted from 2001 to 2003 by the Federal Motor Carrier Safety Administration (FMCSA) and the National Highway Traffic Safety Administration (NHTSA), only coarse estimates of those target populations were possible using data from the Fatality Analysis Reporting System (FARS) and the National Automotive Sampling System's General Estimates System (NASS GES). Both of these databases contain limited information that is coded from police reported data.

The LTCCS conducted on-scene investigations of real world crashes that resulted in a database of 1070 cases rich in detail, specifically related to precrash conditions and factors associated to why the crash occurred. The detail in the data was enough to make clinical (case by case) estimations of the applicability of crash avoidance countermeasures for each crash, based on our knowledge of these systems and how effective they are in certain scenarios. Final benefit estimates would take into account the applicable target populations and the effectiveness of a system, as determined through field operational tests or some other measure.

This study presents the results of clinical reviews of truck crashes from the LTCCS to determine which target populations of crashes could be candidates for prevention given the multiple factors that came into play. Countermeasures related to the truck, truck driver, or trucking industry might have prevented 61 percent of the crashes in LTCCS, including 50 percent that might have been prevented by advanced technologies that are currently available for trucks. The newly coded data from these clinical reviews can be used to further refine the applicable crash populations estimated from FARS and GES. This research indicates that only a portion of applicable crash scenarios identified through FARS and the NASS GES are candidates for prevention by crash avoidance countermeasures.

The results present an option for a more accurate methodology for estimating the size of crash populations addressable by crash avoidance countermeasures. Using these results it is possible to prioritize research on crash avoidance countermeasures.

BACKGROUND

In 2007, an estimated 413,000 heavy vehicles were involved in crashes which resulted in 4,808 deaths and 101,000 injuries. Of the fatalities that resulted from heavy truck crashes, 75 percent were occupants of a light vehicle, 8 percent were nonoccupants, and 17 percent were occupants of a large truck [1]. Crashes involving heavy vehicles are severe events. Due to the nature of crashes which involve heavy trucks and another vehicle (extreme differences in mass and energy), the greatest potential to save lives and reduce injuries comes from crash avoidance countermeasures. Advances in crashworthiness aim to protect motor vehicle occupants given that a crash occurs. Advances in crash avoidance technologies present the opportunity to prevent these crashes from occurring in the first place. Preventing heavy vehicle crashes can result in a big impact by focusing on a specific population of crashes, whose prevention would result in a significant number of lives saved and injuries avoided.

INTRODUCTION

The first step to prevent crashes is to gain a complete understanding of how and why they happen. Through a joint effort by the Federal Motor Carrier Safety Administration and the National Highway Traffic Safety Administration, a major on-scene data collection effort was undertaken to identify events leading up to crashes and factors that contribute to them. It was called the Large Truck Crash Causation Study.

The LTCCS data were collected on-scene by trained crash researchers at 24 representative locations throughout the United States. The on-scene nature of the study allowed for richer and more accurate data

than a study based on after-the-fact investigations would have.

Data collected on-scene and from follow-on investigations were compiled for each case and a crash event assessment was made using all of the available information. The crash event assessment for a crash occurrence consists of three elements for each vehicle involved in the crash: the “critical precrash event”; the “critical reason for the critical event”; and “associated factors”.

The “critical precrash event” is the action or event that placed the vehicle on a collision course such that the collision was unavoidable given reasonable driving skills and vehicle handling. In other words, the “critical precrash event” makes the crash inevitable. The “critical precrash event” is typically coded in relation to a pedestrian, nonmotorist, object, other motor vehicle, or animal that the subject vehicle was attempting to avoid. It is important to note that culpability/fault is not considered when making the “critical precrash event” determination.

The “critical reason for the critical event” is the immediate reason for this event and is often the last failure in the causal chain (i.e., closest in time to the “critical precrash event”). This variable establishes the critical reason for the occurrence of the critical event. Although the critical reason is an important part of the description of the crash event, it is not the cause of the crash nor does it imply the assignment of fault. The primary purpose for the “critical reason for the critical event” is to enhance the description of crash events and allow analysts to better categorize similar events [2].

While there is only one critical reason coded per crash, this variable is documented at the vehicle level. Therefore, for each multiple-vehicle crash, there is at least one vehicle for which the critical reason is coded as “No driver error,” which means the critical reason was coded to another vehicle in the crash. Table 1 shows the results from the LTCCS for the “critical reason for the critical event” codes. A general level of detail is shown, but each level contains several more detailed elements.

**Table 1 [3].
Weighted Number of Involved Vehicles
By Critical Reason (General Level), Crash Type, and Involved Vehicle Type**

Critical Reason (General Level)	Single-Vehicle Crash		Multivehicle Crash						Total					
	Truck		Truck		Vehicle		Total		Truck		Vehicle		Total	
	#	%	#	%	#	%	#	%	#	%	#	%	#	%
No Driver Error	1447	4	61913	60	58252	58	120164	59	63360	45	58252	58	121612	50
Physical Driver Factor	7744	20	1377	1	6214	6	7590	4	9121	6	6214	6	15335	6
Driver Recognition Factor	6309	17	15883	15	12421	12	28304	14	22193	16	12421	12	34613	14
Driver Decision Factor	12621	33	16886	16	11106	11	27992	14	29507	21	11106	11	40612	17
Driver Performance Factor	4425	12	2758	3	7617	8	10375	5	7182	5	7617	8	14800	6
Vehicle Related Factor	4831	13	2956	3	1577	2	4533	2	7787	6	1577	2	9364	4
Environment - Highway	599	2	950	1	510	1	1460	1	1549	1	510	1	2059	1
Environment - Weather	127	0	114	0	541	1	655	0	241	0	541	1	782	0
Unknown Reason	23	0	238	0	1591	2	1829	1	261	0	1591	2	1852	1
Total	38127	100	103047	100	99829	100	202902	100	141200	100	99828	100	241028	100

Source: NHT SA, NCSA, LT CCS. Study time span: April 1, 2001 - December 31, 2003.

Associated factors can be related to the drivers involved in the crash, the vehicles, and/or the environment. The NASS researcher collected as

much data as possible related to factors present prior to the crash. Factors were coded when present; no determination was made as to whether or not they

contributed to the crash. These factors are important to provide more detail for each crash and to set the stage for relative risk analyses using the entire data set. Relative risk analyses will determine whether the presence of certain factors increases the risk of a crash occurrence. For example, in the LTCCS, alcohol would still be coded for a drunk driver stopped for a red light who got rear-ended even though alcohol did not play a role in this crash. Statistical analysis in the end would show if alcohol was more prevalent in striking or struck vehicles in similar crash scenarios.

ANALYSIS

Heavy vehicle research must be focused to have the highest impact to prevent crashes involving large trucks. To accomplish this, crash types must be accurately quantified and mapped to potential countermeasures. This results in the identification of the largest crash problems and identifies possible solutions to them. Analysis of LTCCS data can play an important role in this process by improving the accuracy of crash population estimates for specific countermeasures.

A Volpe study shows that 90 percent of crashes are caused by driver error (see Figure 1) [4]. LTCCS data also shows that more than 80 percent of associated factors are coded as driver-related factors.

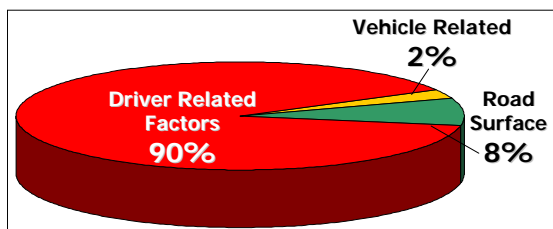


Figure 1. Crash Causal Factors [5].

Until we had the rich precrash data from the LTCCS, we relied solely on estimates from FARS (for fatalities) and GES (for injuries). Crash scenarios were coded, technologies were mapped to the scenarios they may be able to prevent, and then populations were defined to feed into effectiveness estimates. But, for example, how many run-off-road scenarios might actually be prevented by lane departure warning systems, if a portion of those are due to a physical inability to control the vehicle (i.e. heart attack or seizure). We can't get this information from FARS and GES. But we can get it from LTCCS.

Findings from the LTCCS analysis show that regardless of which vehicle or the types of factors that contributed more to the crash, in 52 percent of truck vs. light vehicle crashes, countermeasures on the truck may have helped to prevent the crash. And in 70 percent of the truck vs. nonmotorist crashes, countermeasures on the truck may have helped to prevent the crash. These are the target populations which would then be multiplied by system effectiveness estimates to give overall benefits estimates of each countermeasure.

As for individual countermeasures – how do we prioritize them? Which are applicable to largest target populations and present us with an opportunity to prevent the most crashes and save the most lives?

The objective of the analysis presented in this paper is to estimate the size of crash populations addressable by crash avoidance countermeasures using very detailed real world crash data. NHTSA uses multiple data sources to prioritize research on advanced technologies, to support regulatory activities, and to provide information to consumers. The precrash data from each of these resources, thus far, has been extremely limited, with details focused on crash configurations and injury mechanisms. The detailed precrash data from the LTCCS can explain how and why crashes occurred which leads to more accurate target population estimates, which in turn will lead to more accurate benefits estimates.

There are different ways to analyze a data set such as the LTCCS. One can perform relative risk analyses to determine whether the presence or absence of certain factors increases the likelihood of a crash. Another method, which was used in the analysis this paper presents is a clinical method.

In depth, clinical reviews of each case were completed to make individual determinations as to what happened in each crash and what could have prevented each crash.

New data elements were coded for each case, specifically whether the crash should be included in the target population of crashes that may be prevented by a countermeasure. The list of countermeasures included was identified using several factors. Only advanced technologies that are newly penetrating the commercial vehicle market or are soon to penetrate were included. They had to have a reasonable expectation to be successful in preventing crashes or mitigating injuries by reducing crash severity. The following advanced technologies,

from warning systems to active vehicle interventions, were included in the analysis:

Augment Driver Performance

- Lane Departure Warning (LDW)/Lane Keeping Assist(LKA)
- Forward Collision Warning (FCW)
- Blind Spot Detection (BSD)/Lane Change Warning
- Drowsy Driver Detection
- Backover Crash Prevention
- Night Vision
- Tire Pressure Monitoring System (TPMS)

Augment Vehicle Performance (intervene when driver action would be insufficient to prevent a crash

- Roll Stability Control (RSC)
- Electronic Stability Control (ESC)

In addition to the technologies listed here, non-technological countermeasures were considered, such as:

- Stricter Vehicle Maintenance Requirements
- Enhanced Conspicuity
- Driver Training and Education
- Stricter Driver Licensing Requirements
- Alcohol and Drug Enforcement
- Miscellaneous Others

With these countermeasures in mind each case was reviewed using the following clinical review process. First, by reviewing case summaries, then scene diagrams, pictures, the crash event assessment forms and any other coded data identified as necessary, a determination was made as to whether or not each crash should be included in the target population for each countermeasure considered.

In the case example illustrated in Figure 2, a truck was traveling in the center lane next to a light vehicle in lane 1. The truck initiated a lane change maneuver to the right and impacted the car. The crash event assessment form shows the critical event, critical reason for the critical event and all of the associated factors in the crash. The case data (Shown in Figure 3) includes separate tabs for different kinds of factors. Drugs and alcohol are rarely coded as critical reasons for the critical event, but if they are present, they are included as associated factors.

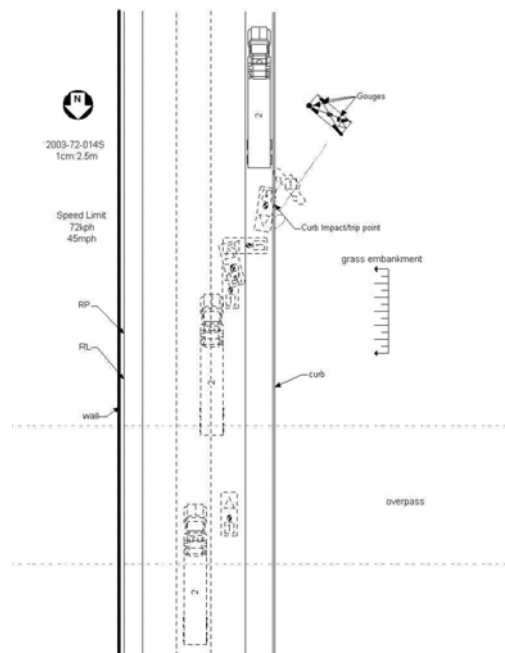


Figure 2. Photos and Scene Diagram from Example Case 2003-72-014.

The screenshot displays the 'TRUCK Case # 2003-72-0145: Display Mode - [Crash Assessment Case No: 2003-72-0145/ Vehicle No: 2/ Mode - Display]' window. The interface includes a menu bar (File, Components, Actions, Process, View, Report, Review, Options, Window, Help) and a tabbed toolbar with categories like Pre-Crash Events, Jackknife Event, Cargo Shift, Support Data, Driver Physical Factors, Driver Assessment, Traffic Factors, Vehicle Factors, Roadway Factors, Weather/Other Environment, and Source.

The main data entry area is divided into several sections:

- Movement:** Pre-event movement is set to 'Changing lanes'.
- Critical Pre-Crash Event/Reason:**
 - Event:** Category is 'This vehicle traveling', and Events is 'Over the lane line on right side of travel lane'.
 - Reason:** Category is 'Driver Recognition Factor', and Reasons is 'Inadequate surveillance (e.g., failed to look, looked but did not see)'.
- Pre-Crash Details:**
 - Avoidance Maneuver: 'No avoidance maneuver'.
 - Pre-Impact Stability: 'Tracking'.
 - Pre-Impact Location: 'Stayed on roadway but left original travel lane'.
 - Right of Way: 'No'.
- Crash Type:** A diagram shows a vehicle labeled '44' with an arrow indicating a lane change. Below the diagram, 'Crash Type' is set to '44', and the selected crash type is 'Sideswipe/Angle'.

At the bottom, there is a 'Close' button and a status bar showing 'Queries >> 16'.

Figure 3. Screen Capture of Case Data from Example Case 2003-72-014.

In this case, the critical reason was coded as inadequate surveillance (See Figure 3). The car was in the truck's blind zone. This case was fairly straightforward because the countermeasure that could have prevented this crash was some kind of blind zone detection system or lane change assist. There could be confounding factors that would exclude a case from the target population (such as when a driver suffered a heart attack that precipitated the crash), but this case was kept in because there were no such factors. For many other cases in the LTCCS countermeasures were coded not only for the truck, but for the light vehicles and the environment as well.

RESULTS

The advantage of such a clinical review is to gain a better understanding of what kinds of crashes define the target populations that are preventable by crash avoidance technologies and what percentage of the applicable population of crashes could actually be mitigated. In addition, we can identify crashes that may be prevented by advanced technologies that otherwise would have gone unnoticed based solely on the data in a police report. This increases our target population and gives better benefits estimates.

Only 10 percent of the LTCCS crashes could be considered unpreventable with the rest having a reasonable expectation of being included in target populations that have the potential to be prevented by some countermeasure on either the heavy vehicle or a passenger vehicle, if one was involved. Countermeasures include advanced technologies, stricter vehicle maintenance requirements, alcohol enforcement, etc. If you go far enough back in the chain of events, almost everything is preventable.

A breakdown of the unpreventable crashes is shown in Table 2 including some reasoning as to why countermeasures would not have been able to address each.

Table 2.
Unpreventable Crash Types from the LTCCS

Unpreventable Crash Types	Number of LTCCS Crashes Applicable
Medical Condition	25
Intersection Crash	19
Poor Driving Skills/Bad Decisions	16
False Assumption of Other Road User's Actions	14
Caused by Previous Event	10
Blew Red Light/Stop Sign	8
Unpredictable Pedestrian Behavior	8
Vision Obscured	5
Rare Occurrence	1
Total*	106
Source: LTCCS Analysis, Kingsley, 2009.	

*The total in the table represents 10 percent of all crashes in the LTCCS.

A surprising number of crashes in the LTCCS involved some kind of medical condition which precipitated the physical inability to act. There were seizures, heart attacks and diabetic episodes.

Many of the crashes occurred at intersections and may only be prevented by technologies that are further off into the future, such as vehicle to infrastructure or vehicle to vehicle communications.

There were a number of crashes that happened because of poor driving skills or poor decisions made on the part of one of the drivers. For example, a truck backed into a bicyclist after ignoring the audible warning from the vehicle's rear object detection system. One of the codes in the LTCCS is "False Assumption of Other Road User's Actions." Many of these may be preventable, depending on the crash type, but an example of the type that are unpreventable is crashes occurring at an intersection controlled by a 2-way stop sign. Five of the cases in the LTCCS involved a driver stopping at the stop sign, viewing the crossing vehicle, but continuing ahead anyway because of the assumption that the other driver also had a stop sign.

An unpreventable crash was one where a driver swerved to avoid another vehicle or another crash, but ended up in their own crash. Other examples are crashes that involved erratic pedestrian behavior (e.g. one pedestrian who was under the influence climbed under a truck who stopped briefly at an intersection unbeknownst to the truck driver).

The unpreventable crashes are only a small percentage of the crash population as a whole. This leaves a large target population that has the potential to be addressed by countermeasures.

Countermeasures for trucks may have prevented 61 percent of these crashes, regardless of who was at fault, and regardless of who was assigned the critical reason for the critical event.

In order to prioritize individual countermeasures, to have the greatest impact, new codes were added to each LTCCS case. These codes were queried and then tallied to provide the results.

Analysis shows the technologies ranked in order by their potential to prevent the largest number of crashes (See Table 3). Unweighted data were used and pilot study cases were included. The total number of cases reviewed was 1070.

Table 3.
Advanced Technologies and Their Potential to Prevent Crashes from the LTCCS

Advanced Crash Avoidance Technologies	Percentage of LTCCS Crashes Applicable
FCW	23.8%
ESC	19.3%
RSC	10.2%
LDW	6.1%
BSD	5.9%
Drowsy Driver Warning	4.1%
TPMS	1.7%
Backover Prevention	0.3%
Night Vision	0.5%
Total*	49.9%
Source: LTCCS Analysis, Kingsley, 2009.	

*The total value in the chart takes into account overlap among the systems. It is not the sum of the percentage of crashes applicable for each technology. Most of the crashes may be included in target populations of more than one advanced technology. See the drowsy driver warning example below.

Forward collision warning (FCW) systems have the potential to prevent the most crashes, based on in-depth clinical reviews of LTCCS cases. Although not included in this analysis, some form of automatic braking technology (e.g. collision mitigation braking)

would likely address similar crashes in addition to those in the target population for FCW. The most common crash scenario for heavy vehicles is rear-end crashes (23 percent) as can be seen in the chart below. Figure 4 shows the most common accident

types, which total 75 percent of all of the LTCCS crashes. An additional 25 percent of crashes are miscellaneous accident types and are not included.

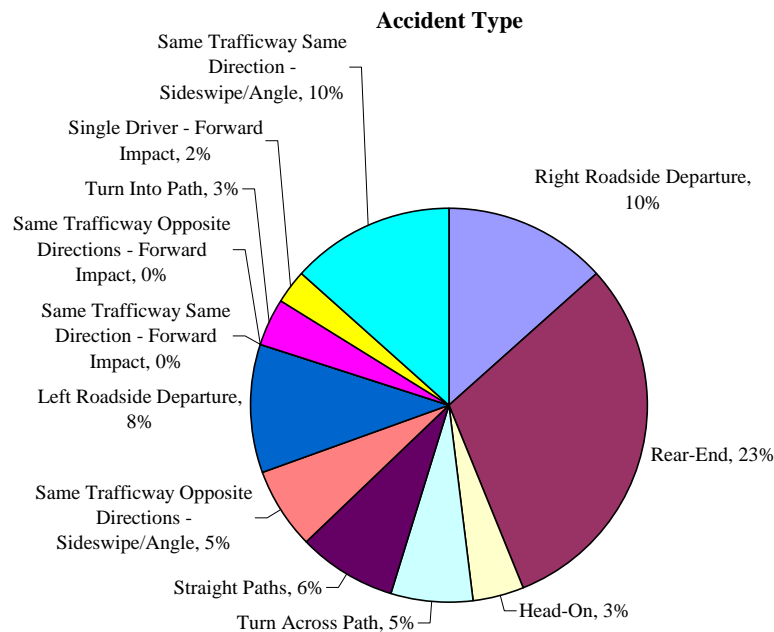


Figure 4. LTCCS Accident Types (Most Common Types Included – 75 percent of Cases).

Understanding that there is an incremental benefit to a crash imminent braking system in addition to FCW, those target populations were not broken out in this analysis. Results shown here define the target population for FCW, the difference coming into play based on the driver's response to the warning, which is outside of the scope of this analysis.

An example of the type of crash that LTCCS would shed enough light on to exclude from an FCW target population is one in which the heavy vehicle driver is aware of the danger of the situation and makes the conscious decision to "follow too closely" in traffic.

Another technology with significant potential, because of its large target population, is electronic stability control. Cases were reviewed separately for yaw stability and roll stability and it was found that the target population for a combined system was two times the size of the target population for roll stability alone. While ESC and RSC target populations would

include rollover crashes some of the accident types these technologies map to in Figure 4 include Right and Left Roadside Departures.

Notable were the crashes that may have been prevented by a drowsy driver warning system. All of them in LTCCS could have benefited from either a lane departure warning system or a forward collision warning system as well. See Table 4.

Table 4.
Drowsy Driver Crashes
Also Addressable by LDW or FCW

Advanced Crash Avoidance Technologies	Number of Crashes in Drowsy Driver Population	Percentage of Drowsy Driver Population
DDWS	44	100.0%
LDW	33	75.0%
FCW	8	18.0%
LDW or FCW	3	7.0%

Source: LTCCS Analysis, Kingsley, 2009.

Although only LDW and FCW systems were considered in the analysis above, if one assumes that a drowsy driver warning system (DDWS) would have alerted the driver at a point earlier in the pre-crash timeline, a DDWS would potentially offer the driver more of an opportunity to avoid a crash. For example, for cases in which a driver was actually asleep at the wheel and awoke to either the sound of rumble strips, or the jar of a road departure, it can be assumed that an LDW system might not give the driver sufficient warning to avoid that crash. In these types of crash imminent cases, it was assumed that even if a person were awakened by an LDW (or FCW system in the case of a rear-end crash scenario), the driver would not be able to successfully correct in time.

Another interesting countermeasure, though limited in crash population, was the TPMS. Each of those crashes that would be in a target population for TPMS would also be in a target population of crashes that have the potential to be prevented by some other non-technological countermeasure, such as stricter vehicle maintenance or better driver training. Advanced driver training courses teach drivers to handle blowouts and tread separations in such a way that they are non-events. And TPMS is not a replacement for regular vehicle maintenance, including checking tire pressures and tread depth.

Surprisingly, a significant impact can be made with non-technological countermeasures. See Table 5. Though vehicle-related factors rank well below driver error, as a causal factor in just 2 percent of crashes [6], almost 30 percent of the trucks in the LTCCS were coded with some vehicle deficiency. Based on this analysis, better vehicle maintenance could have prevented 13 percent of the crashes.

Table 5.
Additional Countermeasures and
Their Potential to Prevent Crashes from the
LTCCS

Additional Crash Avoidance Countermeasures	Percentage of LTCCS Crashes Applicable
Vehicle Maintenance	12.5%
Conspicuity	2.7%
Driver Training	1.1%
Stricter Licensing	0.8%
Alcohol and Drug Enforcement	1.4%
Misc.	0.6%
Total*	17.9%

Source: LTCCS Analysis, Kingsley, 2009.

*The total value in the chart takes into account overlap among the countermeasures. It is not the sum of the percentage of crashes applicable for each countermeasure. Most of the crashes may be included in target populations of more than one advanced countermeasure.

Alcohol and drug involvement do not play as big of a role for truck drivers in heavy vehicle crashes as it does for crashes involving passenger vehicles. The percentage of large-truck drivers involved in fatal crashes who had a blood alcohol concentration (BAC) of .08 grams per deciliter (g/dL) or higher was 1 percent in 2007. For drivers of other types of vehicles involved in fatal crashes in 2007, the percentages of drivers with BAC levels .08 g/dL or higher were 23 percent for passenger cars, 23 percent for light trucks, and 27 percent for motorcycles[7].

Overall, 61 percent of the crashes in the LTCCS are represented in target populations of crashes that may be avoided by trucks equipped with advanced technologies or truck drivers who have the benefit of other non-technological countermeasures. The total of 61 percent represents the sum of the totals from Tables 3 and 5, minus the crashes that were included in both tables (e.g. crashes where either advanced technologies or some other non-technological countermeasure may have prevented the crash).

CASE EXAMPLES

There are several cases in the LTCCS where the truck and its driver did nothing to contribute to the crash, but a countermeasure on the truck could have prevented it from happening. An example is CASEID 820003685. A heavy truck impacted a pedalcyclist who was riding in the middle of the lane down the highway. The impact occurred late at night on an interstate highway. It is not reported whether the pedalcyclist was under the influence of alcohol or drugs at the time. The critical reason for the critical event was coded to the pedalcyclist, but advanced technologies on the truck (such as forward collision warning with object detection, collision mitigation braking, and/or night vision) may have helped to prevent this crash and others like it (there are also two similar cases in LTCCS where alcohol was a factor for the nonmotorist).

There are several cases in the LTCCS which, based solely on police reported data, might be included in effectiveness estimates for advanced crash avoidance technologies. But upon clinical review of the cases, it is clear that the scenario would not have been applicable. An example is CASEID 333006978. Other data sources would show that a truck rear-ended another truck. This should be a prime candidate for forward collision warning. But upon further review of this case, one can ascertain that the driver of the striking truck was following too closely when a car suddenly cut off the truck in front of him. A forward collision warning system would not have helped, but some form of automatic braking technology (e.g. collision mitigation braking systems) may have mitigated the severity of the crash.

The last example is CASEID 342006805. The truck departed the roadway in the curve of an exit ramp. One might conclude that the truck was traveling too fast for the curve and either electronic stability control or roll stability control would have slowed the vehicle sufficiently to prevent this crash. The LTCCS data shows that this driver lost control of his vehicle due to a heart attack, and therefore no advanced technologies could have helped in this situation. There were many cases in the LTCCS like this.

FUTURE WORK

It is envisioned that the refinement of target population estimates from FARS and GES would be conducted using the following steps:

1. Define pre-crash scenarios from FARS and GES like the 37-crashes typology

[8], but specific to trucks (this is currently being done by NHTSA).

2. Map crash avoidance technologies to each of the scenarios to estimate target populations.
3. Identify the same scenarios in the LTCCS data.
4. Refine target population by:
 - a. Calculating the percentage of those LTCCS cases which were coded during the analysis presented in this paper as being a candidate for inclusion in the target population of the countermeasure being studied.
 - b. Identifying other cases in the LTCCS which were coded as being a candidate for inclusion in the target population of the countermeasure, but were not pulled out using the query based on crash scenarios.
5. Apply those proportions back to the FARS and GES estimates for a more robust target population.

CONCLUSIONS AND CURRENT STATUS REPORT

Clinical reviews of the cases from the Large Truck Crash Causation Study show that 90 percent of those crashes could be prevented by highly effective countermeasures and programs. Sixty-one percent of the crashes have the potential to be prevented by some countermeasure related to the truck, truck driver, or trucking industry. An additional 29 percent could be prevented by countermeasures related to light vehicles, light vehicle drivers or the environment. The truck-related countermeasures include vehicle maintenance and driver training in addition to advanced technologies. Almost 50 percent of the crashes in the LTCCS have the potential to be prevented by advanced technologies that are currently available for trucks.

The in-depth cases reviews and analysis conducted in this paper can be used to prioritize research, refine effectiveness estimates from FARS and GES, and to define crash scenarios that can be used in follow-on research (e.g. simulation studies) to estimate the effectiveness of advanced technologies.

REFERENCES

- [1], [7] Traffic Safety Facts 2007 Data: Large Trucks, DOT HS 810 989.
- [2] Toth, Gary R., et al, Large Truck Crash Causation Study in the United States, ESV 2003, Paper Number 252.
- [3] Starnes, Marc, Large Truck Crash Causation Study: An Initial Overview, DOT HS 810 646, August 2006.
- [4], [5], [6] Najm, Wassim, et al, Synthesis Report: Examination of Target Vehicular Crashes and Potential ITS Countermeasures, DOT HS 808 263, 1995.
- [8] Najm, Wassim, et al, "Pre-Crash Scenario Typology for Crash Avoidance Research," DOT HS 810-767, April 2007.

DEVELOPMENT OF A THORAX PROTECTOR FOR MOTORCYCLISTS

David Manzardo

Dainese

Marco Pierini

University of Firenze

Italy

Aline Delhay

FEMA

Belgium

David García Ruiz

CIDAUT

Spain

Samuel Bidal

Altair Development

France

Steffen Peldschus

Ludwig-Maximilian University

Germany

Paper Number 09-0465

ABSTRACT

This paper describes the development of a new thorax protector as part of the personal protective equipment for motorcyclists. The function of the protector is the mitigation of injuries in impacts to the frontal or lateral parts of the thorax. A sandwich structure was selected. The outer shell of polypropylene was designed to spread concentrated impact forces, a shock absorbing aluminium honeycomb material was coupled with a comfort layer for the inner part of the protector.

The materials were characterized and an FE model was created for impact simulations with the HUMOS2 model. Frontal and lateral impact tests against which the HUMOS2 model had previously been validated were simulated. The simulations highlighted that the main benefit of such a device is derived from the force distribution and that the shock absorbing material provides smaller contribution to the protector's performance.

After a pre-selection of the design variants by means of simulation, a series of thorax protector prototypes were manufactured and tested in terms of comfort (ergonomic tests) and impact protection. Ergonomic tests confirmed the quality of the design, showing that the protector does not interfere with the normal rider's movements. A series of frontal impact tests using the Hybrid III Dummy was carried out. It was concluded that the protector reduces the compression of the thorax and the probability of sustaining rib fractures in the analysed impact conditions and thus reduces the potential injury risk.

INTRODUCTION

The APROSYS project aims, within Sub-Project 4 "Motorcycle Accidents", at reducing the number and severity of powered two wheelers (motorcycle and moped) user injuries for the most relevant accident scenarios.

In order to accomplish this result, an in-depth analysis based on four accident databases (COST 327, MAIDS, GIDAS and DEKRA) and a literature review have been carried out at the beginning of APROSYS for investigate in the injuries mechanisms and in the most frequent injuries that motorcyclists sustain during accidents [Manzardo 2006].

THE IMPACT TEST CONDITIONS

From these analyses it has been pointed out that, even though, thorax is not the most frequently injured body region, injuries in the thorax area often have a high severity index. In the light of these results, the development of a device able to protect from and reduce the severity of injury to the thorax region has been addressed within APROSYS project.

The development process has been started defining a validation plan, able to check the impact safety performance of a thorax protective device. The test plan included four impact conditions, frontal and lateral at 5 and 10 m/s carried out with a cylindrical impactor with a diameter of 15.2 cm and weight 23.4 kg, impact locations are shown in Figures 1 and 2.

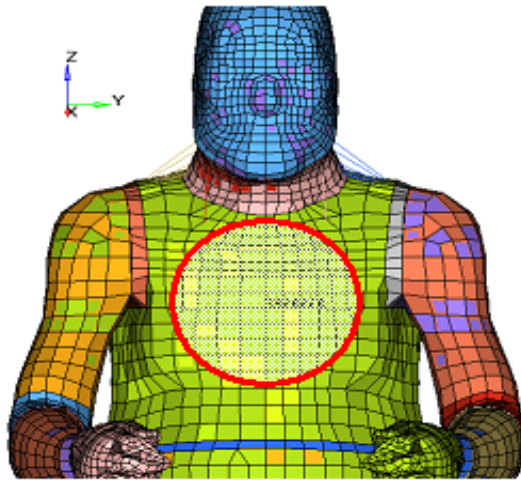


Figure 1. Frontal impact location.

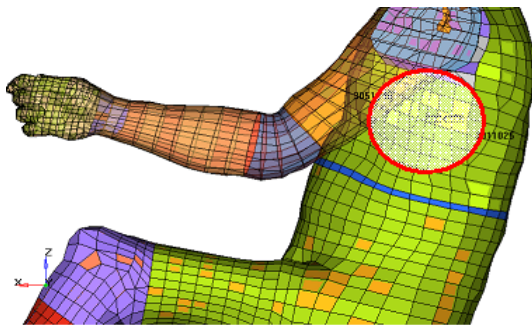


Figure 2. Lateral impact location.

The simulation and test analysis were carried out considering the following injury criteria associated with ECE-R94 (frontal) and ECE-R95 (lateral):

- for the frontal impact the thorax compression and the peak viscous response VCmax
- for the lateral impact the compression of the impacted half of the thorax was evaluated

Simulations and real tests data coming from the

validation had then to be analysed comparing measurements with and without protector. No absolute limits have been set for measurements: the evaluation criterion was the maximization of the difference between the values with and without protector.

DESIGN OF THE PROTECTOR

The design concept activity has been driven by the necessity to achieve a good impact energy distribution and, at the same time, the capability to shift the forces from the central to the lateral area of the thorax reducing the flexural moment, thus fracture risk, on ribs.

Furthermore, these safety requirements should be accomplished taking into account also ergonomic and comfort issues. An integral solution has been preferred, with a one piece semi-rigid external shell, connected to lateral rigid plates. The shell's internal side has been provided with a reticular structure.

The honeycomb absorbing structure has been selected to grant, besides impact absorption, a proper breathability on the chest zone.

Once the structural and ergonomic design issues have been defined, also the aesthetic aspect has been taken into account.

The final step for the design process had been the elaboration of the thorax protector CAD model. Figure 3 shows the design of the protector.

NUMERICAL STUDY

Brick elements have been used to mesh the protector. The interior face of the rigid shell is constituted of reinforcements which had to be taken



Figure 3 Thorax protector draft design

into account during the simulation. To model these surfaces, a series of brick elements, with a size equal to the reinforcement's width (2 mm) have been used.

The thorax protector final mesh had 100238 nodes and 54972 elements. 9056 bricks defined the honeycomb structure, 45306 bricks the rigid shell and 610 shells were included to represent the zip parts (see figures 4 and 5).



Figure 4. Rear-lateral view of FE model of the thorax protector



Figure 5. Frontal-lateral view of FE model of the thorax protector

In order to simulate impacts, thorax protector mesh has been placed on HUMOS 2 model (see figures 8 and 9).

Thorax compression and VCmax have been calculated for each frontal impact. Half thorax compression and VCmax have been calculated for each lateral impact.



Figure 6. Set-up for simulation of lateral impact including the thorax protector.



Figure 7. Set-up for simulation of frontal impact including the thorax protector.

Referring to the injury criteria table (table 1), the main benefits of the thorax protector had been expected in frontal impacts. The simulations highlighted that honeycomb did not records any deformation and for that reasons its behaviour has

been further investigated in the optimization phases, firstly changing impactor's shape then modifying the honeycomb mechanical properties in order to simulate stiffness behaviour.

Simulations then demonstrated that honeycomb compression was similar for cylindrical and for kerbstone impactors, but that it was varying with its stiffness. Taking into account injuries criteria, the honeycomb stiffness changes in combinations with impactor changes, which have been carried out during optimization phase, did not cause a remarkable effect on the thorax protection performance.

PROTOTYPE AND CRASH TESTING

After the numerical optimization phase, the prototype manufacturing has been started with the mould construction (figure 8).



Figure 8. Mould for the protector shell.

Then, a series of prototypes for the validation tests have been prepared. In order to further investigate the honeycomb behavior, protectors have been prepared in different configurations, one without honeycomb, one with honeycomb between the rigid shell and the thorax and one with honeycomb outside (see figures 9 to 11).



Figure 9. Protector without honeycomb



Figure 10. Protector with honeycomb outside.

Table 1.
Impact simulations: Parameters measured for the assessment of protection level.

IMPACT CONFIGURATION	FRONTAL			LATERAL
	<i>Chest compression</i>	<i>Vcmax</i>	<i>Chest deflection</i>	<i>Half thorax compression</i>
5 m/s – without protector	27 %	0.66	46.5 mm	27 %
5 m/s – with protector	20 %	0.41	34.5 mm	29 %
10 m/s – without protector	71 %	3.21	120 mm	61 %
10 m/s – with protector	51 %	2.53	85.8 mm	56 %



Figure 11. Protector with honeycomb inside.

Tests have been carried out with an instrumented HYBRID III test dummy seated in a plane and an octofilar pendulum that guide a cylinder probe with the impactor mounted on one its side, to hit the dummy in the sternum area (see figures 12 and 13).

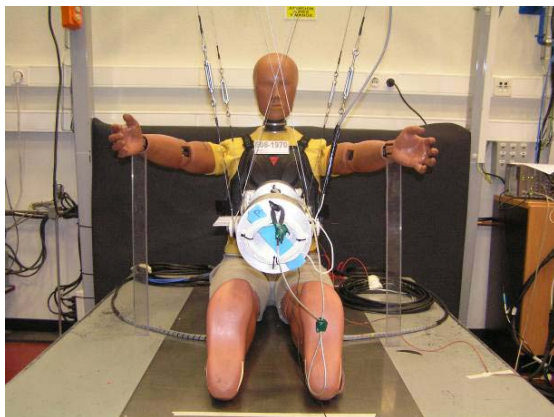


Figure 12. Impact test with Hybrid III – frontal view.

In table 2 the matrix of tests shows the test results. From the data it can be easily observed that comparing data on the chest compression, viscous criterion recorded in the test, with and without protector, for each type of prototype a reduction on the recorded values in case of use of the protector have been achieved. Taking into account sternum accelerations only the thorax protector without honeycomb demonstrate to be able, in all the test conditions, to reduce or at least maintains the accelerations values without any degrade on the data.

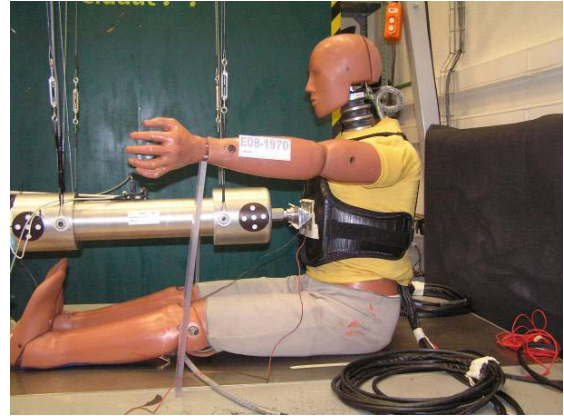


Figure 13. Impact test with Hybrid III – lateral view.

CONCLUSIONS

From the simulations results as well as from the physical impact tests it can be concluded that the presented thorax protector reduces the compression of the thorax and the probability of sustaining rib fractures in the analysed impact conditions and thus reduces the potential injury risk.

Apart from offering an additional protection to the thoracic area of a motorcyclist, ergonomic tests confirmed the quality of the design, showing that the protector does not interfere with the rider's normal movements.

This study highlights the importance of the distribution of the impact forces on the human body in case of an impact. This is an important fact that should be taken into account for the future development of motorcyclists protective equipment and for any draft or revision of standards for the testing of such equipment.

ACKNOWLEDGEMENTS

Part of this work was funded by the European Commission within the APROSYS project under the 6th Framework Programme.

REFERENCES

Manzardo, D., 2006. "APROSYS SP4.1: Analysis on protective clothing for motorcyclists ". Deliverable 4.1.4. AP-SP41-0004

Table 2.
Impact tests: Parameters measured for the
assessment of protection level.

IMPAC TOR	PROTECTIVE CLOTHING	Target probe velocity (m/s)	Measured probe velocity (m/s)	Chest_S (mm)	Chest VC (m/s)	Sternum_a x (g)
FLAT	NO	5,00	4,88	49,8	0,51	93,11
FLAT	YES, WITHOUT HONEYCOMB	5,00	4,88	43,8	0,50	84,52
FLAT	YES, WITH HONEYCOMB INSIDE	5,00	4,92	42,6	0,49	78,78
FLAT	YES, WITH HONEYCOMB OUTSIDE	5,00	4,92	42,5	0,47	101,88
FLAT	NO	6,70	6,68	72,2	1,07	135,44
FLAT	YES, WITHOUT HONEYCOMB	6,70	6,74	63,9	0,99	136,21
FLAT	YES, WITH HONEYCOMB INSIDE	6,70	6,75	62,1	0,96	146,15
FLAT	YES, WITH HONEYCOMB OUTSIDE	6,70	6,74	62,0	0,93	130,31
KERB	NO	5,00	4,92	50,5	0,61	70,02
KERB	YES, WITHOUT HONEYCOMB	5,00	4,95	43,4	0,45	69,78
KERB	YES, WITH HONEYCOMB INSIDE	5,00	4,95	43,1	0,47	92,10
KERB	YES, WITH HONEYCOMB OUTSIDE	5,00	4,95	42,2	0,34	81,04
KERB	NO	6,70	6,74	73,6	1,20	203,29
KERB	YES, WITHOUT HONEYCOMB	6,70	6,8	65,7	0,87	112,16
KERB	YES, WITH HONEYCOMB INSIDE	6,70	6,74	59,6	0,84	109,40
KERB	YES, WITH HONEYCOMB OUTSIDE	6,70	6,80	62,3	0,89	102,61

METHOD OF DRIVING ASSISTANCE SYSTEM DESIGN TO IMPROVE HUMAN-VEHICLE INTERACTIONS AND SAFETY TECHNOLOGIES DEVELOPMENTS FOR TRUCKS

Benoît, Mathern
Arnaud, Bonnard
Hélène, Tattegrain
LESCOT/INRETS
France
Paper Number 09-0472

ABSTRACT

This paper presents a method to develop coherently a Driving Assistance System (DAS) and its supporting technologies in order to reach efficiently the best added value in terms of Human-Vehicle interactions and technology specification.

This method is an iterative development process based on a Human Centred Design approach. It requires a driving simulator and a development framework in order to simulate technologies. The first step of the method is to validate the DAS prototype through 3 iterative tasks: Study of the drivers needs, Design of the DAS with “perfect” technologies, Evaluation of driver-vehicle interactions to validate the effectiveness of the assistance. Then the second step is to obtain the best trade off between effectiveness of the assistance and technological requirements through 2 iterative tasks: Modification of the technology performance by changing the specifications (toward existing, emerging or futuristic technologies), Evaluation of driver- vehicle interactions to validate that the assistance is still effective. This guides the final decision for the DAS production: use existing technologies, or develop better safety technologies.

This method is developed inside VIVRE 2 project, which aims to design an innovative DAS to help truck drivers engaged in low speed manoeuvres in urban areas.

We first developed a prototyping platform, which we then used along with the method to design the DAS and to determine the best compromise in terms of Human-Vehicle interactions and technology specification. Even if the method inherits of the limitations of simulated environments, it permits a “driver in the loop” development of innovative DAS which would be difficult otherwise.

Instead of using the classical approach “From technologies, to DAS design, to DAS evaluation”, this approach shift the problem to “From driver needs, to DAS evaluation, to technologies”.

INTRODUCTION

With the massive arrival of electronics, systems designed to support and assist the driver in his/her driving activity (like ABS, Navigation systems...) started to be implemented inside vehicles. These systems raised different research questions not only in the field of technological development, but also in the field of drivers’ needs in terms of assistance. However, as the number of DAS inside a single vehicle increase and as they are designed and implemented separately, it becomes more and more difficult to determine the impact of the sum of these assistances on the driving activity. In order to avoid a negative impact of these systems on the driving activity, a detailed study of the interaction between the human and the vehicle systems is required. Human Factor research provides the key concepts to tackle this issue. Thus, the design of DAS becomes a joint work for engineers and Human Factor researchers.

In this context, we propose a DAS design process based on a Human Centred Design approach that permits to develop coherently a driving assistance system and its supporting technologies in order to reach efficiently the best added value in terms of Human-Vehicle interaction and technology specification.

In this paper, we present in details this design process and its results through the case of VIVRE 2 project which aims to design an innovative DAS to help truck drivers engaged in low speed manoeuvres in urban areas.

METHODOLOGY

Human Centred Design Approach

While developing a DAS, thorough technical specifications have to be made, as the safety of drivers and other road users are engaged.

The usual way of working starts by identifying what safety issue could be solved by a DAS.

Then, it consists in finding which technology could be employed to solve this issue. Then, in developing a prototype and testing its functioning in all situations in which it is designed to work. After the validation of the functioning, when the

technology is considered as mature enough, the DAS is spread on the market. This type of method is called technology driven approach, as it consist to start from a technological description of the problem, and solve it via a technical solution. This method is thorough, efficient and safety-proof. These criteria are sufficient for a DAS manufacturer who needs to be sure a technology is safe and can be used by drivers. However, this approach does not guarantee that the DAS is useful, and that it is correctly used by drivers. In order to solve these issues, DAS designers have to consider the drivers' feedbacks earlier in the design process: at its very beginning. Thus, they have to shift their way of doing from such a technology driven approach to a human centred design approach.

Human Centred Design (HCD) approach places the users and their needs at the centre of the development process. The key principle of user centred approaches, as defined by Gould & Lewis (1985)[1] is to focus on users and tasks and to apply an iterative design.

In the case of DAS design, it consists in studying the driver and his/her driving activity all along the DAS development process.

HCD for DAS design consists in iteratively:

1. Studying the driving activity (e.g. through DVE model...)
2. Deriving the contextualised needs in term of assistance (related to safety, control, information, comfort...)
3. Formalizing the functional specifications of the DAS
4. Developing the DAS
5. Testing the impact of the DAS on the driving activity

Our Approach

General Overview – Considering that the driver might not use the DAS as the designers was expecting, or more generally, that the driver will adapt it's driving behaviour to the DAS, we adapted the HCD approach, in a way where we can evaluate the modified behaviour of the driver at the early stage of the development process.

We actually adapted the 5-steps development process loop into two different steps. The first one focuses on the interaction between the Driver and the DAS (leaving technological limitations aside). The second step consists in making the DAS realistic, by adapting the DAS to existing or forthcoming technologies.

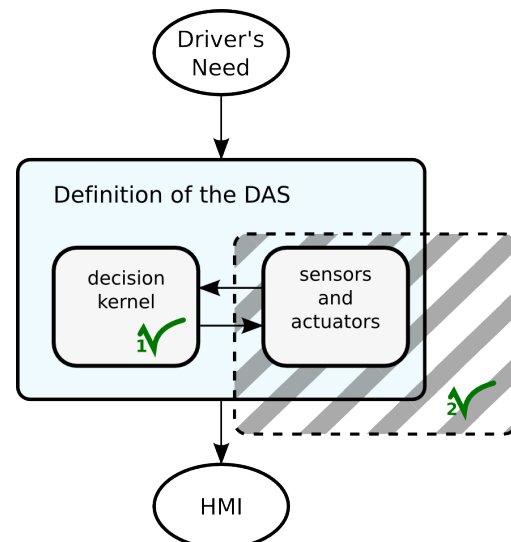


Figure 1: General overview of our approach.

The figure 1 illustrates this approach. We start from driver's needs, that have to be identified by ergonomics researchers studying driving activity. From this needs, we can design the kernel of the DAS. But we don't limit this DAS with technological constraints on sensors and actuators. And we test, at an early stage, the behaviour of both the driver and the DAS when put together.

Of course, this step can only be done on a driving simulator.

This steps should be executed in a loop until the drivers coupled to the DAS behaves satisfyingly. This validates the kernel of the DAS, and the effectiveness of the assistance.

Then, we can focus on the technological constraints. On this second step we expect to find a good trade-off between the effectiveness of the DAS and the technological requirements. The kernel that was defined specify at some point the technologies that would be needed. But what if the technology selected to support this DAS is not efficient enough? For such reasons we could be interested in seeing how far from the "ideal" technologies we can get while the DAS stays satisfyingly efficient for the driver.

We will present in details these two steps in the following of this chapter.

First Step – Focus On Driver / System

Interaction - The objective of the first step is to validate the effectiveness of the assistance system according to the drivers needs.

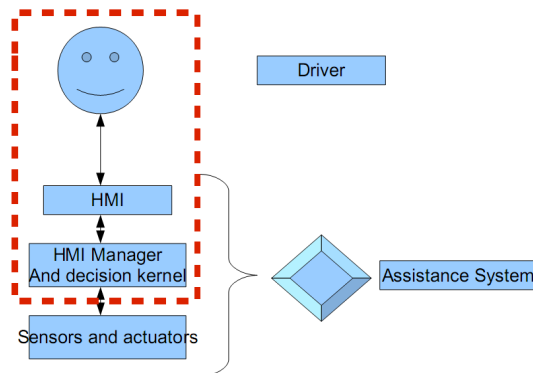


Figure 2: first step to Focus on driver / system interaction

The methodology for this first step is inspired from a human centred approach.

The first phase of this step consists in defining accurately what kind of assistance the driver needs in what situation. This knowledge is gained through a detailed analysis of the driving activity. Various scientific approaches can bring knowledge on the driving activity. Naturalistic observations or experimental observations in real traffic condition are specifically suited for this purpose.

Once the situations and the respective assistance that is needed by the drivers are defined, the design of the DAS can begin.

The central question is to determine the best possible way to provide the driver with the relevant assistance: the right information/action at the right moment.

So the second phase of this first step focuses on the design of the Human/Machine Interface. This second phase consists in an iterative process with 2 tasks. The first task is to develop an HMI and an HMI manager that give, for the target situations, the relevant assistance to the driver. The second activity is to study the interactions between the driver and the assistance system and to evaluate the effectiveness of the system. These two tasks have to be repeated until the cooperation between the driver and the system reaches the targeted objectives.

At this stage, the development of the assistance decision kernel is based on technologies that have an ideal functioning, and that are always capable of delivering perfect information to the HMI manager.

This first step permits to design a DAS and to assess very quickly if the DAS suits the drivers needs in terms of driving assistance.

Though this first step is meaningful to validate a concept of assistance, it is disconnected from the constraints of the technological offer. Therefore, a second step is necessary to tackle this issue.

Second Step - Focus on system / sensors

interactions - The objective of the second step is to materialize the DAS in order to determine the best technological specifications to support its functioning.

To reach this objective, two tasks have to be realised as an iterative process. The first tasks is to simulate technologies that can provide the assistance kernel with informations. These technologies does not necessarily have perfect performances (sensors range, decision algorithms...). When changing their specifications, from ideal technologies toward existing, emerging or futuristic technologies, the modifications might have an impact on the global functioning of the assistance. Therefore, the second task consists in evaluating driver-vehicle interaction to validate that the assistance is still effective and that its functioning was not significantly reduced.

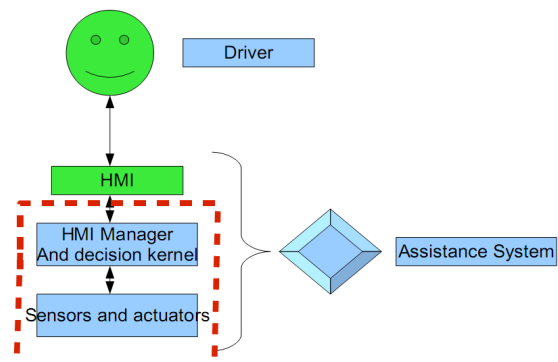


Figure 3: second step to Focus on system/technology interactions

Through the iterations, it is possible to find out the best compromise in terms of Human-Vehicle interactions and technology specification.

RESULTS: CASE STUDY ON VIVRE II PROJECT

Context

VIVRE2 project focuses on reducing the number of accidents involving trucks and vulnerable road users (pedestrians, cyclists...) in urban areas [2]. Part of the project consists in designing and testing on a Renault Trucks simulator called “SCOOP”, a system assisting truck drivers engaged in low speed manoeuvres.

SCOOP simulator runs various applications from Oktal. This software is controlled by specific Labview diagrams. These diagrams give an easy access to several parameters that describes driving activity, such as information on driver's actions, truck dynamics, dynamics of mobiles around the trucks, properties of these mobiles and roads characteristics.

Development of a Framework that Support our Methodology

To support our design process, tools are necessary. These tools should offer flexibility for the DAS development : a dedicated architecture for the DAS HMI manager and decision kernel, a dedicated architecture to easily simulate technologies, and a feature to connect the DAS to driving simulators. Thus, the development of a dedicated prototyping platform would be useful. That is why we specified and created a framework platform with the features required to support the design process we described in chapter 3. This framework is based on a architecture composed of several dedicated modules: Two specific interface modules (that transfer and translate data from simulator to prototyping platform back and forth), a module to pilot the HMI of the DAS, a module with the DAS decision kernel and finally different modules that simulate technologies required by the DAS.

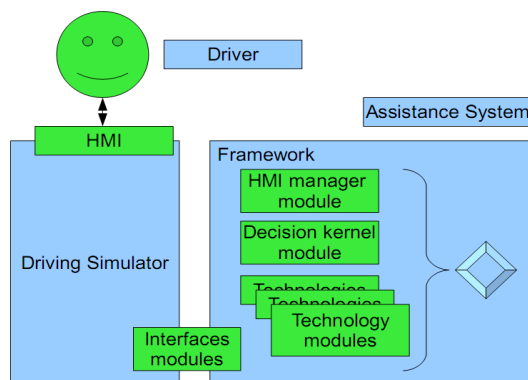


Figure 4: Architecture for DAS design

These modules act as containers for DAS algorithms and are connected according to the architecture.

Using this framework, the DAS designer focus on creating the relevant algorithms of each module.

Application of the Methodology Through the Framework

To design VIVRE 2 DAS, the ergonomics researchers of the project defined the needs in terms of assistance and the target situations. They also started the design of the HMI to provide the driver with the assistance.

At first, we focused on the development of the interface modules algorithms in order to be able to receive data from the simulator, and to pilot the HMI.

Then, we drafted the HMI manager algorithms and the decision kernel algorithms, and developed them until they corresponds to the expectations of the ergonomics researchers and prove their effectiveness on a sample of drivers. At this stage, the technology modules algorithms only deliver perfect information from the simulator (exact position of the pedestrians, infinite range of perception...).

This achieve the first step of our methodology, that focus on driver/system interaction.

To continue, we selected a set of sensors that could support this DAS (laser scanners and ultrasonic sensors) in a real implementation. We modified the technological modules algorithms accordingly, by adding physical constraints that simulate the behaviour of these sensors.

This is the second step of our methodology. At the time we write this paper, we are testing the effectiveness of the assistance with this selected set of sensors on a sample of drivers.

The following steps will be to take into account the feedbacks of the drivers to validate the specification of the technologies : either the technologies are sufficient to support the correct driver/assistance interaction, or new specifications are required to support the driver/assistance interaction. These new specifications can come from another set of sensors, or from the suggestion of specifications improvement.

CONCLUSIONS

Instead of using the classical approach "From technologies, to DAS design, to DAS evaluation", we shifted the problem to "From driver needs, to DAS evaluation, to technologies". Indeed, we developed a DAS design process inspired from a Human Centred Design approach and we successfully applied it to a real case. This design process consists in 2 different steps. To support this method, we developed a framework.

This framework proposes a reference architecture for DAS design.

It permitted us to quickly realise the first step of the method, focused on driver/assistance interaction, and to obtain a prototype that provide the driver with an effective assistance.

Then, it permitted us to begin with the tasks of step 2, focused on assistance/technologies functioning. Experimentation with drivers are currently performed to complete step 2. The overall objective is to obtain, through this method, the best compromise in terms of Human-Vehicle interactions and technology specification.

DISCUSSION

To be optimal, this method requires a high number of iterations and tests with drivers, which is costly and time consuming. This is a first limitation of this design process. This parameters has to be taken in to account during the development in order to optimise the number of iterations. However, the modification between each iteration can be done very quickly and easily, which accelerate the general design process.

Even if the tests on drivers inherits of the limitations of simulated environments, it permits to evaluate innovative DAS which would be difficult otherwise.

This “driver in the loop” development can only be achieved by considering the couple driver and assistance. A step further would be to develop a driver model, that simulates the behaviour of a real driver, in order to rationalise this couple and to be able to perform more iterations for the system evaluations.

REFERENCES

- [1] J.D. Gould & C. Lewis, “Designing for Usability: Key Principles and What Designers Think”, 1985.
- [2] VIVRE2, “Véhicule Industriel et usagers Vulnérables de la RoutE”, PREDIT GO4 project proposal, 2005

DESIGN OF THE DECISION LOGIC FOR A PTW INTEGRATED SAFETY SYSTEM

Giovanni Savino

Avinash P. Penumaka

Marco Pierini

Niccolò Baldanzini

Università degli Studi di Firenze

Italy

Bernd Roessler

Ibeo Automobile Sensor GmbH

Germany

Paper Number 09-0500

ABSTRACT

The Powered Two Wheeler Integrated Safety (PISa) project is developing an integrated safety system for a range of powered two wheelers (PTWs). This system includes state of the art sensors, innovative warning devices and rider assistance systems.

This paper reports on the design of the decision logic for deploying autonomous braking (AB) and enhanced braking (EB) safety functions in the PISa system, for a PTW travelling towards leading obstacle, using on-board inertial measurement unit (IMU) and Laserscanner.

The decision logic deploys the AB and EB systems based on a theoretical kinematic parameter: the required deceleration to avoid a collision. The criterion for deployment is to trigger the AB and EB systems when the collision is physically unavoidable.

The decision logic is tested off-line for datasets acquired using the PTW integrated with the IMU and the Laserscanner.

INTRODUCTION

According to the European Road Safety Observatory (ERSO), in 2006 more than 24,000 road traffic fatalities were registered in the EU-14 (EU-15 without Germany). About 5,400 were PTW riders. During the period 2000 - 2006, the car fatalities decreased by 35%. During the same period moped fatalities also decreased by 30%, while motorcycle fatalities increased by 10%. The risk of fatality for PTWs (including mopeds and motorcycles) is 26 times higher per km travelled compared to passenger cars [1].

Within the European Commission's 6th Framework Program, the PISa project is developing an innovative approach for PTW safety to address the growing fatality rate. The aim of the PISa project is to develop and implement an integrated safety system for a range of PTWs, to contribute in the reduction of casualties by avoiding accidents and reducing injury severity.

In the PISa project, PTW accident analysis was performed using existing statistical data to identify

important accident types and causation factors. Subsequently, a sample of existing in-depth motor-cycle accident datasets were selected and predictive assessments were made regarding the ability of a range of safety systems to influence the accident outcome. This analysis was used to identify and prioritise the most effective safety functions to be implemented in the PISa system [2].

The following components of the PISa system were defined:

- sensors to obtain the state parameters to describe the relevant vehicle behaviour;
- human machine interfaces (HMIs) - a vibrating saddle to warn the rider;
- actuators - the braking assistance system and the semi-active suspension;
- decision logic to coordinate the activation or inhibition of the elements of the PISa system to appropriately deploy the selected safety functions.

Accidentology

A total of sixty in-depth real cases with relevance to the seven main accident scenarios identified in the Aprosys project [3] were extracted from COST 327, OTS and Fatal databases. The selected cases were analysed in detail to determine the characteristics of the accident, including relative vehicle behaviour (positions and speeds prior to collision), environmental and human contributing factors, casualties [4]. The outcome of the accident analysis led to the identification of the most frequent and severe PTW accident configurations (ACs) shown in Figure 1.

Safety Functions

A total of forty-five safety functions were identified based on the possibility to avoid the accidents or to reduce their outcomes at the different phases of the accident, i.e. pre-crash, crash, post-crash. These functions were prioritised by a group of experienced analysts of the PISa project, according to the effectiveness to influence the accident outcome for the sixty in-depth cases. The method to prioritise the safety functions was to rate each function in

each case from 0 to 5 (0 being no effect, 5 being most effective). For each function, the ratings in all the sixty cases were summed up to obtain the ranking for the safety functions in the order of effectiveness. In Table 1, the prioritised list of safety functions is shown, filtering out the least effective functions from the forty-five safety functions.

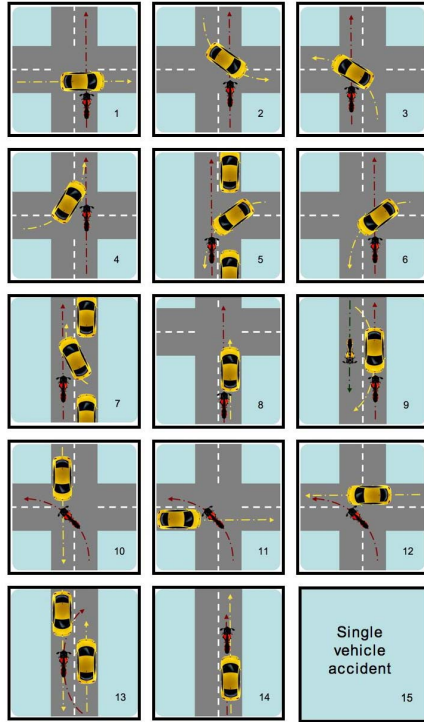


Figure 1. PISa accident configurations.

The most relevant safety functions based on the scope and the capability of the PISa Consortium were identified. In Table 1, the six selected functions are highlighted in bold. These functions will be implemented within the PISa project on two demonstrator PTWs. Taking into account the PISa project time scale, among the 15 accident configurations shown in Figure 1, two configurations (AC1 - cross intersection; AC8 - car following) were selected for implementation and validation of the safety system.

In the present work, the focus is on the development of the AB and EB functions for AC8, with two different states for the obstacle:

- PTW travelling towards a moving obstacle;
- PTW travelling towards a fixed obstacle.

The functionality of the AB is to automatically slow down with a precise deceleration, or eventually stop the PTW by braking without rider input. The intention is to reduce the PTW speed when the rider is unaware of a dangerous situation. This function is meant to warn the rider by braking at low deceleration value, anticipating the rider to react. If the rider does not react, the AB helps in reducing the consequences of the collision. If the rider reacts by braking, the EB will assist the rider in obtaining a pre-

determined deceleration of the PTW by amplifying the braking force during the emergency braking.

Table 1.
List of prioritised safety functions

n.	Prioritised function list
1	Warn other vehicle of PTW presence
2	Automatically slow/stop other vehicle without input from driver
3	Amplify braking force – Enhanced braking system (EB)
4	Improve conspicuity – Special fairings/active lighting
5	Balance front to rear braking force – Combined braking system (CBS)
6	Detect and warn PTW that vehicle travelling from left, right or oncoming is crossing the PTW path – PTW to detect other vehicle and warn rider
7	Avoid locking of wheels in straight line – Antilock Braking System (ABS)
8	Automatically brake PTW without input from rider – Autonomous braking (AB)
9	Communicate and warn PTW that vehicle travelling from left, right or oncoming is crossing PTW path
10	Restrict PTW to posted speed limit
11	Reduce closing speed – Distance support system (DSS)
12	Protect rider's legs
13	Advise rider of approaching permanent hazard (sharp bend, steep decline, fixed obstacles)
14	Help rider to maintain steering and prevent loss of control

Integrated Safety System

The safety functions are implemented in an integrated safety system, which is comprised of sensors, actuators and interfaces. The system is on board along with the decision logic on a PTW. Sensors provide input to the safety system about the state of the PTW, the rider behaviour and the PTW surroundings.

The IMU provides the following information regarding the PTW:

- speed;
- acceleration;
- roll angle and roll rate;
- pitch angle and pitch rate.

Pressure sensors on the hydraulic braking system, an encoder mounted on the throttle and a load cell provide the following information about the rider behaviour:

- brake pressure applied on the front and rear wheels;
- throttle position;
- steering input.

A Laserscanner mounted in front of the PTW provides information about the surroundings. The objects in front of the PTW are detected, tracked and assigned with an ID. For each assigned object, the following data is computed:

- classification (PTW, passenger car, van, etc.);
- dimensions (width, length);

- relative position (longitudinal and transverse distance from the PTW);
- yaw angle (current direction of the object);
- both relative and absolute speed (longitudinal and transverse).

Because the Laserscanner is mounted to the fixed frame of the PTW, detection of objects that are far away is sometimes not possible for high PTW roll angles. For this reason, it is convenient to work only on the configurations where PTW is travelling in a straight-line path. Nevertheless, to take into account of the curvature of the path even for small roll angles, a correction on the data coming from the Laserscanner is performed, based on the hypothesis of steady curve manoeuvre. In Table 2 the list of data acquired by the aforementioned sensors is shown.

Table 2:
Data acquired by the sensors

Element	Parameters
Host vehicle	Speed, acceleration
	Yaw and roll angles, roll rate
Rider	Throttle position
	Front/rear brake pressure
	Steering input
Surrounding object	Classification and dimensions
	Relative position from PTW
	Speed, acceleration

The actuators included in the integrated safety system are the braking assistance system with the AB and EB functionalities, and the vibrating seat to warn the rider. The development of the components will be finalised in the later stages of the PISa project.

DECISION LOGIC

The decision logic is the set of rules and algorithms that take care of the deployment of the AB and EB in a reliable manner, which means without false triggering. The AB and EB are implemented on a PTW for car following configuration, i.e., PTW following leading vehicle in straight path.

Deployment strategy

The AB and EB functions are deployed in emergency situation, without rider input, by performing an evaluation of the kinematic situation. The main criterion for deploying the functions is the risk for collision. The risk evaluates the possibility for a collision to occur and the severity of the outcomes associated with that event. Also the rider continuously performs risk evaluation and reacts accordingly, trying to keep the risk within a subjective reasonable level. A deployment of the AB or EB functions can be dangerous when the rider does not expect or even desire such a response. To overcome such a danger, the system will take the physical limits of the PTW into consideration to set the

threshold for triggering. Accordingly, the system intervenes with the braking assistance only in case of an unavoidable collision against the leading vehicle. In such a situation, if the risk perceived by the rider is still within the personal safety limit it is probably due to rider misjudgement, distraction or physiological limitations. As a consequence, the system decision to deploy the braking assistance will be safer, no matter what the rider's intentions are.

Once the AB is triggered, the deployment is postponed by a delay time τ_{AB} to pre-warn the rider by the vibrating saddle, thus avoiding totally unexpected deceleration. The delay reduces the effects of the AB in terms of reduction of the impact speed, but it is fundamental to prepare the rider for the consequences of the deceleration.

Risk evaluation

A substantial amount of work has been done in defining the methods for risk evaluation to deploy safety functions in car following configuration. Zhang et al. [5] reviewed the different methodologies for computing a risk parameter based on kinematic quantities and proposed a new synthetic parameter for evaluating the threat. Among the different methodologies, focus must be laid in the required deceleration parameter. According to Kiefer et al. [6], the required deceleration measure is the constant deceleration level required for the driver to avoid colliding with the lead vehicle at manoeuvre onset. The assumption for this parameter is to consider constant deceleration of the leading vehicle. The inputs for evaluating the required deceleration (d_{req}) are PTW speed (v_{PTW}), lead vehicle speed (v_L), lead vehicle acceleration (a_L), relative distance between PTW and lead vehicle (L).

$$d_{req} = \frac{(v_{PTW} - v_L)^2}{L} - a_L$$

The importance of this parameter is the direct correlation with the kinematics of the situation associated with a low complexity. The risk parameter will be directly related to d_{req} . According to the research conducted by Kiefer et al. on passenger cars [7], it is not possible to establish a direct correlation between d_{req} and the driver perception of the threat. Therefore the deploying strategy based on d_{req} will be relied on the physics of the situation and not on the rider's evaluation.

Triggering

The required deceleration is a theoretical parameter with a practical significance related to the possibility of avoiding the collision by braking. The deceleration of the PTW is obtained by the longitudinal forces between the tyres and the road and by the aerodynamic forces. The latter is a function of the

speed and depends on the geometry and the mass of the PTW including riders, while the former is limited by the friction coefficient between tyre and asphalt. Below 20 m/s the aerodynamic forces are negligible, so the maximum deceleration mainly depends on the maximum friction coefficient μ_p (traction coefficient). Under these assumptions, the maximum deceleration is $\mu_p g$. For this reason, the braking assistance will not be activated until d_{req} is less than $\mu_p g$, since the collision is theoretically avoidable by braking. When the d_{req} overcomes $\mu_p g$, the system will trigger the brake assistance to contribute in the reduction of the impact speed because the collision is reasonably inevitable.

Since the braking traction coefficient is difficult to be measured locally with precision, the triggering deceleration (d_{trigg}) is set to 10 m/s², estimated when $\mu_p=1$, which is the maximum value for common road conditions with dry surface. If locally $\mu_p < 1$, e.g. on wet surface, the triggering limit of 10 m/s² is still fail-safe because the maximum braking deceleration that the PTW can feasibly achieve is $\mu_p g < 10$ m/s², so the system still deploys when d_{req} is beyond the physical limits.

In principle, in normal road conditions ($\mu_p=1$), the triggering threshold identified referring to the physical possibilities of the PTW with maximum traction coefficient could be reduced to the actual possibilities of each rider with a specific PTW. Nevertheless the present work refers to a generic rider and PTW. Winkelbauer et al. [8] showed that on a population of riders with various levels of riding experience, comprehensive of novices, on different PTW equipped with ABS, the braking performances after a short training were so high that to include the 90% of them in the deploying criterion of the maximum feasible performances, d_{trigg} must be higher than 9.5 m/s². Considering that the EB function is not allowed without being associated to ABS, d_{trigg} cannot be reduced because of the real performances of the riders.

Inhibition

Triggering is inhibited in cases where system activation might cause dangerous consequences. Two parameters are taken into account before deploying the braking assistance system.

Firstly, if roll angle and roll rate are not close to zero, the PTW is not in the proper conditions for the deployment of the braking assistance, as the AB or EB deployment would lead to a destabilisation of the PTW and dangerous outcomes. If roll angle or roll rate are greater (in modulus) than a threshold, the system will inhibit the deployment of the braking assistance.

Secondly, before triggering the braking assistance system, it is important to assess that collision avoidance against the lead vehicle is no longer feasible by swerving. It is assessed by measuring

the relative distance between the PTW and lead vehicle (L) and comparing it with the minimum distance required to avoid the collision by swerving (L_{swerve}), which is calculated using the speed of the PTW and lead vehicle and by defining a maximum value for the roll angle. Until L is higher than the feasible limit L_{swerve} , the AB is inhibited. The minimum distance to avoid the collision by curving is computed under the following hypotheses:

- v_{PTW} and v_L are constants;
- radius of the path R suddenly changes from infinite (straight path) to a constant value R_{min} :

$$R_{min} = \frac{v_{PTW}^2}{g \cdot \tan \varphi_{max}}$$

where φ_{max} is the maximum feasible roll angle for the PTW during emergency curving.

$$L_{swerve} = \sqrt{2 \cdot k \cdot v_{PTW}^2 \cdot s + s^2} + k \cdot v_{PTW} \cdot v_L \cdot \arccos \left(\frac{k \cdot v_{PTW}^2}{k \cdot v_{PTW}^2 + s} \right)$$

where $k = \frac{1}{\tan \varphi \cdot g}$ and s is the tolerated distance between the centres of gravity of the PTW and the obstacle.

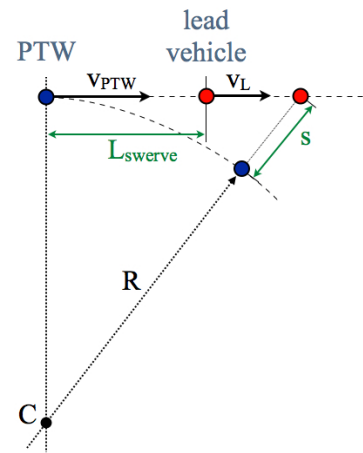


Figure 2. Kinematic representation to calculate L_{swerve} .

Theoretical benefits

The AB and EB are meant to reduce the consequences of inevitable collision principally by decreasing the impact speeds. The theoretical performances depend on the following intervention parameters for triggering:

- required deceleration for triggering (d_{req});
- reference deceleration for the AB (d_{AB});
- reference deceleration for the EB (d_{EB});
- delay-time for deploying the AB (τ_{AB}).

The reference deceleration for the AB must be small enough to avoid the rider falling off the PTW,

since the rider may not be aware about the deployment of the AB. Specific tests will be required to identify the maximum acceptable deceleration for the AB.

For the EB, since the braking assistance is deployed when the rider is already braking, a high value of deceleration could be acceptable, as the rider is aware of the emergency situation. Further investigation will be necessary to assess the deceleration value for the EB.

Table 3 shows the values for the assumed intervention parameters.

Table 3.
Intervention parameters

Parameter	Value
d_{trigg}	10 m/s ²
d_{AB}	4 m/s ²
d_{EB}	8 m/s ²
τ_{AB}	0.1 s

The impact speed reduction is a function of Δv and does not depend on v_{PTW} itself. For the assumed values of the intervention parameters, in Table 4 the reduction of impact speed and energy when the rider performs no braking manoeuvre are shown.

Table 4.
Relative impact speed reduction
(only AB, no reaction from the rider)

Δv [m/s]	5	10	15	20	25
Impact speed reduction (%)	12	17	19	20	21
Impact energy reduction (%)	23	32	35	36	37

In theory, when the AB triggers, the rider is expected to start braking. In that case the system will switch from the AB to the EB. Hypothetically, if the delay-time between the instant when the AB actually deploys and the rider brakes is $\tau_{EB} = 0.2$ s, the final impact speed reduction is still a function of Δv . Under these assumptions, the theoretical benefits are not negligible, as shown in Table 5.

Table 5.
Relative impact speed reduction
(AB followed by EB)

Δv [m/s]	5	10	15	20	25
Impact speed reduction (%)	12	24	34	39	42
Impact energy reduction (%)	23	43	56	63	66

PRELIMINARY TESTS

Tests were conducted to validate the triggering strategy in real conditions in terms of reaction time to trigger and false triggering. This will form the basis for a future evaluation of the theoretical benefits of the AB and EB.

For evaluating the triggering, the deployment of the braking actuators is not necessary. Hence the tests are conducted off-line, by elaborating the datasets acquired on a PTW.

Test preparation

The PTW, a 500cc Malaguti SpiderMAX scooter, is integrated with the Laserscanner (Ibeo LUX) manufactured by Ibeo Automobile Sensor GmbH to monitor the surrounding and the IMU (MTi-G, Xsens) to acquire the information about the state of the PTW.

The Laserscanner is utilised with the following characteristics:

- scan frequency: 12.5 Hz;
- field of view (horizontal): 100°;
- range: 0.3 m to 200m.

In Figure 3 the Ibeo Laserscanner mounted in front of the PTW is shown.

The characteristics of IMU are the following:

- maximum update frequency: 120 Hz;
- heading estimation (dynamic accuracy): 2° RMS;
- speed estimation.



Figure 3. Ibeo Laserscanner mounted on board the PTW.

Table 6.
Processed variables acquired for the tests

n.	Variable
1	time
2	speed of the PTW
3	obstacle id
4	relative x distance of the obstacle
5	relative y distance of the obstacle
6	relative x speed of the obstacle
7	relative y speed of the obstacle
8	absolute x speed of the obstacle
9	absolute y speed of the obstacle

The raw scan data and the state of the PTW acquired respectively from the Laserscanner and the IMU are processed together using an application software developed by Ibeo. An object tracking and classification are performed, providing the information shown in Table 6.

The software runs on an electronic control unit (ECU) connected to a hard drive to store the data. Both the ECU and the hard drive are mounted on-

board the PTW. Then the processed data stored in the hard drive is utilised to perform an off-line elaboration. Figure 4 shows the acquisition system set up on board the PTW.

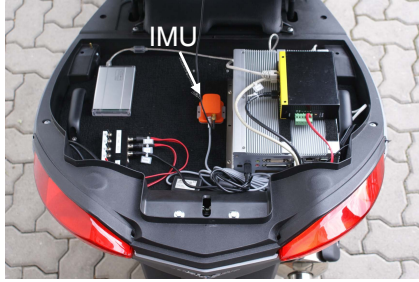


Figure 4. Acquisition system on board the PTW.

Test description

A total of ten tests were conducted for AC8 with both moving and fixed obstacle, while PTW travelling towards it. Six tests were conducted for the PTW travelling on a straight path towards a leading car proceeding at different speeds. These tests were performed on a straight road in real traffic conditions. In all the cases the car was approaching an intersection and slowed or stopped, with the PTW following. The PTW rider was aware of the situation and braked with an appropriate deceleration, thus avoiding the collision.



Figure 5. PTW travelling towards a fixed obstacle.

Four tests were conducted with the PTW travelling on a straight path towards fixed foam as obstacle in a parking lot along with other fixed objects (Figure 5). The tests were performed simulating different rider behaviours in terms of awareness of the imminent collision:

- no awareness – proceeding with constant speed against the obstacle;
- late reaction – proceeding with constant speed before braking too late, thus colliding with the obstacle;
- full braking – proceeding with constant speed before hard braking, thus avoiding the collision;
- complete awareness – proceeding with constant speed before braking on time to avoid the collision.

Elaborations

For each test, the Laserscanner identifies several objects with the related information about the state. In principle, for each object it is possible to calculate the risk for collision. On-line elaborations will be performed alternatively by computing the information of all the detected objects simultaneously or by utilising a specific algorithm to automatically identify and compute only the information related to the principal object. Since in the present work the elaborations are conducted off-line, the principal object is selected manually and the information is obtained about it. For each test, the outcome of the elaboration is the trend as a function of time for the following parameters:

- d_{req} ;
- L_{swerve} ;
- trigger for the AB.

For these preliminary tests, the throttle position and the braking forces are not measured.

Results

The results of the evaluation are shown in a graphical manner. These graphs are divided into two groups, the first representing d_{req} and the trigger. On the x-axis the time duration of the test is shown. On the left y-axis, the distance between the PTW and the obstacle (black line) is shown together with the v_{PTW} (green dotted line), on the same scale. On the right y-axis d_{req} (red line) is shown. The trigger is represented as a step function (zero means no triggering).

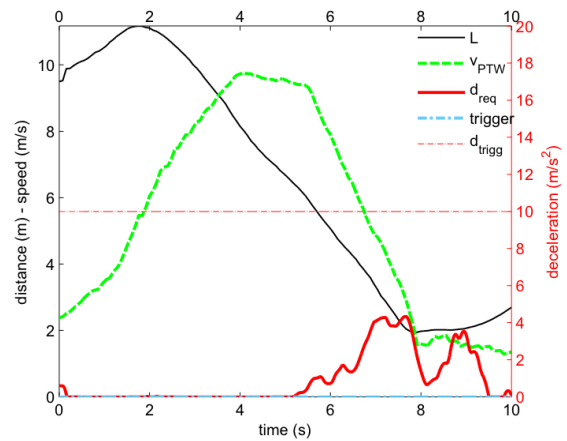


Figure 6. Risk evaluation for a specific PTW following a car.

Moving obstacle - For the PTW following a leading car, six tests were conducted when the rider was completely aware of the situation, hence there was no necessity to trigger the AB. In fact, in all these cases the rider reacted on time by braking to avoid the collision. In Figure 6, risk evaluation for a specific PTW following a leading car is shown. It is representative of all the six cases for car following, as they were similar. During these preliminary tests

conducted in real traffic conditions with an attentive rider, d_{req} is always less than or equal to 5 m/s^2 , which is far below the defined threshold for triggering.

Fixed obstacle - As expected, for the three different rider behaviours, while travelling towards a fixed obstacle, the deployment algorithm computes different responses. Figure 7 represents the PTW travelling towards a fixed obstacle without performing any collision avoidance manoeuvres, to simulate the rider behaviour with no awareness of the imminent collision. The result of this elaboration shows that while the PTW is approaching the obstacle, d_{req} increases and exceeds the triggering threshold limit. The triggering deploys 0.7 s prior to the collision, coherent with theoretical estimation.

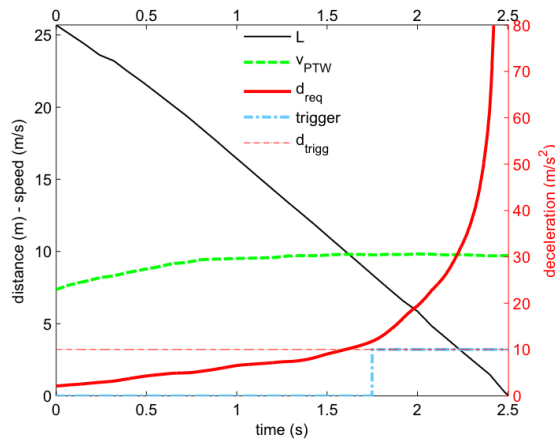


Figure 7. Risk evaluation for a specific PTW travelling towards fixed obstacle with no awareness.

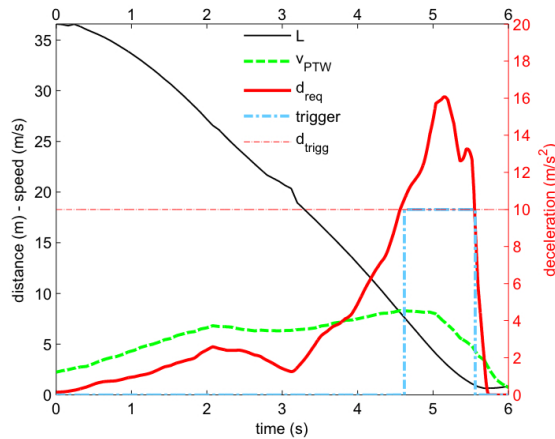


Figure 8. Risk evaluation for a specific PTW travelling towards fixed obstacle and reacting too late.

Figure 8 represents the PTW travelling towards a fixed obstacle with the rider performing the braking manoeuvre too late to avoid the collision, thus simulating the rider behaviour of late reaction. The

result of this elaboration shows that also in this case d_{req} exceeds the triggering threshold limit. The triggering is 0.2 s prior to the full braking applied by the rider.

Figure 9 represents the PTW travelling towards a fixed obstacle when the rider reacts to the emergency situation with a last second braking, thus representing a full braking manoeuvre with no collision. In this case the global maximum of d_{req} is below the threshold limit, in fact the rider was able to avoid the collision.

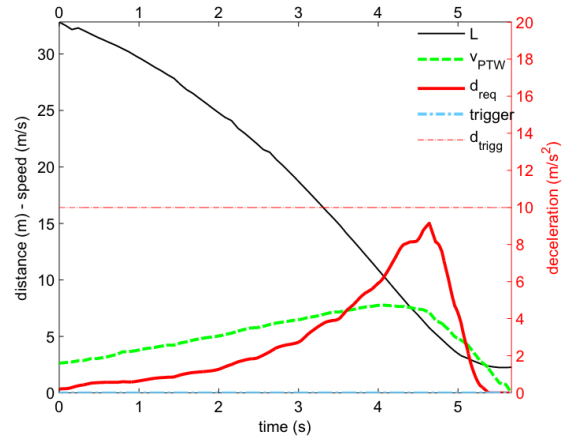


Figure 9. Risk evaluation for a specific PTW travelling towards fixed obstacle with full braking.

The second group of graphs (Figure 10 and Figure 11) shows d_{req} (red line) and the distance to avoid collision (dotted blue line) together with the distance between the PTW and the obstacle (black line). They represent the cases in which the activation occurred, to highlight the influence of the distance to avoid collision by swerving on the triggering. On the x-axis, the time duration of the test is shown. On the left y-axis both the distances are shown, while on the right y-axis d_{req} is shown. To compute L_{swerve} , the values assumed are shown in Table 7.

Table 7.
Intervention parameters

Parameter	Value
s	3 m
Φ_{max}	30°

In Figure 10, d_{req} exceeds the threshold (point A). At this point, the rider cannot avoid the collision by braking, but still has the possibility to avoid the collision by swerving, as L_{swerve} is lower than L . Hence there is no trigger. When L becomes lower than L_{swerve} (point B), the collision avoidance is no longer possible neither by swerving and therefore the trigger is activated.

In both Figure 10 and Figure 11, for the PTW speeds less than or equal to 10 m/s, approximately at the same time d_{req} exceeds the threshold for trig-

gering and L becomes lower than L_{swerve} . For this reason, even with a lower value of d_{trigg} there will be no anticipation in the triggering, because of the inhibition produced by L_{swerve} .

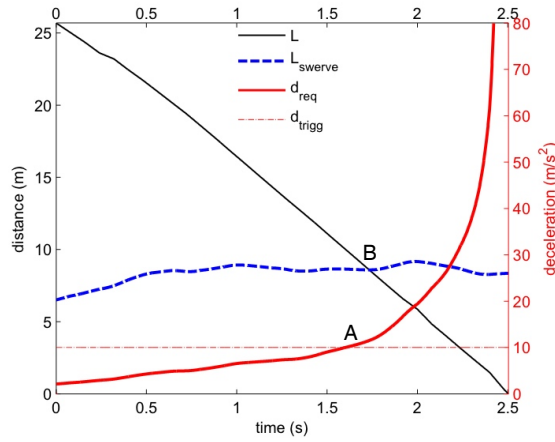


Figure 10. Triggering activation/inhibition parameters for no awareness case.

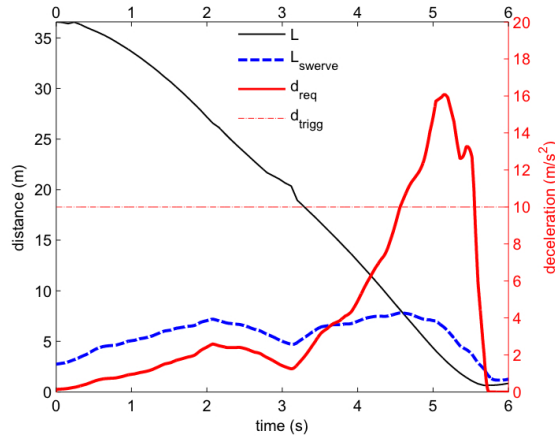


Figure 11. Triggering activation/inhibition parameters for late reaction case.

CONCLUSIONS

The decision logic described in the paper defines the deployment criteria for the AB and EB of a PTW integrated safety system in order to reduce the casualties in car following configuration.

The criterion is to deploy the braking assistance functions only when the collision has become physically unavoidable, since a prior deployment is potentially dangerous for the rider. The collision is considered unavoidable based on two parameters:

- required deceleration to avoid the collision (d_{req});
- distance to avoid the collision by swerving (L_{swerve}).

When d_{req} is higher than d_{trigg} (10m/s^2), the collision is unavoidable by braking. When the distance of the leading vehicle is lower than L_{swerve} the collision is unavoidable by swerving. The triggering is deployed when both the conditions are satisfied, hence avoiding the possibility of false triggering.

The computed theoretical benefits for the AB and EB reveal significant reduction in the impact speeds and energies. Further studies are required to identify the appropriate values for intervention parameters.

The PTW, integrated with the Laserscanner and the IMU, was used to perform preliminary tests for the car following configuration. The tests were conducted with PTW following a moving car and PTW travelling towards a fixed obstacle with simulated different rider behaviours. The datasets acquired are utilised for performing the off-line evaluation of the decision logic deployment strategy. The results show that in none of the cases false triggering is generated.

Further investigation is still necessary to validate the deployment strategy in real traffic conditions.

ACKNOWLEDGMENTS

The present work is part of the ongoing research conducted within the EC FP6 PISa project (Powered two-wheeler Integrated Safety, contract no. 031360). The authors would like to acknowledge the contributions of the members of the PISa consortium, in particular Rachel Grant and Richard Frampton (VSRC), Erich Schuller and Steffen Peldschus (LMU), Ard De Ruiter and Aernout Oudenhuijzen (TNO), Harry Kroonen (Carver) and Mike McCarthy and Wesley Hulshof (TRL) for their valuable suggestions.

REFERENCES

- [1] European Road Safety Observatory, www.erso.eu.
- [2] R. Grant, R. Frampton, S. Peldschus, E. Schuller, A. Oudenhuijzen, J. Pauwelussen, V. StClair, M. McCarthy, R. Babu, M. Pierini, G. Savino. 2008. "Use of In-depth Crash Studies to Identify and Prioritise the Functions of an Integrated Safety System for Motor Cycles." 52nd AAAM Annual Conference, San Diego, CA (USA), 05-08 October 2008.
- [3] M. Pierini, H. Cappon, J. Koenig, B. García, F. Lopez-Valdes. 2005. "APROSYS SP4: Motorcyclists: Accident National Data." APROSYS, Deliverable, AP-SP41.
- [4] R. Grant, R. Frampton, S. Peldschus, E. Schuller, V. StClair, M. McCarthy, R. Babu, M. Pierini, G. Savino. 2008. "Powered two-wheeler Integrated Safety. Project objectives, achievements and remaining activities." 7th International Motorcycle Conference, Cologne, Germany, 6-7 October 2008.
- [5] Y. Zhang, E. K. Antonsson and K. Grote. 2006. "A New Threat Assessment Measure for Collision

Avoidance Systems.” Proceedings, IEEE on Intelligent Transportation Systems, 968 – 975.

[6] R. J. Kiefer, D. J. LeBlanc, M. D. Palmer, J. Salinger, R. K. Deering, and M. A. Shulman. 1999. “Development and validation of functional definitions and evaluation procedures for collision warning/avoidance system.” CAMP, NHTSA, Final report DOT HS 808 964.

[7] R. J. Kiefer, M. T. Cassar, C. A. Flannagan, D. J. LeBlanc, M. D. Palmer, R. K. Deering, and M. A. Shulman. 2003. “Refining the CAMP crash alert timing approach by examining “last-second” braking and lane change maneuvers under various kinematic conditions.” CAMP, NHTSA, Final report DOT HS 809 574.

[8] K. Vavryn, M. Winkelbauer. 2005. “Braking Performances of Experienced and Novice Motorcycle Riders – Results of a Field Study.” Presented at the 2004 International Conference on Transport and Traffic Psychology, Nottingham, United Kingdom.

TESTING OF HEAVY TRUCK TIRE PRESSURE MONITORING SYSTEMS (TPMS) IN ORDER TO DEFINE AN ACCEPTANCE TEST PROCEDURE

Paul Grygier

Samuel Daniel, Jr.

National Highway Traffic Safety Administration

Richard Hoover

Timothy Van Buskirk

Transportation Research Center Inc.

United States of America

Paper No. 09-0551

ABSTRACT

Several manufacturers produce tire pressure monitoring systems for heavy trucks which are designed to detect low tire pressure and alert the driver. This paper reports on a series of test procedures conducted on these aftermarket TPMS to determine the suitability of these tests for use in developing performance requirements.

Five TPMS were installed one at a time on two heavy trucks. The minimum activation pressure of the TPMS was determined. After driving for a period of up to fifteen minutes, the vehicle was stopped and air was released from one tire to bring its inflation pressure to a point below the minimum activation pressure for the system. The vehicle was driven and the time needed for the system to detect the loss of pressure and alert the driver was recorded. Multiple tire deflations and failure modes were also tested.

Data were obtained from independent onboard instrumentation that measured tire pressure, vehicle speed and distance, and ambient temperature. A video of the TPMS driver display was recorded. Other properties were also evaluated, including temperature compensation accuracy of system pressure measurement and failure modes. The study's results are limited to the five systems tested. Although these systems were chosen to be representative of TPMS on the market, this was not an exhaustive study of all such systems.

INTRODUCTION

In 2000, Congress enacted the Transportation Recall Enhancement, Accountability, and Documentation (TREAD) Act, amending Title 49, United States Code, to require reports concerning defects in motor vehicles and tires, and other mandates to improve vehicle safety. Section 13 of this Public Law 106-414 requires that tire pressure warning systems be

installed in new motor vehicles to indicate when a tire is significantly underinflated. Following a one-year research project [1], NHTSA established Federal Motor Vehicle Safety Standard (FMVSS) No. 138, *Tire Pressure Monitoring Systems (TPMS)* [2], which mandated TPMS for vehicles of no more than 10,000 pounds in Gross Vehicle Weight Rating (GVWR). However, this rule did not cover heavy vehicles over 10,000 pounds GVWR. In 2006, the Federal Motor Carrier Safety Administration performed a test-track evaluation of a number of commercially available tire inflation and pressure monitoring systems [3]. This study reported the advantages and disadvantages of the tested systems.

This heavy truck test program addresses TPMS requirements for these heavy vehicles and it explores a series of test protocols which could be applied for verifying basic heavy truck TPMS performance capability.

DEFINITION OF TPMS

A Tire Pressure Monitoring System senses tire pressures and alerts the driver if pressures are outside of safety set points or pressure leakage rates. The "Monitor" systems read the actual pressure in each tire (direct TPMS) or estimate the relative pressure in a group of tires comparing the rotational speed of the tires using the antilock brake system (ABS) wheel speed sensors (indirect TPMS).

Five Types of Direct Pressure Reading TPMS

Using ABS wheel speed sensing is not a practical approach to determining if one tire in a pair of "duals" is low in tire pressure because both tires are mounted to the same hub. Although each tire has an individual rim, the rims are coupled such that the wheel speed for both tires is the same. Therefore, tire pressures must be measured directly to assure the

operator receives accurate information that will enable him to respond and ensure that each tire is provided with sufficient pressure to safely meet the expected load requirement placed upon the tire, as well as to ensure that the tire operates within its limits of pressure design criteria.

There are five types of tire pressure monitoring systems that are capable of directly reading the pressure of the air contained in individual tires of a heavy vehicle. The types are: rim mount (inside tire envelope), tire patch (mounted to tire inside tire envelope), interior valve stem (inside tire envelope), flow-through (outside of tire) and end-of-valve stem mount (outside of tire).

Systems Tested

This program tested two rim-mount systems, two flow-through systems, and one end-of-valve-stem unit. The two rim-mounted systems, the Dana/ SmartTire Smart-Wave S14486 and the HCI Corp Tire-SafeGuard TPM-W210, used internally mounted sensors (on bands around the rim) and included both pressure and temperature measurement of the air contained within the tire envelope. The SmartWave system applied the measured temperatures for “live” pressure compensation, whereas the Tire-SafeGuard system measured the temperatures for driver benefit to determine if a wheel was running hot and as a baseline for referencing cold inflation temperatures.

The sensors of the other three TPMS were mounted outside of the tire envelope, attached to the valve stem. The HCI Corp Tire-SafeGuard TPM-P310B1 provided tire temperature measurement that was acquired indirectly through the sensors mounted at the outboard end of the valve stems. Both it, and the WABCO/Michelin IVTM, provided auxiliary Schrader valves so the tires could be inflated without removing the sensors. The other TPMS system – Advantage Pressure-Pro CU41807684 - covered the end of the valve stem. The Pressure-Pro sensors needed to be removed from the valve stems in order to inflate the tires.

Characteristically, some TPMS have multiple pressure warnings, such as low tire pressure, extremely low pressure (or flat tire), and over-pressure. Some of the externally mounted TPMS have only one setpoint or pressure value for low tire pressure, but do provide for indication of a slow leak.

TEST VEHICLES AND TIRES

Two 10-tire, Class 8 vehicles were selected for demonstration of the TPMS acceptance procedure - a

Volvo three-axle tractor and a Peterbilt three-axle straight truck.

The Volvo tractor was a 1991 Model No. WIA64T sleeper-cab tractor with a 189-inch wheelbase. The GVWR was 50,000 lb and the Gross Axle Weight Ratings (GAWR's) were 12,000 lb (steer axle) and 19,000 lb (each drive axle).

The vehicle tire placard specified 275/80R24.5 tires at 100 psi, with a load rating of G, for all tire positions and the tires used for this program matched the placard specifications for tire size. The steer tires were Michelin Pilot XZA-1 Plus rated for 6,175 lb (max “single”) at 110 psi (DOT M591-BYUX-0508 and M591-BYUX-4207) and the drive tires were Michelin Pilot XDA-2 rated for 5,675 lb (max “dual”) at 110 psi (DOT M591-CM9X-4307 and M591-CM9X-4407). For safety considerations, the Volvo steer tires were tested at 105 psi. The Volvo drive tires were tested at 100 psi as recommended on the vehicle tire placard.

The Peterbilt truck was a 2004 Model No. 357 day cab straight truck with 273-inch wheelbase. The GVWR was 62,000 lb and the GAWR's were 18,000 lb (steer axle) and 22,000 lb (each drive axle).

The steer tires used were Bridgestone 315/80R22.5, M843 V-Steel Mix, Low Pro, M&S, load range L, rated for 9,090 lb (max) at 130 psi (DOT 2C4D-5BF-3007). They were tested at a cold inflation pressure (CIP) of 130 psi.

The drive tires were Firestone 11R-22.5 – 14PR, FD663 Radial, load range G, rated for 5,840 lb (max) at 105 psi (DOT 4D3T-3E3-0708). For the Peterbilt truck TPMS tests, the drive tires were inflated to the maximum specified on the tire sidewall, 105 psi. Therefore, all tires on the Peterbilt were inflated to their maximum tire pressures as labeled on the sidewalls.

INSTRUMENTATION

The setup of the TPMS components, including initialization of the Central Processing Unit (CPU), programming of the tire pressure warning setpoints, as well as documentation of significant events during testing, were vital to the mission of this project. All of these activities were established and recorded using a digital Computerized Data Acquisition System (CDAS), a thermal probe, and a video camera.

Data Channels

A ruggedized benchtop-PC computer collected 16 channels of data during the TPMS testing. Parameters measured included: 10 individual tire pressures, vehicle speed and distance, 3 types of event indications, and ambient temperature.

Tire Pressures

Individual tire pressures were transferred to the cab using a network of rotary unions, valves, tee couplings, hoses, and transducers. To allow for wheel rotation, rotary unions were installed in the air lines at each wheel to couple the pressures in the tire envelopes directly to the in-cab data acquisition system. The drive wheels used two port unions so pressures from both inner and outer tires of each dual set were monitored live. Air line tee couplings were added at each valve stem to allow for simultaneous connection to both TPMS and data collection system. Standard ¼-inch SAE J844 truck air line tubing connected the rotary unions to a manifold system mounted in the truck cab.

The manifold system consisted of 10 pressure-control ball valves and pressure transducers. The pressure transducers were configured for a range of 0 to 200 psi with accuracies of 0.5 percent of full scale. The tire pressure controllers allowed for remote inflation or venting of one or more tires simultaneously, zeroing of transducers, and logging of real-time tire pressures.

Vehicle Speed and Distance

Vehicle speed was measured using an ADAT DRS-6 Radar Speed Sensor by B&S Multidata. This dual antenna microwave device provided high accuracy logging of vehicle velocity over the dry surfaces driven without contact with the roadway surface. The digital output was then directly fed into a Labeco Model No. 625 Performance Monitor to log accumulated distance traveled.

Event Channels

Three event channels were configured on the CDAS data collection system to interface events real-time into the data set. A driver event button was installed so the observer riding in the truck during the track tests could signal the data set that an observation was made (this freed the driver to actually concentrate on driving). Driver events were logged when significant events occurred about the test track, such as when the vehicle reached the target speeds (i.e. “now at 60 mph”), when the vehicle stopped for intersections, or

at the end of the driving segment of the test. If the observer heard a TPMS buzzer, the driver event button was also actuated.

Temperatures

Live tire temperature measurements were not logged for this project; however, constant vigilance was maintained for any indication of tire heating. Before and after each track run, individual tire temperatures were measured using a Fluke k-type thermal probe. The probe was inserted deep into the tread of each tire, maintained until the readings stabilized, and then the tire temperature measurements were recorded.

The CDAS maintained a real-time log of the variations measured in the ambient temperature experienced while the tire pressures were being adjusted in the preparation bay, and while the truck was being driven on the test track.

Video Log

A mini-DVD tape camera, zoomed in to view the TPMS displays and a portion of the CDAS monitor, was used to log all in-cab TPMS activity. The camera logged changes applied to pressures in test tires, TPMS events and display warnings, audible buzzer sounds, and verbal commentary from both the driver and the observer.

TEST PROCEDURES

Direct pressure reading TPMS do not rely upon ABS wheel speed sensing to indicate low tire pressures. Actual driving with the systems installed did not appear to modify any calibration parameters used by the TPMS tested. However, a calibration run was made before any low-pressure detection tests were begun to allow time for all sensors to begin active transmission of measured pressure values.

Once the calibration runs were completed, a series of tests were performed that evaluated the sensing capabilities of the various TPMS on individual tires with reduced tire pressures. After detecting the low tire pressure, the ignition switch power to the TPMS was cycled to assess the short-term memory retention of the alarm condition. After cooling the tires, the test tire was re-inflated to CIP and the re-inflation identification response of the TPMS was noted.

Preparation to Test TPMS Performance

To prepare to run the TPMS performance test program, the test vehicle was outfitted with new tires, plumbed with a tire pressure control system that regulated pressure in all tires, and instrumented with

individual tire pressure sensors and a central data acquisition system. A video camera was installed in the cab to log test events, along with both driver and observer commentary.

Once prepared, the truck was parked in a shaded area (such as the truck bay with the garage doors open) and the tires were inflated to the specified CIP. Then, the TPMS was turned on and observations made of the validity and completeness of the lamp check sequence. The TPMS was programmed to identify each tire pressure sensor (if needed) and actual TPMS pressure readings were collected. Tire temperature readings were made if the TPMS was so equipped, and a thermal probe was used to measure the external tire temperatures, between the ribs or lugs.

TPMS Calibration Test – Sensor Identification

The FMVSS No. 138, “Tire Pressure Monitoring Systems” [2] as written for light vehicle TPMS, specified that a calibration run should be provided before beginning any low-pressure detection tests. Following this lead, all heavy truck tests herein were given ample vehicle-in-motion time prior to actual low-pressure detection tests. The calibration test is part of the light vehicle test procedures, designed to allow the systems to make any necessary adjustments prior to the low tire detection test. The calibration procedure is intended primarily for indirect TPMS, but the procedure is recommended for the heavy vehicle TPMS test procedures so that the procedures are technology neutral.

After initial installation and preparation, the TPMS was subjected to a system “calibration” test. With the pressures successfully set to CIP at ambient temperature, the TPMS was powered up. Initial tire pressure and temperature readings of both the CDAS and TPMS were recorded. If a sensor did not immediately transmit a pressure signal, its reading was taken after the vehicle was put into motion for the calibration procedure. The truck was driven once around a 7.5-mile test track with constant running speeds near 60 mph and returned to the starting point. The total tire rolling time ranged from 12 to 15 minutes. During this time, all sensors “woke up” and began actively transmitting pressure signals.

A variation of the calibration procedure was applied for the tractor (the second test vehicle). In this “cool” calibration test, the tractor was driven for 8 to 10 minutes over a flat road. The vehicle speed was limited to 25 mph for the 2-mile loop. The tire temperatures rose 5 to 10 degrees above ambient and

were fairly stable at the time of the subsequent low-pressure detection tests. With tighter pressure ranges, the pressure detection tests frequently did not require driving the tractor to detect the set low tire pressure levels. As there was little heat added during these tests, the tire cooling period was reduced, thereby lowering the total test-cycle time required for testing each tire.

TPMS Low-Pressure Detection Test

The pressure was reduced in one test tire while the TPMS was turned off. After the pressure was adjusted, the TPMS was turned on. If the display immediately alarmed, the low-pressure detection test was considered successful and complete. If the display initialized, but did not identify the low-pressure tire, the truck was driven once around a 7.5-mile test track (for a period of 12 to 15 minutes) on a low tire pressure detection run, where steady state speeds reached or exceeded 60 mph for at least 5 minutes of the run. If the TPMS still did not identify the low tire pressure, the sensor channel for that tire was listed as “failed to detect” at that low-pressure setpoint. When the TPMS did display the low tire pressure alert, the time to alert was recorded.

After returning to the starting point, a five-minute memory check was performed to determine if a temporary lapse of power to the system (such as turning off the engine during a snack break or stop at the shipping office) would lose the low pressure warning display. The ignition power to the TPMS was turned off. After five minutes had elapsed, power was restored to the TPMS and the status of the alarms recorded. The TPMS was turned off again while the tires cooled.

The low-pressure tire was re-inflated to CIP and the TPMS was then turned on back to read the now-correct tire pressure levels. If the TPMS correctly identified the restored pressure, the Low Tire Pressure Detection Test was complete. However, if the TPMS failed to clear the previous low-pressure warning, the truck was again driven once around the 7.5-mile test track for a Reset Identification Test, in expectation that it would clear the warning.

This procedure was repeated for each of four individual tires. An additional test was run with simultaneous multiple low pressure tires to determine the order and extent of the warnings presented by the TPMS.

TPMS Malfunction Tests

This section of testing was unique, as each TPMS system contained different setup procedures, programming methods, and electronic components. One common feature for the systems tested was that none of the sensors had batteries that were user-replaceable. The transmitters could not be powered down to identify lack of communication. Therefore, each system was tested for absence of a transmitter by removing the tire and transmitter from the vehicle and physically moving them to a remote location over 100 feet from the receivers in the trucks. For the TPMS with remote antennas, the antennas were removed to simulate loss or damage to them as might occur while traveling on the highway.

SYSTEM TEST RESULTS FOR LOW PRESSURE DETECTION

Data were collected in multi-media style to ensure no details were missed. The highlights of the data collected for the various low-pressure setpoints are tabulated in separate tables by TPMS system, by vehicle, and then by setpoint pressure. Within each table, there is a comparison of the four individual tires tested at the same relative pressure setpoint (e.g., CIP - 10 percent), the test pressure actually applied, corresponding tire temperature at the time the pressure was reduced, the type of alarm expected to be displayed for the low-pressure level, a description of the alarm indication - when and where it occurred, and a description of the alarm indication moments after the tire was re-inflated to CIP.

System A – SmartWave – Rim Mount

The SmartWave system, tested first, was subjected to the prescribed tests at three different test pressure levels. Because it did provide two distinct low tire pressure identification setpoints, the first two test pressures were set to a allowance of 2 psi below the setpoints (which were factory set at -10 and -20 percent below CIP respectively) and the third test pressure at 2 psi below the CIP minus 25 percent level.

After reviewing the results of the first few tests run at pressures beyond the initial setpoint, it appeared that the test pressure allowance may have been set too tightly. A brief experiment was run using the truck to explore the possibility of increasing the allowance from 2 psi to 3 psi. This increase allowed for differences in the compensation scheme of the SmartWave system that tended to run 2 psi to 3 psi lower than data system reference pressures in random pressure comparisons. All TPMS tests performed

after this initial truck/TPMS configuration applied the 3-psi allowance for all test pressures (3 psi below the TPMS setpoints).

The SmartWave system provided a tire pressure temperature-compensation chart with which to adjust tire pressures at elevated temperatures (beyond ambient) for an initial CIP referenced to 65°F. No other TPMS manufacturer's installation package included a temperature compensation chart.

Because the SmartWave was received with a temperature compensation chart, all target pressures were adjusted (for the Peterbilt truck only) to test pressures specified by the SmartWave compensation chart for the TPMS tire temperatures measured at the end of the calibration test. Therefore, the truck tire test pressures were adjusted to somewhat above the non-compensated target pressure levels used for the other TPMS. In contrast, the later tractor series tests of the SmartWave TPMS used non-temperature-compensated target pressures that were calculated using straight 90 percent and 80 percent of the actual CIP's before subtracting the 3 psi allowance allowance, which was the same approach used for the other TPMS installed on the tractor.

For the 10-percent "Low Deviation" tests on the truck tires, the SmartWave correctly identified the 10-percent low-pressure deviation level (Table 1) before completion of the 15-minute detection run, for 4 out of 4 cases. During one of the tests, the SmartWave identified the low-pressure deviation applied to the subject tire, soon after the TPMS was turned "on". During the other three tests, the SmartWave correctly identified the low-pressure deviation, but the alarm did not activate until the truck was already put into motion for the 15-minute detection run. The test pressures applied (as prescribed by the SmartWave temperature compensation chart) only ranged from 4.8 to 7.6 percent below the actual CIP pressures, as the elevated tire temperatures caused the pressures in the test tires to rise somewhat above CIP during the "hot calibration" test. As such, a pressure loss of 10 percent below the "hot" tire pressures was detected by the SmartWave TPMS. With temperature compensation, the SmartWave detected a pressure loss of 10 percent of the hot tire pressure reading, making it more sensitive to detecting pressure loss than TPMS without compensation.

In Table 1, a yellow highlighted Detection Status box indicates that the truck was actually driven to allow the TPMS to detect the low-pressure condition applied. Once the warning activated, the truck was

driven back to the shaded starting point (truck bay). Driving was discontinued to allow time for the low-pressure alarm to clear due to an increase in pressure caused by increasing tire temperature (thermal lag from the previous drive). A box in Table 1 that is not highlighted indicates that the TPMS properly identified the low-pressure deviation condition before the truck was driven; therefore, it was not driven for this step of the test procedure.

Table 1.
SmartWave (rim mount) low deviation setpoint = 10 percent below CIP - Truck

Tire	CIP (psi)	Test Pressure Used	Detection Status	Re-inflation Status After Cool Down
LF	130	123 psi. @95°F	alarm before driving	clear before driving
RF	130	123 psi. @95°F	alarm during driving	clear before driving @ 10.7min
LII	105	97 psi. @86°F	alarm at gate while driving	clear before driving
RRO	105	100 psi. @100°F	alarm backing out while driving	clear before driving

Tire positions: LF=left front, RF=right front, LII=left intermediate inner, RRO=right rear outer

For the second low-pressure setpoint on the truck installation of the SmartWave TPMS, the test tire pressures were reduced to 2 psi below the 20-percent-low level. The applied test pressures ranged between 14 and 19 percent below the actual CIP values (again as interpolated from the SmartWave tire pressure correction chart).

For this series, the level of alert appeared to be affected by the timing of setting the compensated test pressures. After the “hot calibration” tests, the tires began to cool quickly. The first tire temperature value read after the calibration test ended was used to determine the compensated test pressure for the following low tire pressure detection test. The test procedure guidelines followed allowed only 5 minutes to adjust the tire pressure for the low pressure detection test. The SmartWave alarm activated at the test pressure, but incorrectly displayed the low deviation alert instead of the critical low pressure alert. It was felt that the less severe warning activated because the test pressure applied was obtained using the temperature compensation chart, and was a value higher than would have been applied if a straight uncompensated test pressure were applied.

The SmartWave correctly identified the reset pressure immediately after the tires were re-inflated for 3 of 4 tests. For the fourth test, re-inflation identification “reset” automatically cleared the previous warning from the display screen as the truck was being backed from the building (Table 2). Therefore, the SmartWave did alert to the low-

pressure conditions on each application, but it did not correctly indicate the severity level expected for the lower pressure tests using temperature compensation and allowing only a 2-psi allowance for the setpoint.

Table 2.
SmartWave (rim mount) critical low-pressure setpoint = 20 percent below CIP - Truck

Tire	CIP (psi)	Test Pressure Used	Alarm	Detection Status	Re-inflation Status After Cool Down
LF	130	108	Low Deviation, NOT Critical Low	alarm while driving T=7.8min Dist=0.6mi	clear before driving
RF	130	109.2	Low Deviation, NOT Critical Low	alarm while backing T=2.4 min Dist=16ft	clear while backing T=3.4min, Dist=132ft
LII	105	85.1	Critical Low Pressure	alarm while backing T=1.6min Dist=100ft	clear before driving
RRO	105	89.7	Low Deviation, NOT Critical Low	alarm before driving >1.9min	clear before driving
Multi	130 & 105	LF-95 RF-94 LII-75	Critical Low Pressure	alarm before driving	clear before driving

Note – 130 psi -25% = 97.5 psi; and 130 psi – 20% = 104 psi (the uncompensated setpoint)

An additional test was performed where three of the four test tires were simultaneously subjected to the same 20 percent pressure reduction. For detection of multiple low pressure tires, the SmartWave TPMS correctly identified a critical low tire pressure for each tire and alerted the driver before the vehicle needed to be driven on the detection run. Upon resetting the tire pressure to CIP, the TPMS display cleared all warnings without needing to drive again.

For the SmartWave TPMS, using temperature compensation to adjust tire pressure appears to be beneficial in determining early alerts of low tire pressure. Inflating a tire to CIP at 65°F provides sufficient load carrying capacity to meet tire design specifications. With compensation, a low tire pressure of 10 percent below expected pressure can be repeatedly detected, even at elevated tire temperatures.

To continue the original test procedure guidelines for the second vehicle (the tractor), the SmartWave pressure setpoints were re-programmed to the CIP requirements of the tractor tires. Because the “cool” calibration procedure was applied to all tractor tests, the measured tire temperatures were near ambient temperature when lowering the tire pressures down to the test pressures. The data presented in Table 3 reflect the procedural change to “testing without applying temperature compensation” to adjust the test pressures. All five TPMS systems tested on the tractor used the same “cool” calibration procedure

and no temperature compensation. For the SmartWave system, all test pressures were set to a fixed allowance of 3 psi below the 10-percent-low deviation setpoint without regard to measured tire temperature.

Table 3.
SmartWave (rim mount) low deviation setpoint = 10 percent below CIP - Tractor

Tire	CIP (psi)	Test Pressure Used (psi.)	Detection Status	Re-inflation Status After Cool Down
LF	105	92	alarm before driving	clear before driving
RF	105	92	alarm before driving	clear before driving
LII	100	87	alarm before driving	clear before driving
RRO	100	87	alarm before driving	clear before driving

For each tire position tested, the SmartWave detected the reduced tire pressure and activated a “low deviation” alert. After cooling the tires for one-half hour, the tires were re-inflated to uncompensated CIP. When the ignition power was restored to the TPMS, the previous warning flashed briefly on the display, then cleared without needing to drive the tractor on a re-inflation identification run.

Similar results were attained for the more severe Critical Low pressures summarized in Table 4. The test pressures 81 psi (steer) and 77 psi (drives) were set at 3 psi below fixed pressure decrements of 20 percent below CIP.

Table 4.
SmartWave (rim mount) critical low-pressure setpoint = 20 percent below CIP - Tractor

Tire	CIP (psi)	Test Pressure Used (psi.)	Detection Status	Re-inflation Status After Cool Down
LF	105	81	alarm before driving	clear before driving
RF	105	81	alarm before driving	clear before driving
LII	100	77	alarm before driving	clear before driving
RRO	100	77	alarm before driving	clear before driving
Multi	105 & 100	81 & 77	alarm before driving	clear before driving

*1: TPMS alarmed for RIO non-test tire that went out of normal operating pressure range.

Following are two pictures which show the installation of the sensor on a rim without the tire (Figure 1) and the array of antennas, sensors, display, rim bands, and hardware associated with the SmartWave TPMS (Figure 2).



Figure 1. SmartWave sensor mounted on the tractor steer axle rim.



Figure 2. SmartWave components kit.

System B – Tire-SafeGuard – Rim Mount

The Tire-SafeGuard “rim mount” was tested second. Its sensors mounted with bands onto the rims, similar to those of the SmartWave system. The primary difference between the SmartWave and the Tire-SafeGuard was that the Tire-SafeGuard only had one low-pressure setpoint for each axle group of tires. The setpoints needed to be programmed as actual declared pressures, rather than deviation percentages of an initial pressure. The pressures added to the program corresponded to the nearest whole unit psi resulting from an assumed low-pressure indication (similar to some other TPMS units tested) of CIP minus 12 percent. Actual test pressures applied were presented as 3 psi below the low-pressure setpoints. Upon operation, a low-pressure alert was expected to activate for each tire that was set to run low on inflation pressure. Figure 3 shows the three receiving antennas, ten sensor transmitters, and the steel mounting bands.



Figure 3. Tire-SafeGuard (rim mount) components kit.

Care was taken when installing the tire onto the rim to ensure no damage was incurred by the sensor transmitter antennas. Figure 4 shows the tight clearance encountered when lifting the tire over the sensor to seat the tire on the bead.



Figure 4. Tire-SafeGuard sensor and rim-mounting band – showing antenna.

For the straight truck tests, the steer tire low-pressure warning setpoints were set to 114 psi, which was approximately 12 percent below the 130 psi CIP. The setpoints for the drive tires were set to 92 psi, or approximately 12 percent below the drive tire CIP of 105 psi. The test pressures applied were 3 psi below the setpoints at 111 psi (steers) and 89 psi (drives). The “hot calibration” procedure was used for all tests on the straight truck. For all four individual tire tests, the Tire-SafeGuard rim mount TPMS displayed the correct low pressure alert. Three of the four tests responded quickly, before moving the vehicle. The fourth unit alarmed while the truck was being driven to the test track on the detection run. After cooling the tires, all four sensors showed the appropriate response to re-inflating the tires by displaying a

“ready” display after cycling through system power-on and a quick check of sensors. After lamp check, the display would briefly show the previous low tire warning, and then abruptly clear and reset to ready mode (Table 5).

Table 5.
Tire-SafeGuard (rim mount) low-pressure setpoint = ~ 12 percent below CIP – Truck

Tire	CIP (psi)	Setpoint Pressure or Delta %	Test Pressure Used (psi)	Detection Status	Re-inflation Status After Cool Down
LF	130	114 psi (~ -12%)	111	alarm before driving	clear before driving
RF	130	114 psi (~ -12%)	111	alarm before driving	clear before driving
LII	105	92 psi (~ -12%)	89	alarm before driving	clear before driving
RRO	105	92 psi (~ -12%)	89	Alarm at gate while driving	clear before driving
Multi	130 & 105	114 & 92 psi (~ -12%)	111 & 89	alarm before driving	clear before driving

A simultaneous multi-tire low-pressure detection test followed (last row in Table 5), to identify more than one tire in a low-pressure condition. The results duplicated the single tire tests in that the Tire-SafeGuard alerted to all four tires being low in pressure (and without driving the detection run). After re-inflating the four tires, the display promptly cleared the faults and displayed a ready screen.

When the Tire-SafeGuard “rim mount” TPMS was transferred to the tractor, the setpoints were adjusted to meet the new CIP requirements. The steer tire low-pressure warning setpoints were set to 92 psi, which was approximately 12 percent below the 105 psi CIP. The setpoints for the drive tires were set to 88 psi, or 12 percent below the drive tire CIP of 100 psi. The applied test pressures were 89 and 85 psi, respectively. The “cool calibration” procedure was used for all tests on the tractor (Table 6).

Table 6.
Tire-SafeGuard (rim mount) low-pressure setpoint = ~ 12 percent below CIP - Tractor

Tire	CIP (psi)	Setpoint Pressure or Delta %	Test Pressure Used (psi)	Detection Status	Re-inflation Status After Cool Down
LF	105	92 psi (~ -12%)	89	alarm before driving	clear before driving
RF	105	92 psi (~ -12%)	89	alarm before driving	clear before driving
LII	100	88 psi (~ -12%)	85	alarm before driving	clear before driving
RRO	100	88 psi (~ -12%)	85	alarm before driving	clear before driving
Multi	105 & 100	92 & 88 psi (~ -12%)	89 & 85 psi	alarm before driving	clear before driving

Note: only one setpoint pressure was tested for this unit as it only had one level to test.

For this configuration, in all four tests using single tires with low pressure, the Tire-SafeGuard “rim

mount” TPMS rapidly responded with a low-pressure warning before the truck was driven for the detection run. The same response resulted from the four-tire multiple-low-tire pressure test, as well. As in the truck tests, the system again reset appropriately after re-inflating the multiple deflated test tires to CIP.

System C – Tire-SafeGuard – Flow Through

An additional Tire-SafeGuard TPMS was tested, except, instead of mounting the sensors on the rims, the sensors were mounted on the valve stems externally, in a flow-through mode. It had a driver display and operating functions similar to the previous Tire-SafeGuard unit. One drawback to the flow-through sensors was the fact that the temperature measurements provided by the TPMS were measured in the valve stems, outside of the captive air inside of the tire envelope (Figure 5). The flow-through sensors traded ease of installation and maintenance for temperature precision. This flow-through system only required the use of one receiving antenna. Figure 6 shows the receiving antenna, 10 small valve-stem mounted flow-through sensors, and small driver display.



Figure 5. Tire-Safeguard (flow-through) sensor with test hose attached for remote inflation.



Figure 6. Tire-Safeguard (flow-through) components kit.

The installed sensors appeared compact and unobtrusive to would-be vandals. These flow-through sensors attached directly to the valve stem, thereby eliminating the need for any external connecting hoses for a standard installation. It is not known if the added mass may lead to valve stem leakage or fatigue. (Durability issues are outside the scope of this paper.)

In operation, the “flow-through” Tire-SafeGuard system provided only a single setpoint for determining low tire pressures. Again, the setpoints needed to be programmed as pressure levels, not percentages of CIP, so the pressure levels from TPMS unit B Tire-SafeGuard “rim mount” were also applied for TPMS unit C – the Tire-SafeGuard “flow-through” system.

For the truck tests, the “hot calibration” test procedure was followed. Under subsequent low pressure detection tests, the Tire-Safeguard flow-through system correctly identified all four individual low tire pressure readings using a test pressure of 3 psi below the setpoints (which were set at approximately 12 percent below CIP). The TPMS display responded quickly with a low pressure warning, eliminating the need to run a detection test on the test track.

After cooling and re-inflating the tires, the Tire-SafeGuard quickly reset and cleared the faults, thereby returning to a quiescent ready mode (Table 7). A simultaneous low tire pressure test was not performed for the truck installation, but was conducted later for the tractor installation.

Table 7.
Tire-SafeGuard (flow-through) low-pressure setpoint = ~ 12 percent below CIP - Truck

Tire	CIP (psi)	Setpoint Pressure or Delta %	Test Pressure Used (psi)	Detection Status	Re-inflation Status After Cool Down
LF	130	114 psi (~ -12%)	111	alarm before driving	clear before driving
RF	130	114 psi (~ -12%)	111	alarm before driving	clear before driving
LII	105	92 psi (~ -12%)	89	alarm before driving	clear before driving
RRO	105	92 psi (~ -12%)	89	alarm before driving	clear before driving

For the tractor tests using the Tire-SafeGuard “flow-through” sensor system, results obtained were similar to those measured in the truck tests. The display alarmed before the detection run was begun; therefore the tractor was not driven for this test sequence. After cooling and re-inflating the test tires, the TPMS reset correctly, shortly after repowering the display.

A multi-tire low-pressure test was performed (Table 8) on the tractor installation, following a “cool calibration” preparatory test. The TPMS detected all four low tire pressure readings in rapid succession and did not require the tractor to be driven on a detection run. After cooling and re-inflating the tires, the display showed that the TPMS successfully reset to the ready mode.

Table 8.
Tire-SafeGuard (flow-through) low-pressure
setpoint = ~ 12 percent below CIP – Tractor

Tire	CIP (psi)	Setpoint Pressure or Delta %	Test Pressure Used (psi)	Detection Status	Re-inflation Status After Cool Down
LF	105	92 psi (~ -12%)	89	alarm before driving	clear before driving
RF	105	92 psi (~ -12%)	89	alarm before driving	clear before driving
LII	100	88 psi (~ -12%)	85	alarm before driving	clear before driving
RRO	100	88 psi (~ -12%)	85	alarm before driving	clear before driving
Multi	105 & 100	92 & 88 psi (~ -12%)	89 & 85 psi	alarm before driving	clear before driving

Therefore, the Tire-SafeGuard “flow-through” TPMS correctly measures and responds to test pressures of 3 psi below low-pressure setpoints without temperature compensation. The drawback is that if the tires get hot after the initial tire inflation to CIP at ambient temperature, a 105 psi CIP tire that is heated to running temperature may see an increase of 5 to 10 psi (or more) to over 115 psi. At these temperatures, the tire would have to experience a pressure loss of 23 psi before this system would activate a low tire pressure alarm (below 92 psi). The pressure may drop down to the low 80’s in psi when returned to the original ambient temperature, where the load capacity would be greatly diminished.

System D - WABCO/Michelin IVTM – Flow Through

The fourth TPMS tested was manufactured by WABCO and distributed by Michelin. The IVTM provided a valve stem mounted “flow-through” tee coupling to accommodate simultaneous tire pressure measurement and tire re-inflation through an auxiliary supply port. A short length of flexible hose coupled the tee to the IVTM sensing transmitter. The sensor was mounted on a steel plate that attached to two of the wheel lug bolts after the hub-piloted wheels were installed onto the hub. Normal torque was applied to tighten the wheel lug nuts. If two sensors were used to measure a set of dual wheels (on a drive axle), they were placed opposite one another. When only one tire pressure sensor was used (on a steer axle), a counterbalance weight provided by WABCO was installed on the wheel opposite of the

sensor (Figure 7). The long-term effects of the mounts on lug nut tightness were not studied.



Figure 7. IVTM mounted on right steer tire with plumbing for data system.

This was the most complex of the externally mounted TPMS as the sensors were mounted on wheel-lug plates and included valve stem extension hoses with tee-fittings (Figure 8).



Figure 8. IVTM components kit.

No low-pressure setpoint values were listed in any of the numerous brochures and manuals supplied with the IVTM. Hence, a slow leak-down test was performed to derive empirically the two low-pressure setpoints of the IVTM. A low-pressure setpoint was found to be 20 percent below the CIP and the second setpoint at 35 percent below CIP.

The truck was tested first and used the “hot calibration” procedure prior to the low tire pressure detection tests. For the first setpoint, all four individual tire tests produced timely first level alarms using a test pressure of 3 psi below the CIP minus 20 percent level. Therefore, no low-pressure detection test track driving tests were needed at this pressure

level. After cooling the tires and then re-inflating with air to CIP, the IVTM delayed in clearing the low-pressure alert until nearly the end of the reset identification run, (5.8 miles into the 8.3-mile test track course and after 11.2 minutes) (Table 9). For the other three single tire tests, the IVTM produced a first level alert and cleared promptly after re-inflating, without necessitating any driving on the track, beyond the initial calibration runs.

Table 9.
IVTM (flow-through) low-pressure setpoint 1 = 20
percent below CIP – Truck

Tire	CIP (psi)	Test Pressure Used (psi)	Detection Status	Re-inflation Status After Cool Down
LF	130	101	alarm before driving	clear during driving 11.2 min, 5.8 mi
RF	130	101	alarm before driving	clear before driving
LII	105	81	alarm before driving	clear before driving
RRO	105	81	alarm before driving	clear before driving
Multi	130 & 105	both	alarm before driving	clear before driving

For the multiple-alert test (last row in Table 9), simultaneous-low-tire-pressure test, the same 4 tires were deflated to the previous individual test pressures (3 psi below CIP-20%). The driver display was inadvertently left turned on during the release of air from the tires. Because the “vents” dumped air from the selected tires very rapidly, the IVTM display alerted to critical low pressures every time the vents discharged air. With the test apparatus close coupled in a tee formation at the wheel, the TPMS read the sudden decrease in pressure from the venting lines, thereby indicating critical alerts. Each time the release of air was stopped for more than a few seconds, the critical alert for that channel cleared. The TPMS was turned off at approximately 2.5 minutes into the adjustment period, with the 4 pressures still being vented down to the setpoints. After the test pressures were established in the 4 tires, the IVTM was turned back on. The IVTM quickly displayed 4 first level low-pressure alerts (portrayed by a “turtle” icon). Having passed the multiple-low-tire pressure detection test, the tires were re-inflated. The system cleared the faults after repowering the display.

The CIP values were reprogrammed for the tractor tests to match the lower tire pressure requirements. The tractor was driven on the “cool calibration” circuit before beginning low tire pressure tests. Again, the IVTM displayed appropriate low-pressure warnings for the 20 percent low pressure level, and reset upon restoring the tires to CIP pressures (Table 10).

Table 10.
IVTM (flow-through) low-pressure setpoint 1 = 20
percent below CIP – Tractor

Tire	CIP (psi)	Test Pressure Used (psi)	Detection Status	Re-inflation Status After Cool Down
LF	105	81	alarm before driving	clear before driving
RF	105	81	alarm before driving	clear before driving
LII	100	77	alarm before driving	clear before driving
RRO	100	77	alarm before driving	clear before driving
Multi	105 & 100	81 & 77	alarm before driving	clear before driving

System E - Pressure-Pro – Valve-Stem-End Mount

The fifth TPMS system tested was from PressurePro. That system contained the least number of components and was the simplest to install. The single receiving antenna was mounted directly to the top of the driver display; therefore, the only cable to install was for system power.

The sensors were installed by removing the valve stem caps and replacing them with the sensors. However, there was some concern raised when installing the sensors on aluminum rims with small hand-holes. The sensor nearly filled the opening in the rim, thus making it challenging for the installer to ensure that proper tightness was applied to the sensor. The clearance around the sensor was less of a concern for installation on steel wheels with larger hand-holes in the rim (Figure 9).



Figure 9. Two adjacent PressurePro sensors in initial setup for dual tractor tires.

After consulting the manufacturer, the outer wheel was rotated 180 degrees to balance out the weight of the two sensors.

Figure 10 shows the installation kit for the PressurePro TPMS. The packet contained ten sensors, a driver display, and a power cable.



Figure 10. Components kit for PressurePro valve-stem-mounted 10-tire system.

The PressurePro TPMS came configured with two low pressure level setpoints. The “first stage low pressure” setpoint was 12.5 percent below CIP. The “second stage low pressure” or critical low-pressure setpoint was fixed at 25 percent below CIP. To initialize the system, the tires were properly inflated to CIP. Next, the sensors were installed one at a time in the PressurePro wheel sequence, while confirming both position and pressure on the driver display. No actual setpoint pressure values were programmed into the TPMS. The Pressure Pro used the initial pressure readings as the CIP reference for each wheel. Caution was exercised to ensure that the correct CIP pressure was contained in the tire when initializing the sensors. When lowering the air pressures for the respective low-pressure detection tests, the test pressures were set 3 psi below the setpoints for each pressure warning level and for each vehicle.

For the first level low-pressure warnings setpoints (CIP minus 12.5%), the truck test pressures were set to 111 psi (steers) and 89 psi (drives). For the tractor, the test pressures were 88 and 84 psi, respectively. The results from the individual wheel low-pressure tests showed that the PressurePro correctly read and displayed pressures for the two distinct setpoint levels for each vehicle, and quickly warned of the low tire pressures. Upon re-inflating the tires and turning on the TPMS power, the display indicated that the warnings of low tire pressure had appropriately cleared (Table 11 and Table 12).

Table 11.

PressurePro (valve-stem cap) first stage low-pressure = 12.5 percent below CIP – Truck

Tire	CIP (psi)	Test Pressure Used (psi)	Detection Status	Re-inflation Status After Cool Down
LF	130	111	alarm before driving	clear before driving
RF	130	111	alarm before driving	clear before driving
LII	105	89	alarm before driving	clear before driving
RRO	105	89	alarm before driving	clear before driving
Multi	130 & 105	111 & 89	alarm before driving	clear before driving

Table 12.

PressurePro (valve-stem cap) first stage low-pressure = 12.5 percent below CIP – Tractor

Tire	CIP (psi)	Test Pressure Used (psi)	Detection Status	Re-inflation Status After Cool Down
LF	105	88	alarm before driving	clear before driving
RF	105	88	alarm before driving	clear before driving
LII	100	84	alarm before driving	clear before driving
RRO	100	84	alarm before driving	clear before driving
Multi	105 & 100	88 & 84	All alarmed before driving (in a span of 111 sec.)	clear before driving

Additionally for each vehicle, four tire sensors were tested simultaneously for low tire pressure warning. The display responded with a composite array of red LED's showing the exact mounting locations of the four underinflated tires. After re-inflating the tires, the PressurePro again cleared its display and returned to the ready mode.

MALFUNCTION TESTS

The following procedure was used to test each system for a simulated failed sensor and for a disconnected antenna.

All tires were inflated to the proper CIP. The tire pressures were logged from both the TPMS and the data acquisition system. The right front tire was the target in this test (except for the Flow-Through Tire-SafeGuard System which used the left intermediate axle inner tire). The target tire was removed and rolled out of the area about 100 ft from the truck. The TPMS was then monitored to see if it detected the removed sensor, and if so, the time required for detection. The tire was then replaced to see if the system cleared the display of the failed system (malfunction) signals.

Another malfunction test was performed by disconnecting the antenna. The antenna cable was disconnected and the time logged. The TPMS was then monitored to see if it warned of a fault. The antenna was then reconnected to see if the system

would clear the fault warning from the display. The results for both tests are presented in Table 13.

Table 13.
Results of malfunction testing

System	Sensor Test		Antenna Test	
	Result	Time to Warning	Result	Time to Warning
SmartWave	Passed	36 min	Passed	33 min
Tire SafeGuard (rim mount)	Failed	N/A	Failed	N/A
Tire-SafeGuard (valve-stem mount)	Failed	N/A	Failed	N/A
Wabco IVTM	Passed	30 sec	N/A	N/A
PressurePro	Passed	5 min	N/A	N/A

SUMMARY AND CONCLUSIONS

The data results have shown that the type or brand of vehicle did not alter the individual TPMS results. The results for a given TPMS on a 10-tire truck were repeated when later installed on a 10-tire tractor, without observing any vehicle influence on the test results even though the vehicles were equipped with different tires, rims, and the TPMS were adjusted to different CIP's.

Each of the five TPMS tested during this research project was successful at identifying at least one preset level of low tire pressure, signaling low tire pressure to a driver display, and clearing the low-pressure warning from the display after the tire was re-inflated. Some problems were encountered during installation of the systems onto the test vehicles and there were also some problems with the setup and operation of the systems. The problems were overcome by the engineers and technicians assigned to this research project; however, a commercial carrier may not have similar resources available and may not be able to successfully add these systems to in-service vehicles without aid from the system manufacturer. However, it is anticipated that vehicle manufacturers and TPMS suppliers would work together to develop efficient systems if TPMS is mandated for heavy vehicles.

A major factor in considering TPMS for heavy vehicles is an assessment of the durability of the available systems. There have been several studies of the accuracy of available systems with regard to pressure sensing, but there has been little published information to date on the durability and long term operating costs of heavy vehicle TPMS. The Federal Motor Carrier Safety Administration has initiated a field operation study of heavy vehicle TPMS that is designed to provide durability, as well as cost/benefit data, for several of the systems that were tested by this research project for pressure sensing accuracy and for malfunction recognition.

With and without temperature compensation, tire test pressures set to 3 psi below TPMS "factory" setpoints were satisfactorily detected by each TPMS tested. By adding tire temperature compensation (SmartWave only) the variation between a "hot" over-the-road tire pressure reading and low-pressure alerts for both 10 and 20 percent pressure losses was maintained at tire temperatures elevated to nearly 30° F above initial CIP temperatures. It maintained a fixed ratio of pressure drop from current temperature operating pressures to activate the low-pressure alarm, where the systems without temperature compensation allowed much larger pressure drops before activating their alarms. These large pressure drops could result in significant load reduction capability of the tires; and the tires should be re-inflated as soon as possible after the warnings are received. A disadvantage of temperature-compensation is adverse driver reaction when driving through extreme temperature fluctuations (e.g., mountains and valleys). More research will be required to answer the human factor questions of this technology.

As seen in the malfunction tests performed on these systems, several systems did not recognize or acknowledge through the display that communication had been lost with one of the pressure sensors. In order to maintain the safety benefits of the TPMS, it is important that the system inform the driver when it is not operating normally.

Identification of sensor temperature sensitivity needs to be isolated from raw pressure detection as identified by the low-pressure detection test procedure in this paper. A second test would need to be conducted using either fixed pressures and the tires run through a heating and cooling cycle, or the tires would need to be heated fully to on-the-road operating temperatures and a nominal slow leak rate of 1 psi per minute be established through a test pressure controller (as was used for this test program) while driving to detect the level where the TPMS would detect and alert low tire pressure.

Test Procedure Summary

The following section provides the procedural steps for testing a TPMS as described earlier in the paper, but without commentary.

Inflate all tires to Cold Inflation Pressure (CIP). Take readings by measuring individual tire pressures and temperatures with both TPMS and data collection system, and measure all tire external temperatures

with a noninvasive probe. Log all measurements that are not collected electronically.

Drive for 8 to 10 minutes over a flat road (calibration). Limit the vehicle's maximum speed to 25 mph for a 2-mile loop. Within 5 minutes of completing calibration, read TPMS pressures and temperatures, deactivate TPMS, and deflate test tire to 3 psi below the setpoint (which is set at 10 to 15 percent below the CIP). Immediately reactivate the TPMS, take pressure and temperature readings, observe TPMS display for warnings, and then run a Detection Test (same course as in the calibration). The test is complete when the TPMS signals a low-tire-pressure detection or 15 minutes have elapsed since activating the TPMS. Cool tires and re-inflate to CIP. Go to the next test.

When the TPMS detects the low tire pressure within the 15-minute period, return to the starting point. Take readings. Deactivate the TPMS and wait for 5 minutes (this is a TPMS memory check). After 5 minutes have expired, reactivate the TPMS and confirm that the same warning returns to the TPMS Display. If the same warning does not re-display, the TPMS has failed to remember the fault after a power-down cycle (an engine shutdown).

Deactivate the TPMS and allow the tires to cool to ambient temperature from 30 minutes up to 2 hours. With the TPMS deactivated, re-inflate the tires to CIP. Activate the TPMS, take readings, observe TPMS display for warnings. If no warnings are indicated by TPMS display, the test is complete. Proceed to the next test.

When warnings are present, either activate the TPMS reset function (if available) or run Reset Identification Test (same course as the calibration). If the TPMS fails to clear any unwarranted warnings, then the system has failed to identify a properly re-inflated tire.

Repeat the above steps for each test tire and for each pressure setpoint. Once the Detection tests have been completed, conduct a failed system or system malfunction test by disconnecting the power source to any TPMS component, by disconnecting any electrical connection between TPMS components, by removing a wheel and locating it outside of radio range, or by installing a tire or wheel on the vehicle that is incompatible with the system being tested.

REFERENCES

- [1] Grygier, P., Garrott, W.R., Mazzae, E.N., MacIsaac, Jr., J.D., Hoover, R.L., Elsasser, D., and Ranney, T.A. 2001. *An Evaluation of Existing Tire Pressure Monitoring Systems*, U.S. Dept. of Transportation, DOT HS 809 297.
- [2] FMVSS No. 138. 2006. U.S. Dept. of Transportation, National Highway Traffic Safety Administration, FMVSS No. 138, Tire Pressure Monitoring Systems, 49 CFR, Ch. V.
- [3] Brady, S., Nicosia, B., Kreeb, R., and Fisher, P. 2007. *Tire Pressure Monitoring and Maintenance Systems Performance Report*, U.S. Dept. of Transportation, FMCSA-PSV-07-001.